Multivariate Analysis of Transcriptional Changes Following Restoration of SERCA2a Levels in Failing Rat Hearts

by

Adel B. Tabchy

B.S., Biology, American University of Beirut, 1997

M.D., American University of Beirut, 2001

Submitted to the Department of Mechanical Engineering
in Partial Fulfillment of the Requirements for the Degree of
Master of Science

at the

Massachusetts Institute of Technology

June 2004

Signature of Author.....
Department of Mechanical Engineering
May 7, 2004

Certified by.....
David E. Housman
Ludwig Professor of Biology
Thesis Supervisor

Certified by.....
Ain A. Sonin
Professor of Mechanical Engineering
Thesis Reader

Accepted by.....
Ain A. Sonin
Chairman, Committee on Graduate Students
Department of Mechanical Engineering

Multivariate Analysis of Transcriptional Changes Following Restoration of SERCA2a Levels in Failing Rat Hearts

by

Adel B. Tabchy

Submitted to the Department of Mechanical Engineering
on May 7, 2004
in Partial Fulfillment of the Requirements for the Degree of
Master of Science

ABSTRACT

We have identified the genes responsible for SERCA2a-induced reversal of heart failure, the leading cause of morbidity and mortality in the United States and developed countries. We have previously shown that restoration of a key enzyme that controls intracellular Ca^{2+} handling, the Sarcoplasmic Reticulum Ca^{2+} ATPase (SERCA2a), induces reversal of heart failure in humans and experimental models. We used high-density oligonucleotide arrays to explore the genetic reprogramming responsible for the reversal of heart failure upon adenoviral gene transfer of SERCA2a in a rat model of pressure overload hypertrophy in transition to heart failure. We combined model- and data-driven approaches to analyze the resulting multivariate microarray expression dataset corresponding to 4237 transcript sequences in six experimental groups. A multiscale systems approach was used that incorporated the main mechanisms underlying the control of gene expression at the transcriptional level, and the pathologic compensatory responses that occur in heart failure. The combinatorial control of gene expression that is thought to occur in mammals was implemented in a signal-processing model at the level of the heart cell nucleus; it identified 473 SERCA2a regulated genes. The integration of the main mechanisms underlying the pathologic compensatory responses that take place in heart failure was fundamental to the discovery of 10 functional transcriptional classes within this group of genes. In addition, 226 genes that were not targets of SERCA2a but were natural adaptive responses to aortic banding needed for clinical non-failure, were identified and functionally categorized. Biological functional distribution of SERCA2a targets revealed that SERCA2a activates genes that function mainly in the cytoskeleton, ECM, Ca2+ signaling, signal transduction, cell cycle and growth and development pathways. The integration of model- and data-driven ideas was crucial to the elucidation of specific patterns in the multivariate data and allowed the discovery of novel genes and their potential role in the normalization of multiple pathways within the failing cell. This is a novel, powerful and portable method to elucidate multivariate genome-wide transcriptional networks from primary microarray data.

Thesis Supervisor: David E. Housman
Title: Ludwig Professor of Biology

The real act of discovery consists not in finding new lands but seeing with new eyes.

Marcel Proust

Table of Contents

Acknowledgments

First and foremost I want to thank David Housman for giving me the great opportunity to join MIT and his lab, and for being such an active force in shaping my future. He gave me the autonomy to be creative; freedom is the highway for creativity. David is a brilliant mentor, a model, a friend and a father, and will always be. He is generous in extraordinary ways. As a teacher, David leads you to the threshold of your own mind.

I was fortunate to have Roger Hajjar and Federica del Monte as our collaborators at the Cardiovascular Research Center at MGH. Without their generosity and experimental input, this research work would not have been possible. Roger is my friend and my mentor. I have learned a lot from him. Federica is a brilliant researcher, and this work is largely the fruit of her exceptional dedication to research.

Ain Sonin was the pillar in the Mechanical Engineering Department from day one. His enthusiasm, disposition to life and his smile make him a wonderful human being and mentor. Thanks Leslie for being the best support and for un-stressing us with your beautiful smile. Marvin Minsky destroyed the old shell and fostered new ideas.

I want to thank my brother Marc and my parents for setting the example and the light to follow. Your love means everything to me.

Thanks to all Housman lab members for making the lab such a wonderful environment to work in, especially Kevin, Katie-Rose, Amanda, Junne, J. Michael, and Al. A big thanks to you Hitomi and Connie for taking care of business and letting us concentrate on science.

Thanks to my dear friends Shaptini, Saroufim, Sass, Roger, Schuman, Kevin, Mantoura, Khairallah, Maalouf, Emile, Joseph and Asseyley.

Thanks Ghislaine.

Adel.

I Introduction

Heart Failure is the leading cause of morbidity and mortality in developed countries (1). Once heart failure becomes symptomatic, the 5 year survival is less than 50% , a prognosis worst than most malignancies (1). The only curative treatment available is heart transplant.

Current attempts to analyze large genomic and proteomic data sets have significant limitations:

(1) Most analyses focus only on the data generated by a system: they are data-driven as opposed to being model-driven.

(2) Most analyses are not multivariate in nature or do not take into account the multivariate nature of the data at the price of large approximations which can introduce highly significant error into the analysis. There are no satisfactory described methods to analyze large multivariate genomic data sets.

(3) Most functional gene expression analyses lead to the segregation of samples into two groups (e.g. good prognosis vs. bad prognosis): analytical constructs segregating data in this manner are often poor approximation of biological complexity.

We have previously shown that restoration of a key enzyme that controls intracellular Ca^{2+} handling, the sarcoplasmic reticulum Ca^{2+} ATPase (SERCA2a), induces functional improvement and has a protective effect on cardiomyocyte metabolism and intracellular pathways of hypertrophy and failure in human and experimental models (2). SERCA2a expression has been shown previously to be down-regulated during heart failure, and restored back to its levels in healthy hearts by adenoviral gene transfer (3, 4).

The neurohumoral-hemodynamic defense reactions and the hypertrophic reaction in heart failure exhibit two distinct phases on a time scale: If these reactions are *sustained* in time, the outcome will be adaptive on the short-term but maladaptive on the long-term. SERCA2a induces a long-term adapative response in the failing heart.

Goals of the study:

To guide new therapeutic modalities for reversing heart failure, study design was aimed at furthering our understanding of the molecular events that underlie the pathophysiology of heart failure and its reversal by SERCA2a.

In this model, the insult that leads to heart failure is aortic banding. There are two categories of responses to aortic banding: natural responses (in the absence of gene transfer), and SERCA2a-induced responses. Natural responses can be adaptive or maladaptive. When SERCA2a is introduced into banded failing hearts, it elicits adaptive responses since it brings clinical non-failure.

At the most basic level, we wanted to know which molecular responses to aortic banding are causing failure, and which ones are causing non-failure. Starting from a failing heart or going all the way back to a non-failing heart, we defined the minimal genetic reprogramming required to have non-failure in the face of aortic banding.

There are two categories of responses to aortic banding that are needed to have clinical non-failure: SERCA2a-induced responses (those are the molecular differences that cause the clinical transition from a failing to a non-failing clinical phenotype, upon SERCA2a infection of failing hearts), *and* natural adaptive responses needed for non-failure (those are the genes that have a stable expression in failure and SERCA2a-induced non-failure, yet are responses to aortic banding). We identified these functional categories of reprogrammed genes (Fig 1).

We used oligonucleotide microarrays to characterize gene expression patterns in six experimental groups (see Materials and Methods). 87 rats were initially divided into two groups: 45 animals had an aortic band placed while 42 were sham-operated. Cardiac adenoviral gene transfer was performed after development of left ventricular (LV) dilatation in the aortic-banded animals. In both groups, animals either received gene transfer with Ad.SERCA2a or Ad.ßgal-GFP or did not undergo gene transfer. They make up the six experimental groups NF, NFV, NFS, F, FV, and FS (Fig 2).

II Materials and Methods

Construction of Recombinant Adenoviruses

To construct the adenovirus containing SERCA2a cDNA, we used the method described by He et al (5), whereby the backbone vector, containing most of the adenoviral genome (pAd. EASY1) is used and the recombination is performed in *Escherichia coli*. SERCA2a cDNA was subcloned into the adenoviral shuttle vector (pAd.TRACK), which uses the cytomegalovirus (CMV) long terminal repeat as a promoter. The shuttle vector used also has a concomitant green fluorescent protein (GFP) under the control of a separate CMV promoter. An adenovirus containing both ß-galactosidase and GFP controlled by separate CMV promoters (Ad.ßgal-GFP) was used as control. The adenoviruses were propagated in 293 cells. The titers of stocks used for these studies measured by plaque assays were $3x10^{11}$ pfu/mL for Ad.ßgal-GFP and $1.8x10^{11}$ pfu/mL for Ad.SERCA2a, with particle/pfu ratios of 8:1 and 18:1, respectively. These recombinant adenoviruses were tested for the absence of wild-type virus by polymerase chain reaction (PCR) of the early transcriptional unit E1.

Experimental Protocol

Four-week-old Sprague-Dawley rats (Charles River, Mass; 70 to 80 g) were anesthetized with pentobarbital (60 mg/kg IP) and placed on a ventilator. A suprasternal incision was made, exposing the aortic root, and a tantalum clip with an internal diameter of 0.58 mm (Weck, Inc) was placed on the ascending aorta (6). Animals in the sham group underwent a similar procedure without insertion of a clip. The supraclavicular incision was then closed, and the rats were transferred back to their cages.

The animals were initially divided into 2 groups: 1 group of 45 animals with aortic banding and a second group of 42 animals that were sham-operated. Three animals in the aortic banding group did not survive the initial operation, and 2 animals in the sham-operated group did not survive. In the aortic-banded animals, we waited 26 to 28 weeks for the animals to develop left ventricular (LV) dilatation before cardiac gene transfer. In this banded group as well as in the sham-operated group, 14 animals did not undergo gene transfer and were followed longitudinally. The rest of the animals (28 and 26) underwent adenoviral gene transfer with either Ad.SERCA2a (14) or Ad.ßgal-GFP (12). Figure 2 illustrates the six experimental groups in the study: NF (Non-Failing), heart with no aortic banding and no gene transfer; NFV (Non-Failing Virus), no aortic banding but transfer of viral construct (Ad.ßgal-GFP); NFS (Non-Failing SERCA2a), no aortic banding but transfer of SERCA2a construct (Ad.SERCA2a); F (Failing), aortic banding but no gene transfer; FV (Failing Virus), aortic banding and transfer of viral construct; FS (Failing SERCA2a), aortic banding and transfer of SERCA2a construct.

Adenoviral Delivery Protocol

The group of animals subjected to aortic banding was further subdivided into 3 groups of 14, 14, and 14 receiving Ad.SERCA2a, Ad.ßgal-GFP, or no adenovirus, respectively. The group of sham-operated animals was also subdivided into 3 groups of 14, 12, and 14 receiving Ad.SERCA2a, Ad.ßgal-GFP, or no adenovirus. The adenoviral delivery system has been described previously by our group in detail(7, 8). Briefly, after the rats had been anesthetized and a thoracotomy performed, a 24-gauge catheter was advanced from the apex of the LV to the aortic root. The aorta and main pulmonary artery were clamped for 40 seconds distal to the site of the catheter, and 0.5 ml of adenosine to temporarily slow the heart rate was infused followed by 200 ml of adenoviral solution (10^{10} pfu); the chest was then closed, and the animals were allowed to recover. The antibiotic Cefazolin 20 mg/100 g was injected im as well as Buprenorphine 0.01 mg/100 g for 2 days to alleviate pain.

Serial Echocardiographic Assessment

After 18 weeks of banding, serial echocardiograms were performed weekly in lightly anesthetized animals (pentobarbital 40 mg/kg IP). Transthoracic M-mode and 2D echocardiography was performed with a Hewlett-Packard Sonos 5500 imaging system with a 12-MHz broadband transducer. A mid–papillary level LV short-axis view was used, and measurements of posterior wall thickness, LV diastolic dimension, and fractional shortening were collected. Gene transfer was performed in all animals within 3 days of detection of a drop in fractional shortening of >25% as compared with the fractional shortening at 18 weeks after banding. In the sham-operated rats, gene delivery was performed at 27 weeks.

Characterization of Animals

After 24 weeks of aortic banding, the animals showed echocardiographic signs of LV hypertrophy, including an increase in wall thickness, both posterior (30%) and septal (25%), a decrease in LV dimensions (LVEDD 7.5%, LEESD 15%), and an increase in fractional shortening (4%). After 26 to 27 weeks of banding, these animals had uniformly: 1) small pericardial effusions, 2) pleural effusions, 3) an increase in lung weight, 4) ascites, and 5) dyspnea at rest, all indicative signs of severe heart failure. Echocardiographically, LV end-diastolic dimensions increased (LVEDD 8.7%, LVESD 15.4) and fractional shortening decreased by 14.3%. Heart weight was increased from 1.6±0.18 to 2.3±0.22 g ($p<0.01$) in Failing versus control animals. Heart weight to body weight ratio was increased from 0.27±0.03 to 0.49±0.06 ($p<0.004$). The overexpression of SERCA2a reduced the heart weight to body weight ratio to 0.37±0.01 ($p<0.003$ compared to FV, and $p<0.002$ compared to F).

Immunoblotting

The lysates were prepared at 4°C in a lysis buffer containing (in mmol/L) NaCl 150, $MgCl_2$ 1, and $CaCl_2$ 1, plus detergents and proteinase inhibitors (pH 7.4). The tissue was homogenized and spun at 1400 rpm (Eppendorf) for 30 minutes. The supernatant was then filtered through 4 layers of gauze and centrifuged at 15.000 rpm for 60 minutes (Eppendorf). SDS-PAGE was performed on the supernatant under reducing conditions on 7.5% separation gels with a 4% stacking gel in a Miniprotean II cell (Biorad). For immunoreaction, the blots were incubated with 1:1000 diluted monoclonal antibodies to SERCA2a (MA3-919; Affinity BioReagents), phospholamban (Badrilla), or 1:1000 diluted anti-calsequestrin (MA3-913; Affinity Bioreagents) for 90 minutes at room temperature. Protein levels of SERCA2a were

decreased in failing compared to sham left ventricular tissue. Adenoviral gene transfer of SERCA2a in failing hearts increased SERCA2a protein expression, restoring it to levels observed in the non-failing hearts. Calsequestrin protein levels did not change among the different groups, nor did phospholamban.

Validation of microarray data by Quantitative Reverse Transcriptase PCR (QRT-PCR)

Total RNA was isolated and purified from the rat hearts as described below. Following purification, RNA was quantified using the Agilent Bioanalyzer according to the manufacturer's instructions. RNA (15 μg) was treated (10 min at 20 °C) with amplification grade DNase I (Promega; Madison, WI) following which the DNase I was heat-inactivated (15 min at 65°C). QRT-PCR was performed in duplicate using the Qiagen Quantitect RT-PCR kit containing SYBR Green I (1:30,000, Sigma), forward and reverse primers (50 nM each), and sample RNA (<500 ng). Accumulation of PCR product was monitored in real time (ABI Prism 7000, Applied Biosystems), and the crossing threshold (Ct) was determined using the Prism 7000 software. For each set of primers, a no reverse amplification control was included. Post-amplification dissociation curves demonstrated the presence of a single amplification product in the absence of DNA contamination for each set of primers. Fold changes in gene expression were determined using the ΔCt method with normalization to total RNA using S18 ribosomal RNA as an internal control (9).

Microarray Procedures

Total RNA was extracted from rat hearts in each experimental sample using TRIzol (Invitrogen) according to the manufacturer's recommendations. RNA was resuspended in diethyl

pyrocarbonate-treated H_2O and further purified using the Qiagen (Chatsworth, CA) RNeasy total RNA isolation kit. RNA was quantified and was used to generate cDNA using the Superscript Choice system (Invitrogen) according to the Affymetrix protocol (Affymetrix, Santa Clara, CA). Resulting cDNA was used to generate biotin-labeled cRNA using the ENZO Bioarray High Yield transcript labeling kit (Affymetrix). cRNA (20 μg) was fragmented in fragmentation buffer [40 mM Tris (pH 8.1), 100 mM potassium acetate, 30 mM magnesium acetate] for 35 min at 94 °C. The quality of the cRNA was checked by hybridization to Test3 arrays (Affymetrix). Subsequently samples were hybridized to rat mU34A oligonucleotide microarrays (Affymetrix), and staining and scanning according to Affymetrix protocols identified bound sequences.

Oligonucleotide microarray analysis of gene expression was done essentially as described (Affymetrix). The 8800 oligonucleotide clones on the Affymetrix mU34A microarray are available from Affymetrix. Images of hybridized microarrays were obtained using a GeneArray 2500 microarray scanner (Affymetrix). Images were analyzed with Affymetrix® Microarray Suite software, and intensity data (along with multiple quality control parameters; see Affymetrix® Microarray Suite manual) was stored in a database. The software evaluated the relative level of expression of each transcript represented on the array and labeled it as either present, absent, or marginal. To this end it combined the results from match/mismatch probe pairs that interrogate different fragments of a transcript. Probe pair intensities are used as input, and allow the quantitation and subtraction of signals caused by non-specific cross-hybridization. The statistical significance of each detection call was indicated by an associated p-value. Single spots and areas of the array with obvious imperfections were flagged and excluded from subsequent analyses. Clones that consistently behaved poorly across arrays were excluded from all analyses. To enable comparison between experiments, intensity data was calibrated

independently for each array by globally scaling and normalizing the intensities to an average intensity of 1,500. A minimum value of 150 was assigned to all average differences (AvDiffs) with an intensity measurement below 150.

Data analysis

4,237 out of the 8,800 array elements were identified as 'present' in at least 2 out of the 10 experimental samples and were used for further analysis. The intensity values were stored in a table (rows, individual genes; columns, single mRNA samples). Where the same experimental group had been analyzed on multiple arrays, multiple observations for an array element for a single experimental group were averaged. An algorithm was developed by our group that implemented the signal-processing model presented in the text and addressed the goals of the study. The dataset containing 4,237 array elements was used as the input data. The algorithm extracted SERCA2a targets in the failing heart, and clustered those genes into functionally distinct transcriptional profiles. It also extracted the genes that are part of natural adaptive responses against aortic banding that are needed for clinical non-failure and clustered them into distinct transcriptional profiles. We calculated intensity ratios between different experimental samples and a reference sample. The intensity ratio calculated for each gene reflects the relative abundance of mRNA in the experimental sample versus a reference sample. The use of a common reference microarray allows the comparison of the relative expression level of each gene across all the experimental samples (arrays) (10). A 1.2 cutoff value for the ratios was used (thus the upper cutoff value is 1.2 and the lower cutoff value is 1/1.2 = 0.83). To display the output graphically as clustered expression data for Figures 5 and 6, the output of the algorithm was fed into the program Cluster (M. Eisen; http://rana.lbl.gov/EisenSoftware.htm) (10). Genes

were normalized and mean-centered, then hierarchical clustering was applied to the genes axis using the unweighted pair-group method with complete linkage as implemented in Cluster. The distance matrix used was Uncentered Pearson correlation (it is a slight variant of Pearson correlation; see Cluster manual available at http://rana.lbl.gov/manuals/ClusterTreeView.pdf for computational details). The results were visualized with Tree View (M. Eisen; http://rana.lbl.gov/EisenSoftware.htm) (10). All datasets used to generate Figs 5, 6 are included in Tables 1 and 2.

Statistical analysis

All values were calculated as mean±SD. For the echocardiography data, when the variables were examined at various intervals, ANOVA with repeated measures was performed. Statistical significance was accepted at the level of $P<0.05$.

III Results

What genes does SERCA2a target in the failing heart?

We initially focused on identifying the genes that are causal for the clinical transition from a failing to a non-failing clinical phenotype, upon the introduction of SERCA2a into a failing heart. Starting from a failing heart, the minimal genetic reprogramming required to have non-failure in the face of aortic banding (keeping other genes unchanged), defines the genes affected by SERCA2a. A key element in the analysis is the evaluation of the contribution of the gene delivery system to the gene expression changes which occur in the model system. Previously, we demonstrated that the clinical transition from failure to non-failure is only due to SERCA2a expression, and that other elements that are part of the gene expression construct do not contribute to the clinical transition (7, 11-13). Our goal in this analysis was to substract the effects of these elements on gene expression profiles in order to identify those gene expression changes which specifically were contributory to the ability of SERCA2a expression to prevent heart failure.

Isolating the genes that are targets of SERCA2a:

In analyzing the data, we relied on the current understanding of mammalian regulation of gene expression at the transcriptional level(14, 15). The pattern of gene expression in a cell is the result of a complex molecular computation that the intracellular gene control network performs in response to information from inside and outside the cell. Gene expression is thought to be regulated by combinatorial control. Gene regulatory proteins bind to regulatory sequences in the gene control region. The promoter will integrate activator and repressor signals from this combination of inputs, and then make a decision to turn the gene ON or OFF, like a genetic switch, a digital response. The amount of RNA produced, however, varies, and so RNA abundance is an analogue response, and depends on the strength of the activation signal.

We built a signal-processing model that implements the combinatorial control of gene expression. In this model, the heart cell integrates inputs (aortic banding at time 1 and gene transfer at time 2) to change its gene expression and molecular phenotype, leading to a change in clinical phenotype (outputs) (Fig 2). The myocyte background on which the inputs are added is the non-failing heart cell. The different inputs will lead to different combinations of signals that will affect the expression of a gene.

We built a vectorial representation of this input-output system in order to assign cause to a specific input or combination of inputs when there is a change in expression of a gene (Fig 3). We wanted to isolate genes that are targets of SERCA2a. Each vector represents the molecular signals (gene regulatory proteins) transduced for that input at the level of the cell, that collectively either activate or repress transciption of a gene. The vectors are one dimensional, have a direction and magnitude. Therefore each vector encodes 2 bits of information. The

activity of the gene regulatory proteins is determined by the magnitude of the vector. The model is additive; we ignored synergistic/cooperative effects that might take place when multiple signals interact to control gene expression. The expression level of a gene (output) is the sum of the vectorial inputs that converge on the promoter for that gene. The stochastic vector was added to account for background stochastic fluctuations in gene expression levels. The stochastic vector is a measure of randomness within the system.

Thus, for a gene across the experimental samples, the input-output system can be described by a system of 3 linear equations with 7 unknowns:

$$[1]: \overrightarrow{NF} + \overrightarrow{AoB} + \overrightarrow{Stoch} = \vec{F}$$
$$[2]: \overrightarrow{NF} + \overrightarrow{AoB} + \vec{V} + \overrightarrow{GFP} + \overrightarrow{BGal} + \overrightarrow{Stoch} = \overrightarrow{FV}$$
$$[3]: \overrightarrow{NF} + \overrightarrow{AoB} + \vec{V} + \overrightarrow{GFP} + \overrightarrow{SERCA} + \overrightarrow{Stoch} = \overrightarrow{FS}$$

For each gene, we wanted to know which inputs were contributing to the gene expression levels observed, to identify contributions due to SERCA2a. We can reduce the system of equations to 3 linear equations with 4 unknowns:

$$[2]-[1]: \vec{V} + \overrightarrow{GFP} + \overrightarrow{BGal} = \overrightarrow{FV} - \vec{F}$$
$$[3]-[2]: \overrightarrow{SERCA} - \overrightarrow{BGal} = \overrightarrow{FS} - \overrightarrow{FV}$$
$$[3]-[1]: \vec{V} + \overrightarrow{GFP} + \overrightarrow{SERCA} = \overrightarrow{FS} - \vec{F}$$

When we perform a two by two comparison of the gene expression levels, F, FV, and FS, as dictated by the right hand side of the above equations, we get a total of $3^3 = 27$ (F, FV, FS)

configurations, only 13 of which are possible in real space (only in those 13 does the system of 3 equations have a solution) (Fig 4). These configurations correspond to the global geometric structures of gene expression levels for a gene. Genes within a configuration are controlled by the same inputs.

Because there are more unknowns than there are descriptions of the system, for each configuration, instead of trying to solve these equations, we analyzed all possible solutions to these equations at once. We considered all the possible combinations of inputs that can lead to the specific observed outputs. We then chose the most parsimonious solution (16). When gene expression was found to be affected by SERCA2a, that gene was identified as a target of SERCA2a (Fig 4).

To assess the robustness of our analytical methodology, we identified SERCA2a targets by an additional method. Whereas in the combinatorial control model SERCA2a targets were identified by examining myocytes at the molecular level, here we correlated the molecular phenotype of myocytes with their clinical phenotype. The molecular phenotype at the level of the heart cell determines the clinical phenotype at the level of the cardiovascular system. In a cause-effect sequence, change explains change. The clinical phenotype difference between different experimental samples is caused by an underlying molecular phenotype difference. Therefore some of the genes whose expression changes between the two clinical phenotypes are the cause of the clinical phenotype transition from failure to non-failure. The experimental samples F and FV belong to the failing clinical category, while FS belongs to the non-failing clinical category. Here we identified through the use of a molecular-clinical correlation analysis the genes that are

causal for the clinical phenotype transition. Since SERCA2a is the cause for the clinical phenotype transition, those genes would be targets of SERCA2a.

The 13 possible gene expression configurations (F, FV, FS) for a gene (Fig 4) were obtained above by a pairwise comparison of the gene expression levels in F, FV and FS. Each configuration is thus defined by 3 pairs (for example in Fig 4, configuration 1, FV>F, FS>FV, and FS>F). We analyzed individual configurations: Where in each pair, a difference at the molecular level produced a difference a the clinical level, and a similarity at the molecular level produced a similarity at the clinical level, a triple correlation was recorded, and the gene was assigned the highest probability of being causal for the clinical transition from failure to non-failure (a triple correlation is recorded when the gene expression level in F is the same as in FV [same gene expression levels correlates with same clinical phenotype], F is different from FS, and FV is different from FS [different gene expression levels correlates with different clinical phenotypes]; it corresponds to configurations 11 and 13 in Fig 4). Such a gene would have the highest probability of being a target of SERCA2a. Lower correlation scores (correlation in 2 pairs only, one pair only, or no correlation) were assigned progressively lower probabilities. Each configuration in Fig 4 was analyzed individually and a correlation score assigned to it (see Fig 4).

There was agreement between the two methodologies for the identification of SERCA2a targets. To increase accuracy, we combined the results from both analyses into a composite probability score describing the likelihood that a gene is a SERCA2a target. All potential SERCA2a targets (i.e. probability> 0) had a gene expression level in FS different from FV, *and* in FS different from F.

Transcriptional profiling of SERCA2a targets in the failing heart:

The transcriptional reprogramming induced by SERCA2a increased survival to aortic banding as compared to gene expression levels in NF and F.

Since SERCA2a is decreased in failure and restored back to normal levels in non-failure, we reasoned that one functional category of SERCA2a targets might be proteins that were brought back to non-failing levels upon SERCA2a infection (Fig 5, profiles 5, 6). However, if keeping the transcriptome-proteome state of the normal cell was the most adaptive alternative against aortic banding, then the cells would not have changed their expression profile from normal. Therefore, there must be other beneficial responses caused by SERCA2a other than just normalizing cellular proteins.

SERCA2a acts on a basis of already established natural adaptive and maladaptive responses to aortic banding. Natural maladaptive responses will be reversed by SERCA2a, while natural adaptive responses are either optimized or unchanged. In addition, SERCA2a will introduce new adaptive responses to aortic banding. We isolated these functional categories of reprogrammed genes.

Transcriptional profiling of SERCA2a targets defined ten categories of responses to aortic banding. We compared gene expression levels in NF, F, and FS, at a 1.2 cutoff. Because the category FS=F did not include SERCA2a targets, it was excluded. We ended up with 3x3x2= 18 (NF, F, FS) configurations, only 12 of which were possible in real space. SERCA2a effect was significant in 10 of these solutions (Fig 5).

In profile 1 (Fig 5, A, B), the gene expression level is stable from NF to F. This gene is not in the natural repertoire of compensatory reactions against aortic banding. Here SERCA2a is bringing a new adaptive reaction to overload. In profiles 5 and 7, the natural responses to aortic banding are

maladaptive. In profile 5, the gene expression level will be restored back to its level is normal hearts. The response is maladaptive and is cancelled. In profile 7, the adaptive response (SERCA2a) is the opposite of the natural response to aortic banding. For profiles 3 and 9 the response in F maybe adaptive, a first step in the right direction that needs optimization, or it maybe maladaptive. For profile 3, since the more adaptive gene expression level is in between and different from gene expression levels for NF and F, survival is most probably a non-linear function of transcriptional activity, and we cannot tell if the level in F is adaptive as compared to NF and being optimized, or maladaptive. For profile 9, if survival increases linearly in the range NF to FS with increasing level of gene product, than the response in F is adaptive as compared to NF but not as adaptive as in FS. The natural response to aortic banding was amplified by SERCA2a. On the other hand, if survival is a non-linear function of transcriptional activity, then the response in F maybe maladaptive as compared to NF.

The same applies to the mirror images of these individual profiles.

Using the same primary data set, the program Cluster (M. Eisen; http://rana.lbl.gov/EisenSoftware.htm) (10) failed to reproduce the clustering obtained with our algorithm unless the already clustered output from our algorithm was submitted. This further demonstrates the need to incorporate specific biological knowledge and guidance into the mathematical framework for gene expression analysis.

What genes encode natural adaptive responses to aortic banding, needed for clinical non-failure?

There are two categories of responses to aortic banding that are needed to have clinical non-failure. We examined SERCA2a-induced responses earlier. The other category are natural adaptive responses needed for non-failure. Those are the genes that have a stable expression in failure and SERCA2a-induced non-failure, yet are responses to aortic banding, they are reprogrammed in failure. A natural adaptive response that is optimized and needed for non-failure, will be conserved from failure to SERCA2a-induced non-failure. Those genes are not targets of SERCA2a (or other components of the SERCA2a construct). Their level of expression is the same across all aortic-banded states F, FV and FS, since they are a reaction against this insult. Out of 2006 genes changed from NF to F (those are the natural responses against aortic banding), 226 genes were found to encode optimized adaptive responses against aortic banding that were conserved when SERCA2a infected the cells (Fig 6).

Distribution of genes by biological functional category reveals patterns in the genetic reprogramming events to reverse heart failure:

We further classified genes from Figure 5 and 6 according to their published biological function available in public databases (NCBI).

SERCA-induced responses vs. Natural adaptive responses (i.e. Figure 5 vs. Figure 6 genes):

As expected (Figure 7), SERCA2a targets are more often Ca2+ signaling genes than the natural adaptive responses to aortic banding from Figure 6. Up to 15% of SERCA2a targets function in Ca2+ signaling pathways, while 2% function in Ca2+/Calmodulin signaling. This may offer a mechanistic model for SERCA2a targeting of these genes, namely that SERCA2a effect on these genes is mediated by Ca2+. The Figure also shows that natural adaptive responses are much more biased towards mitochondrion and metabolism/energy responses, whereas SERCA2a targets more specifically the cytoskeletal pathways and extracellular matrix components, for structural and contractile optimization on the one hand, and remodeling on the other.

As expected, the genes upregulated in failure in Figure 5 vs. in Figure 6 (see Figure 8A) fall in different categories since the changes in Figure 6 are going to persist into the FS state (adaptive responses) whereas most of the responses in Figure 5 are maladaptive and are going to be corrected by SERCA2a (downregulated). The same applies to Figure 8B. In Figure 8A, a large proportion of genes activated in both Fig 5 and 6 belong to the development/growth differentiation categories; organs use as defense mechanism genetic programs already used during evolution and embryological development of the organ.

SERCA2a and adaptive natural responses target different functional categories of genes: Comparison of genes activated by SERCA2a vs. genes naturally activated in response to aortic banding (Figure 9A), shows that SERCA2a specifically activates genes in the cytoskeleton, ECM, and Ca2+ signaling categories, while activation by SERCA2a of the cell cycle, growth and development genes is comparable to that achieved naturally.

In Figure 9B, the pattern of gene inactivation by SERCA2a and natural responses is more comparable, except for a larger proportion of mitochondrial and metabolism energy genes being turned off by natural adaptive responses.

SERCA-induced responses (Figure 5 genes):

SERCA2a activates and inactivates different categories of genes:

SERCA2a activates genes in the cytoskeleton, ECM, Ca2+ signaling, signal transduction, cell cycle, growth and differentiation pathways, and inactivates genes mainly in the signal transduction, transcription, cell cycle and metabolism/energy categories (Figure 10).

Comparison of genes in profile 1 and profile 2 of Figure 5 (Figure 11A), demonstrates an important activation of cytoskeletal, Ca2+ signaling, signal transduction, cell cycle and development and growth genes. In contrast, metabolism genes are inactivated, in addition to other genes involved in the cell cycle.

Comparison of profiles 5 and 6 (Figure 11C) reveals that signal transduction, cytoskeletal, Ca2+ signaling, RNA processing/translation, cell cycle and development growth and differentiation

genes are activated with SERCA2a restoration, while prominently transcription, and metabolism/energy genes are inactivated.

Among the genes that were upregulated in failure and then restored to non-failing levels by SERCA2a (Fig 5, profile 5) is notably tau protein kinase 1 (GSK3beta) which is known to protect from cardiac hypertrophy as well from apoptosis in the heart (17, 18). GSK3beta was upregulated 1.3 folds upon cardiac failure. It is a kinase with profound effects on fetal development and tumorogenesis. A Ca2+-mediated or direct interaction between SERCA2a and the PI3K/GSK3beta pathways (17, 18) has recently been described. The activity of GSK3beta is negatively regulated by Akt in many cell types, and inhibiting GSK3beta seems to be critical to the anti-apoptotic effect of Akt and to the hypertrophic response (17).
Interestingly, Akt was found to be decreased in failing hearts and rescued by overexpression of SERCA2a (Figure 5, profile 6). Akt is a powerful survival signal in many systems and is activated by several cardioprotective ligand-receptor systems including insulin-, IGF-1- and gp130-signaling pathways. Its rescue probably plays a very important role in the survival benefit observed with SERCA2a overexpression.
Furthermore, two upregulated genes in failure (Figure 6, profile 2) interact with Akt. Akt phosphorylates PEA15 (19) to stabilize its anti-apoptotic function. Hsp 27 was found to regulate apoptosis by regulating Akt activation (20).

Among the failing downregulated genes that were rescued by SERCA2a (Fig 5, profile 6) was the small peptide Tensin. This protein localizes to focal adhesions, regions of the plasma membrane where the cell attaches to the extracellular matrix. This protein crosslinks actin

filaments and contains a Src homology 2 (SH2) domain, which is often found in molecules involved in signal transduction. Tensin is a substrate of calpain II. Tensin is part of the integrin complex consisting of structural and signaling proteins serving both as physical link between the extracellular matrix and the cytoskeleton as well as signal transduction (21-24). The normalization of Tensin gene expression by SERCA2a gene transfer in the failing heart may represent an interesting target in cardioprotection from apoptosis and cell survival signaling pathways in heart failure.

Interestingly, Tropomyosin 1 is downregulated in failure and rescued with SERCA2a infection (Fig 5, profile 6). Mutations in this gene cause hypertrophic cardiomyopathy (25). Tropomyosin 1 is a structural component of the cytoskeleton that binds actin and has an important role in regulation of muscle contraction and heart rate.

Activins are dimeric differentiation and growth factors belonging to the transforming growth factor-beta (TGF-beta) superfamily of signaling proteins. Activins signal through a heteromeric complex of receptor serine kinases. The receptors are transmembrane proteins, composed of a ligand-binding extracellular domain and a cytoplasmic domain with serine/threonine specificity. Type I and II receptors form a stable complex after ligand binding, where type II receptor phosphorylates type I receptors (26). The gene that encodes Activin A type I receptor which signals a particular transcriptional response in concert with activin type II receptors, was found to be restored by SERCA2a from a downregulated state in failure (Figure 5, profile 6). The follistatin-like gene, which was increased in failure (Figure 6, profile 2) is an Activin binding protein which also binds Ca2+ (27).

Heme oxygenase (Fig 5, profile 8) is downregulated in failure (6 fold) and then strongly upregulated upon SERCA2a infection (9 fold). It is an essential enzyme in heme catabolism that cleaves heme to biliverdin. It is also involved in signal transduction and activates the NF-kappaB and MAPK signaling pathways (28). It is an interesting candidate in failure reversal because of its prominent roles in cardiovascular pathways: It is a survival signal (29); it protects against oxidative stress; it binds nitric oxide (30); and it regulates the cell cycle in vascular endothelial and smooth muscle cells (31).

In profile 9 of Figure 5 (Figure 11E), activation of genes for ECM molecules, Ca2+ signaling, signal transduction, cell cycle, growth and development appears to be amplified.

Among the amplified responses by SERCA2a (Figure 5, profile 9) are Endothelin receptor type B (Ednrb), and the mitochondrial uncoupling protein 2 (UCP2). Endothelin receptor type B is a G protein-coupled receptor which activates a phosphatidylinositol-Ca2+ second messenger system. Its ligand, endothelin, is a potent vasoactive peptide. Endothelin plays an important role in the pathophysiology of idiopathic dilated cardiomyopathy (32). It is involved in hypertension (33), in development (34), and it activates matrix metalloproteinases (35) important for remodeling.

Mitochondrial uncoupling proteins separate oxidative phosphorylation from ATP production by allowing a leak in the transmembrane proton gradient. UCP2 overexpression prevents mitochondrial death pathways in cardiomyocytes, by protecting them from oxidative stress induced apoptosis. UCP2 overexpression dramatically attenuated both Ca2+ overload and the

production of reactive oxygen species in mitochondria, which contribute to the catastrophic loss of mitochondrial inner membrane potential, a critical early event in cell death (36, 37).

Natural adaptive responses (Figure 6 genes):

Comparison of genes in profiles 1 and 2 of Figure 6 (Figure 12) shows that the metabolic/energy and mitochondrial pathways are inactivated, at the expense of a dramatic activation of cell cycle, development and differentiation, cytoskeletal and ECM genes.

Among the genes downregulated in failure is S100 calcium binding protein A1 (Fig 6, profile 1). This protein is a member of the S100 family of proteins containing 2 EF-hand calcium-binding motifs, involved in the regulation of cell cycle progression and differentiation. This protein stimulates Ca2+-induced Ca2+ release, inhibits microtubule assembly, and inhibits protein kinase C-mediated phosphorylation. Reduced expression of this protein has been implicated in cardiomyopathies. It is specifically expressed in the heart at high levels and is thought to be an important regulator of cardiac contractility (38). S100A1 protein acts as a cardioprotective factor during ischemic myocardial injury by inhibiting apoptosis in cardiomyocytes via activation of the extracellular signal-regulated protein kinase 1/2 (ERK1/2) (39). This protein also enhances sarcoplasmic Ca2+ release in skeletal muscle fibers (40). Therefore its downregulation in failure would counteract Ca2+ overload in the failing myocardium.

K+ channels:

The K+ channel was repeatedly targeted. Most of the ion channels genes that were reprogrammed were K+ channels. K+ channels were also affected by the reprogramming of

other genes. This important function for K+ channels in failure reversal is understandable in the light of the strong mechanistic role for K+ currents as underpinning excitation-contraction coupling in the heart along with Ca2+.

Validation of microarray data:

Quantitative Reverse Transcriptase PCR (QRT-PCR) validates microarray data:

QRT-PCR was performed to validate that the microarray data reflects true transcriptional changes. In Figure 14 the profiles of different up-regulated and down-regulated sample genes obtained from the microarray data analysis were compared to the QRT-PCR profiles for the corresponding genes, showing a close correspondence of the data for the two analytical methodologies. The fold changes determined from microarray data analysis and QRT-PCR analysis were used to plot expression profiles, setting the level of the NF sample to 100. As shown, QRT-PCR results track the changes in transcript profiles for Tensin, GSK-3β, Rev-ErbA-α, β-enolase, Atrial Myosin Light Chain 1, Na-channel, Rev-ErbA-β, and Connexin-43 gene.

Other published studies validate microarray data:

Other studies in the literature recorded gene expression changes in failure (Figure 6) similar to our microarray data for genes: SLC2A4 (a glucose transporter), the mitochondrial uncoupling proton carrier UCP3 (41), ICAM1 (42), BNP (43), Natriuretic Peptide Precursor A (41), and Endothelin converting enzyme 1 (44).

Microarray data has its internal controls:

We repeatedly found that genes represented by more than one array element or with high degrees of sequence identity clustered next to each other.

IV Discussion

In the post-genome era, biology is quickly transforming from a data poor to a data rich science, but it still lacks the tools to extract meaningful information from the flood of data. The interface between disciplines is oftentimes a rich reservoir of ideas, and biology needs to take advantage of the rapid expansion of interdisciplinary research, to borrow approaches from other disciplines to extract functional information from its growing share of data. One field which would benefit from such an exchange of ideas is gene expression analysis. Most current attempts to analyze large genomic and proteomic data sets look for specific patterns in the data, focusing on the data generated by a system and treating the system as a black box. This approach does not say much about the underlying mechanisms, a knowledge of which is needed for real-life problem solving, and also limits the analysis to relatively simple systems. This explains why most current gene expression analysis are limited to comparing two groups only. By combining model- and data-driven approaches, we were able to analyze a complex multivariate genome-wide microarray expression dataset. It allowed the isolation of novel genes involved in the pathophysiology of heart failure and its reversal that will be used to guide future therapeutic interventions.

Its reliance on the combinatorial control of gene expression in mammals, a widespread control mechanism for gene expression, to dissect causal contributions in multivariate transcriptional networks, is one aspect of the portability of this gene expression analysis.

Cardiovascular compensatory responses in heart failure are adaptive on the short-term but maladaptive on the long-term:

Evidence from drug trials in heart failure showed that drugs that improve short-term symptoms, worsen long-term survival. Furthermore, the ability of neurohumoral blockade (β-blockers) and ACE inhibitors to prolong survival and improve symptoms, have shown that although these two responses are initially adaptive and improve hemodynamics, they evoke long-term proliferative responses that are deleterious. The long-term beneficial effect of many drugs used in heart failure is due to their slowing of the progressive ventricular dilatation called remodeling. Neurohumoral/hemodynamic activation, and hypertrophy/architectural changes (remodeling) in failing hearts are adaptive on the short-run but maladaptive on the long-run. Hypertrophy is initially adaptive, but on the long-term causes maladaptive responses that dominate the clinical picture and hasten the deterioration of the failing heart (45).

The heart lacks functional redundancy. The heart is unlike any other organ in terms of the selective pressures that shaped its evolution. Our view of the heart as central for mammalian survival is because it is a *functional unit* with no functional redundancy (the right ventricle is a low pressure chamber, the left ventricle has no functional redundancy). The heart is one of the very few biological systems important for survival that have no functional redundancy. For this reason, the heart will prioritize uninterrupted function. Its response to an insult is unique among organs: because there is no functional redundancy at the level of the pump, and the life of the whole organism depends on an uninterrupted blood supply, the heart cannot afford resting to heal while another part takes over function, like what happens in most other organs. This puts a major

constraint on the types of compensations that can take place. Any compensation in this context must prevent cardiovascular collapse at all price.

Compensatory responses have short-term and long-term consequences. In the case of an insult, organs that have functional redundancy will tend to select adaptive long-term responses even if the responses are functionally maladaptive on the short term: the rest of the organ will take over function in the meanwhile. This increases reproductive span. The heart, however, does not have this luxury and will therefore prioritize short-term over long-term adaptiveness. In the case of a non-redundant system, long-term adaptiveness does not exist in the absence of short-term adaptiveness: the organism will not survive a maladaptive short-term response. A response that carries a necessary immediate survival advantage, even if maladaptive on the long-term, will be selected.

In heart failure, most responses that are adaptive on the short-term exclude long-term adaptivity. Proliferative responses in the heart lead to cell death. The failing heart deteriorates rapidly. Insults that increase the load on organs induce proliferative responses leading to hypertrophy and hyperplasia. In the case of the heart, because of the lack of redundancy and the need for continued function and ordered electrical impulse propagation, cells cannot divide in any significant amount. Forcing adult myocytes into the cell cycle leads to apoptosis (46). There is also evidence that hypertrophy itself leads to cell death by mechanisms independent of cell-cycle induction. So proliferative signals lead to hypertrophy and cell death. From here emerges the picture of the vicious downward spiral of heart failure: increased load → proliferative signaling

→ hypertrophy → cell death → increased load. Thus it appears that in the case of heart failure, the consequences of short-term responses would preclude long-term survival.

The Neurohumoral/hemodynamic defense reactions emerged as a response to acute challenges. The neurohumoral/hemodynamic defense reactions act on the heart, blood vessels and kidneys, to compensate for the fall in blood pressure caused by underfilling in the systemic arterial system during exercise and blood loss. Because of their high survival value in acute fight or flight situations and in hemorrhage, these hemodynamic responses emerged as an adaptation for these short-term challenges, however they can become maladaptive when used in long-term challenges, such as chronic illness, like heart failure, where it is the cause of a downward deleterious spiral (47). Natural selection favored much more heavily responses that are adaptive for these short term challenges, because they carry a high survival value, are very common, and occur throughout life, i.e. especially before the reproductive age, as opposed to heart failure.

Heart failure usually occurs after peak reproductive age. This is another important reason why compensatory responses in heart failure are not optimized. The major etiologies of heart failure in developed countries are coronary and hypertensive heart disease. Any disease whose onset is after peak reproductive age will for the most part escape natural selection. A dominant defective gene that manifests through a disease phenotype before reproductive age will be filtered through natural selection in one of two ways: Either the gene will be eliminated from the gene pool because of a decrease in reproductive fitness, or adaptive responses by other genes, either a change in a the transcriptional state or a mutation in another gene (or group of genes) will compensate for the decrease in reproductive fitness and lead to an increase in the gene pool (co-

segregation) of the defective and compensatory mechanisms. In such individuals, the disease might be sub-clinical and undetected, or have a later onset. Because heart failure occurs mostly after reproductive age, most of the compensatory responses that develop are not filtered for adaptive responses by natural selection, therefore a lot of them would be predicted on these grounds alone to be maladaptive, and this is in agreement with observations.

SERCA2a targets a key signaling pathway in the heart cell:

Heart muscle cells make extensive use of Ca^{2+} signaling, where it assumes a central role in excitation-contraction coupling. Ca^{2+} can be used as a signal because its cytosolic concentration is normally kept very low (~10^{-7}M), whereas its concentration in the extracellular fluid (~10^{-3}M) and ER lumen is high. Heart failure leads to increased cytosolic Ca^{2+} (48) (49). Impaired SERCA2a activity is thought to be one of the main mechanisms for abnormal Ca^{2+} handling in heart failure (7). Ca^{2+} has been implicated as a possible cause of necrosis and apoptosis in the overloaded myocyte (48, 49). One way to understand the pathogenic role of Ca^{2+} overload in the failing heart is in thermodynamic terms. In the failing heart, Ca^{2+} increases energy demands and decreases energy production and leads to a vicious cycle of energy starvation. On the other hand, because Ca^{2+} level in the cell is normally very tightly regulated, when it increases in the cytosol it tends towards the extracellular/ER Ca^{2+} concentration, and this can be viewed as an entropic drive that signals cell death.

Unknown genes impact the interpretation of function distribution graphs (Figures 7-13): In the interpretation of the graphs showing the distribution of genes according to function, one has to take into account the fact that a large percentage of the genes belong to the unclassified category. More than 90% of genes in the unclassified category are unknown, i.e. they are transcripts that do not match a gene of known function. The rest (<10%) are genes of known function that do not belong to one of the listed categories. Because the number of classified known genes in the distribution is large enough, one can predict based on population statistics that the unknown gene population most probably obeys the same functional distribution as the known classified gene population, and therefore one should account for the proportion of unclassified genes in the interpretation. The easiest interpretation is when both compared categories have a very low and similar percentage of unclassified genes, or when the percentages of unclassified genes are similar.

Choice of a cutoff value:

A small transcription signal, like a transcription factor, located high up in a transcriptional amplification pyramid, can produce a large transcriptional change at lower levels in the pyramid. Therefore, the level of a transcription factor that initiates a transcriptional programme is expected to be tightly regulated, and even a small change from its basal level will produce a downstream response. Such important signals will often be missed in expression profiles that rely on large fold changes. One has to balance the need to unravel true effects against losing important information. Current array technology is mostly used as a jump stone for further confirmation by other experimental methods, and therefore one has more tolerance for false positives than false negatives. It is not more stringent to use a higher fold change as a cutoff when you are using it as a measure of change and no change. You get a compromise: It is stringent when you are using it as a measure of change, but it is not stringent when you are using it as a measure of no change. Thus, a compromise is made when a cutoff is used as both a measure of change and no change. For example, when 1.2 is used as a measure of no change, it is stringent.

Limitations:

As a first limitation, the use of RNA extracted from the entire heart may confound the interpretation of some results due to the heterogeneity of cell types. In addition, with even the best-controlled experimental setting, expression of the transgene is exhibited in 30-60% of cardiac cells following gene transfer. This variability may affect gene expression.

A considerable variability in studying gene profiling in pathological diseases, including heart failure, has been described, compared to the variability related to the experimental error once stringent parameters are included. Multiple samples and sample repetition reduce but do not eliminate biological variability. Although less relevant specifically for human disease, this study has been initially conducted in a rat model of heart failure and gene transfer where the biological variability within samples is largely reduced by homology of gender (all male rats), age, absence of other disease conditions, medications and disease etiology uniformity. In our study the biological variability is more restricted to the genetic intervention such as the level of viral transfection.

Many genes have alternative splice sites and this may lead to apparently contradictory results for array elements interrogating different regions of one transcript. Such genes are usually excluded from the analysis although they may be functionally important.

The list of genes does not provide a mechanism for all the perturbed genes. Genetic editing by transgenesis or knock-out would be required for each gene to clearly understand gene specific mechanisms.

V Conclusion

First, we have described a novel, powerful and portable method to elucidate multivariate genome-wide transcriptional networks from primary microarray data. As opposed to current attempts to analyze large genomic and proteomic data sets that focus only on the data generated by a system, we have combined model and data-driven approaches, what enabled us to elucidate multivariate transcriptional profiles and classify them into multiple functional classes.

Second, as a result, new genes have been identified that may prove important in understanding the mechanisms of heart failure and its reversal. The observation that most compensatory responses in heart failure are maladaptive suggests that successful new therapeutics might be aimed at the upstream signal-transducing molecules whose activity in the failing hearts leads to expression of pathological transcriptional programs. This study serves as a step toward defining new therapeutic molecular targets in heart failure and demonstrates the potential power of well designed gene expression analyses to identify therapeutic targets in disease states.

VI Figures and Tables

Figures

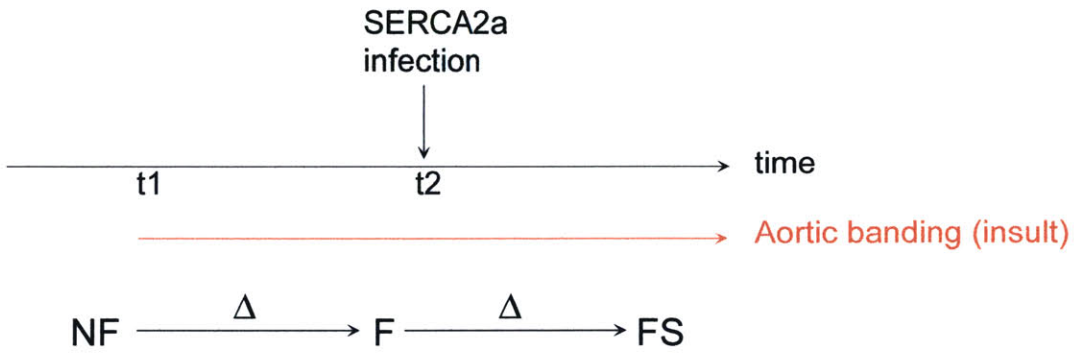
SERCA2a
infection
time
t1
t2
Aortic banding (insult)
NF
Δ
F
Δ
FS

Fig 1

Figure 1:
SERCA2a does not act on a blank slate. Starting all the way back from a non-failing heart, we wanted to define the genetic reprogramming required to have non-failure in the face of aortic banding (a reprogrammed gene is a gene whose expression is changed). The reversal of heart failure by SERCA2a is a two-step process in a sequence. In a cause-effect sequence, change explains change (Δ). The change in inputs explain the change in outputs of the system. Here, the change in inputs explains the change in gene expression. In the NF to F sequence, the input introduced is aortic banding (it is also sustained in time). The genes changed between states NF and F are therefore natural responses to aortic banding; some are adaptive, other maladaptive. Some of the genes changed from NF to F are natural adaptive responses to aortic banding needed for clinical non-failure. In the F to FS sequence, the input introduced is SERCA2a gene transfer (in its adenoviral construct). Therefore some of the genes changed between states F and FS are SERCA2a-induced responses to aortic banding. SERCA2a does not act on a blank state, it acts on a basis of natural adaptive and maladaptive responses to aortic banding. If we start at point F in time, the only genetic reprogramming needed to have clinical non-failure are SERCA2a-induced responses to aortic banding. If however we go back to point NF in time, in order to have clinical non-failure, we need both the natural adaptive responses to aortic banding needed for non-failure, and the SERCA2a-induced responses to aortic banding. We identified these two functional categories of genes.

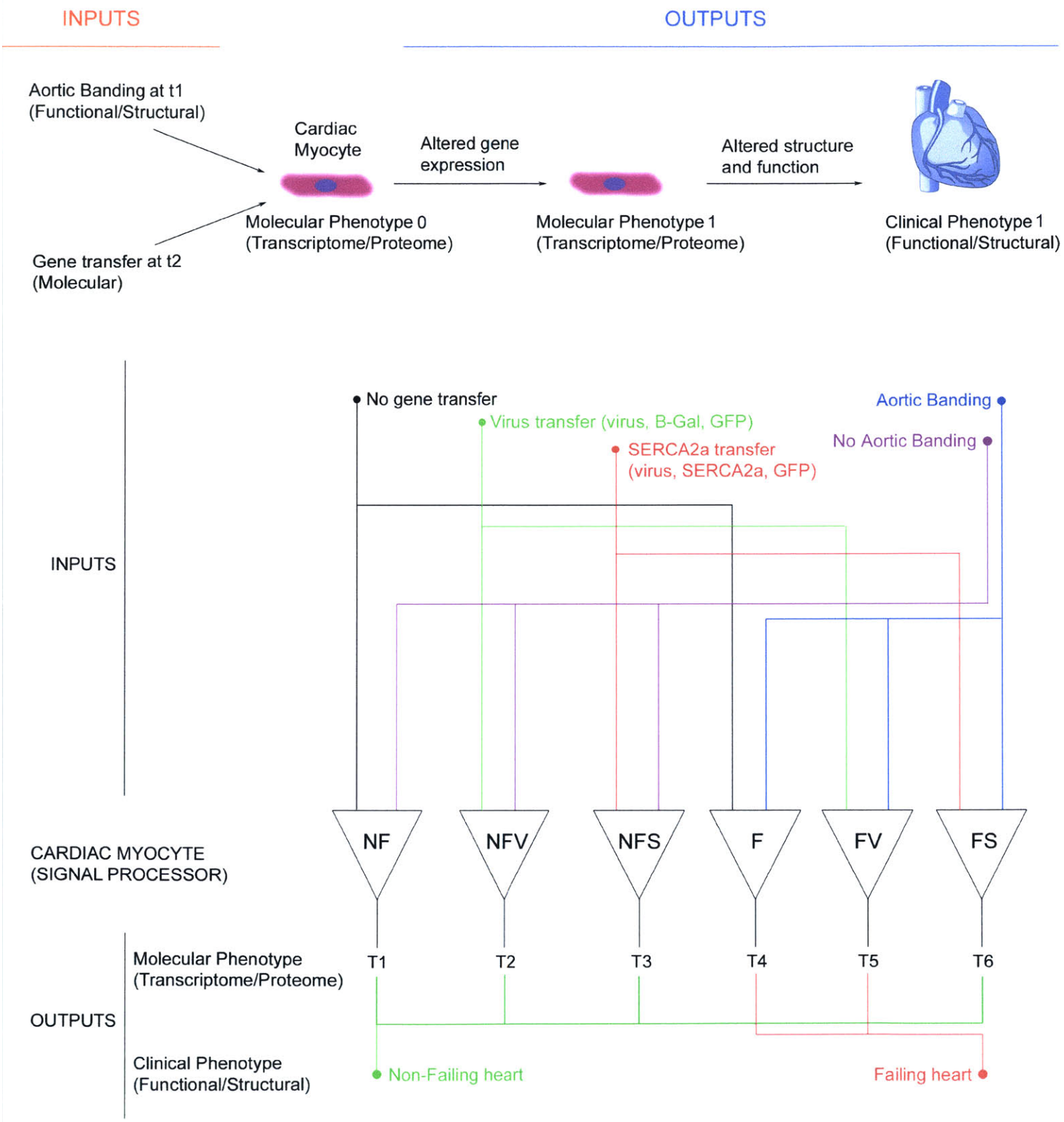
INPUTS
OUTPUTS
Aortic Banding at t1
(Functional/Structural)
Cardiac
Myocyte
Altered gene
expression
Altered structure
and function
Molecular Phenotype 0
(Transcriptome/Proteome)
Molecular Phenotype 1
(Transcriptome/Proteome)
Clinical Phenotype 1
(Functional/Structural)
Gene transfer at t2
(Molecular)
INPUTS
No gene transfer
Virus transfer (virus, B-Gal, GFP)
SERCA2a transfer
(virus, SERCA2a, GFP)
Aortic Banding
No Aortic Banding
CARDIAC MYOCYTE
(SIGNAL PROCESSOR)
NF
NFV
NFS
F
FV
FS
OUTPUTS
Molecular Phenotype
(Transcriptome/Proteome)
T1
T2
T3
T4
T5
T6
Clinical Phenotype
(Functional/Structural)
Non-Failing heart
Failing heart

Fig 2

Figure 2:
The heart cell is the signal processor in an input-output model of gene expression. This model forms the basis of gene expression analysis in this study. The cardiac myocyte is the signal processor that integrates the aortic banding input at time 1, and the gene transfer input at time 2. Notice how the two levels of input are reproduced in the two levels of output: A heart cell can change the expression of its genes and acquire a new molecular phenotype in response to external functional/structural signals (aortic banding) and to internal molecular signals (gene transfer). The new molecular phenotype at the level of the cell will translate into an altered structure and function at the level of the heart and cardiovascular system, and this new clinical phenotype can be assessed by echocardiography and other clinical parameters. The aortic banding input is transduced at the level of the cell into a molecular signal which is relayed to the nucleus where it alters gene expression. The clinical phenotype difference between the different samples is caused by an underlying molecular phenotype difference.

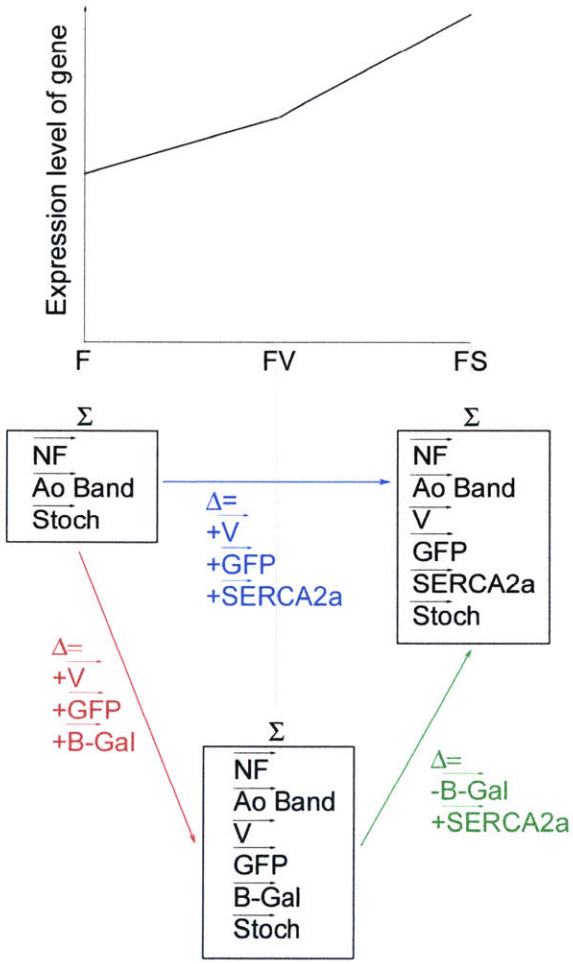
Expression level of gene
F
FV
FS
Σ
NF
Ao Band
Stoch
Δ=
+V
+GFP
+SERCA2a
Σ
NF
Ao Band
V
GFP
SERCA2a
Stoch
Δ=
+V
+GFP
+B-Gal
Σ
NF
Ao Band
V
GFP
B-Gal
Stoch
Δ=
-B-Gal
+SERCA2a

Fig 3

Figure 3:
Gene expression is regulated by combinatorial control. The transcriptional activity of a gene results from a competition between activators and repressors. Combinatorial control of gene expression can be modeled by a vectorial representation of an input-output system. Multiple inputs interact to control the expression of a gene in each experimental sample. The different inputs will lead to different combinations of signals that will affect the expression of a gene. The promoter of a gene will integrate activator and repressor signals from this combination of inputs, and then make a decision to turn a gene ON or OFF. Transcriptional activity is measured by mRNA abundance of a gene for that experimental sample. Shown in color are the inputs that account for differences in expression level of a gene between two experimental samples. The positive direction for vectors is the direction of increased gene expression.

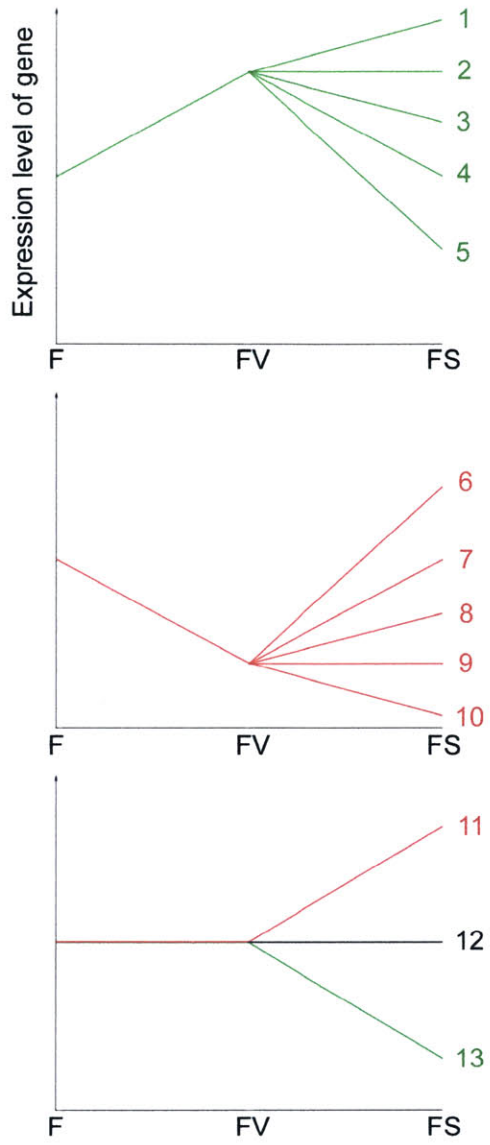
Expression level of gene
1
2
3
4
5
F
FV
FS
6
7
8
9
10
F
FV
FS
11
12
13
F
FV
FS

Fig 4

Figure 4:
The thirteen possible configurations for the relative expression level of a gene across the three experimental samples F, FV and FS. In order to know which genes were targets of SERCA2a, we analyzed the different configurations, and assigned to each the probability of being described by a gene which is a SERCA2a target. We found that a gene probably affected by SERCA2a is a gene where the expression level in FS is different from FV, *and* FS is different from F. Of those genes, a gene that fits configurations 11 and 13 has the highest probability of being a SERCA2a target; configurations 1, 10, 5, and 6 are high probability; configurations 3 and 8 are lower probability.

Solving for SERCA2a target genes: For each configuration, we wrote down all the possible solutions to the system of 3 equations with 4 unknowns. Then out of all possible solutions, we chose the most parsimonious solution. We illustrate this by solving configuration 1:

System of 3 equations with 4 unknowns:

$$[2]-[1]: \overrightarrow{V} + \overrightarrow{GFP} + \overrightarrow{BGal} = \overrightarrow{FV} - \overrightarrow{F}$$

$$[3]-[2]: \overrightarrow{SERCA} - \overrightarrow{BGal} = \overrightarrow{FS} - \overrightarrow{FV}$$

$$[3]-[1]: \overrightarrow{V} + \overrightarrow{GFP} + \overrightarrow{SERCA} = \overrightarrow{FS} - \overrightarrow{F}$$

For configuration 1, it corresponds to:

[2] - [1]: V + GFP + BGal > 0
[3] - [2]: SERCA - BGal > 0
[3] - [1]: V + GFP + SERCA > 0

All possible solutions to the system:
Solution 1:
V>0
SERCA>0

Solution 2:
GFP>0
SERCA>0

Solution 3:
BGal>0
SERCA>0
SERCA>BGal

Solution 4:
BGal<0
V>0
V>|BGal|

Solution 5:
BGal<0
GFP>0
GFP>|BGal|

Solution 6:
V>0
GFP>0
SERCA>0

Solution 7:
....

Solution n:
V>0
GFP>0
SERCA>0
BGal>0
SERCA>BGal

Out of all the possible solutions, the most parsimonious are solutions 1 and 2 (in solution 3 the magnitudes of the vectors are important, which is not the case in solutions 1 and 2):
Parsimony Solution 1 (PS1): SERCA2a>0 and V>0
PS2: SERCA2a>0 and GFP>0

Analysis of each individual configuration:

Configuration 1:
PS1: SERCA2a>0 and V>0
PS2: SERCA2a>0 and GFP>0
Mixed virus/SERCA effect.
Virus effect present, SERCA effect is present.
Molecular-Clinical Correlation (MCC): double correlation (F to FS and FV to FS).
High probability of being a SERCA2a target.
Will be considered as a potential SERCA2a target.

Configuration 2:
PS1: V>0
PS2: GFP>0
Pure virus effect.
No SERCA effect.
MCC: single correlation.
Probability of being a SERCA2a target ~ 0.
Will not be considered.

Configuration 3:
PS1: V>0 and B-Gal>0
PS2: GFP>0 and B-Gal>0
PS3: SERCA2a>0, B-Gal>0, SERCA2a<B-Gal
PS4: SERCA2a<0, V>0, V>SERCA2a
PS5: SERCA<0, GFP>0, GFP>SERCA2a
Pure Virus effect, or Pure SERCA2a effect, or Mixed virus/SERCA effect.
MCC: double correlation.
Lower probability of being a SERCA2a target.
Will be considered.
(Special case: The solution that includes SERCA2a respects the least number of causes condition, but has one more constraint. It is tolerated however, at the price of a lower probability score, because of a double molecular/clinical correlation, and we assume that the clinical difference is caused by SERCA2a).

Configuration 4:
PS: B-Gal>0
No SERCA2a effect.
MCC: single correlation.
Probability of being a SERCA2a target ~ 0.
Will not be considered.

Configuration 5:
PS: B-Gal>0, SERCA2a<0
Probably a pure SERCA2a effect
MCC: double correlation.
High Probability of being a SERCA2a target.
Will be considered.

Configuration 11:
PS: SERCA2a>0
No virus effect.
Pure serca effect.
MCC: Corresponds to clinical phenotype in the 3 conditions perfectly.
Highest probability of being a SERCA2a target.
Will be considered.

Configuration 12:
PS: V = GFP = B-Gal = SERCA2a = 0
No serca effect.
No virus effect.
MCC: single correlation.
Probability of being a SERCA2a target ~ 0.
Will not be considered.

And the mirror images of these individual cases.

By virus effect we mean any difference in expression level between FS and F, due to SERCA2a construct components distinct from SERCA2a: adenoviral genes, or GFP.

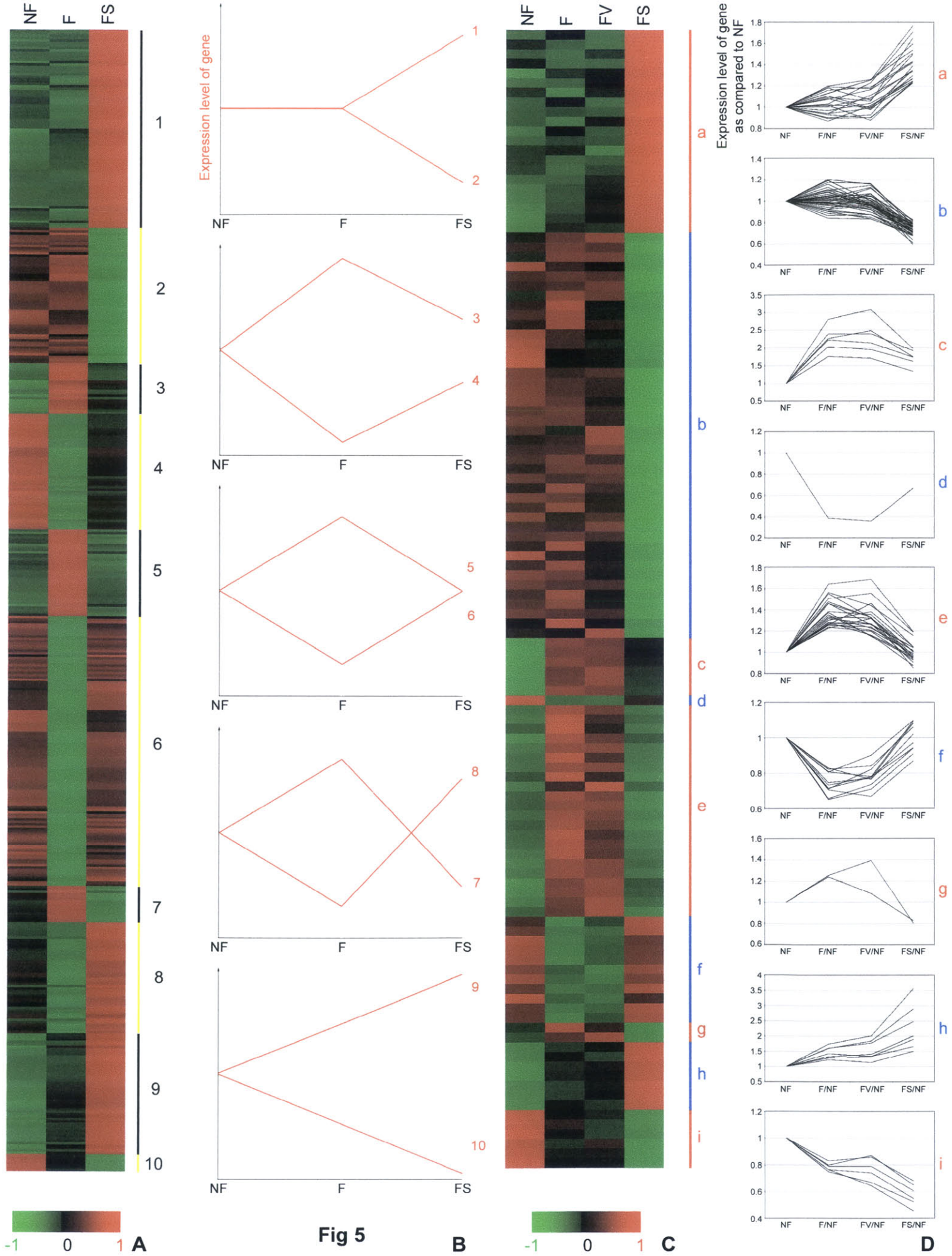
NF
F
FS
1
2
3
4
5
6
7
8
9
10
-1
0
1
A
Expression level of gene
NF
F
FS
B
FV
a
b
c
d
e
f
g
h
i
Expression level of gene as compared to NF
F/NF
FV/NF
FS/NF
C
D

Fig 5

Figure 5:
Transcriptional profiling of SERCA2a targets defines ten categories of responses against aortic banding. Depicted in (A) is a hierarchical clustering analysis of gene expression data from the 473 gene targets of SERCA2a. Each row represents a separate transcript on the microarray and each column a separate mRNA sample. Each small red bar indicates that the given gene in the given sample is expressed at a level higher than the mean across all samples. Each small green bar indicates a less-than-average expression level, and each black bar denotes an expression level that is close to the mean. The color intensity represents the magnitude of the deviation from the mean (10), and is depicted according to the color scale shown at the bottom. (B) shows the 10 possible transcriptional profiles for SERCA2a target genes. The 473 genes were first clustered by our algorithm according to the profiles in (B) before they were submitted to a hierarchical clustering algorithm for visualization (A). (C), Hierarchical clustering was applied to a 118 gene subgroup of the 473 genes in (A), selected because they had the highest probability of being targets of SERCA2a. In another visual representation of the results for this subclass of genes (D), the use of a common reference microarray (NF) allows the comparison of the relative expression level of each gene across all the experimental samples. Notice the plateau between the samples F and FV indicative of a pure SERCA2a effect accounting for the gene expression level in FS.

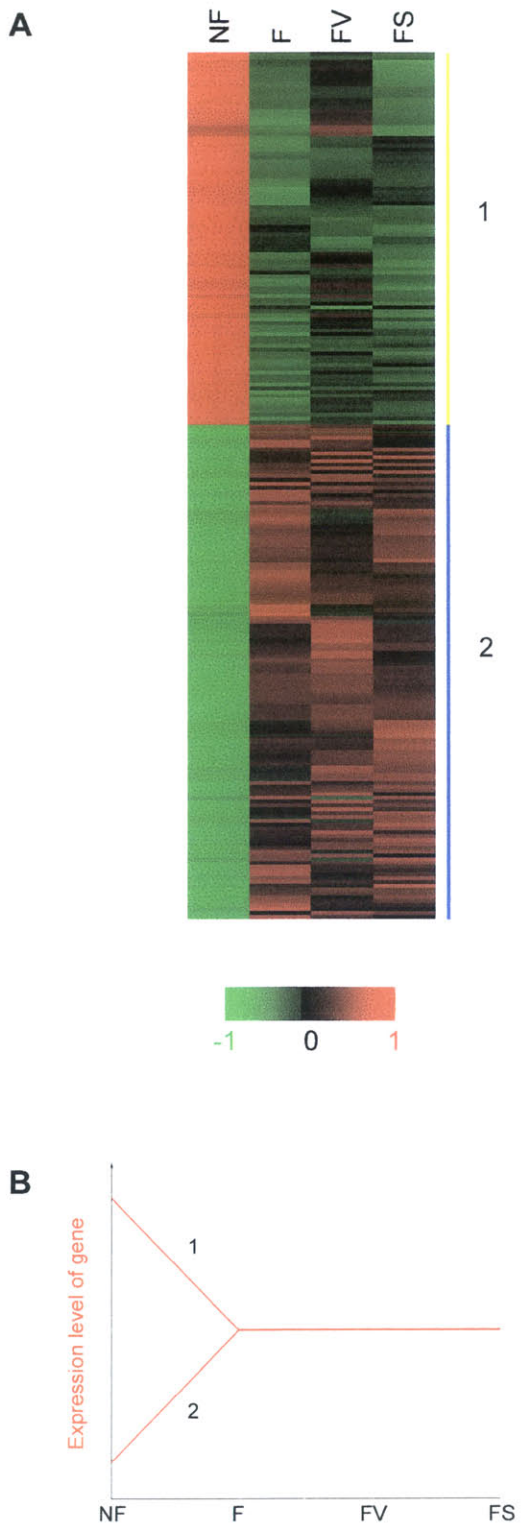

Fig 6

Figure 6:
There are natural adaptive responses to aortic banding that are needed for clinical non-failure. Depicted in (A) is a hierarchical clustering analysis of gene expression data from the 226 genes that encode natural adaptive responses to aortic banding needed for clinical non-failure. (B) shows the 2 possible transcriptional profiles for such genes. The 226 genes were first clustered by our algorithm according to the profiles in (B) before they were submitted to a hierarchical clustering algorithm for visualization (A). Notice how the transcriptional states change from absence to presence of the aortic banding insult (NF to F), and how they are sustained in the presence of aortic banding (F, FV, FS), pointing to their crucial/important compensatory role. These genes are not affected by SERCA2a, yet they are essential for non-failure.

Figures 7-13:
Distribution of genes by functional category. The genes are classified according to biological function from information available in public databases (NCBI EntrezGene; and NCBI UniGene, an EST database). Multiple comparisons are performed to expose important functional patterns underlying the genetic reprogramming that takes place to reverse heart failure. Some genes belong to more than one functional category, therefore percentages may not add up to 100%. All genes under category Ca2+/Calmodulin signaling are part of the higher category Ca2+ binding/Ca2+ signaling. In addition, all genes under metabolism/energy: lipids, metabolism/energy: carbohydrates, and metabolism/energy: proteins, belong to the same higher category metabolism/energy. More than 90% in the "unclassified" category are unknown, i.e. they are transcripts that do not match a gene of known function. Less than 10% of the "unclassified" transcripts have a known function but do not belong to any of the listed categories. ECM= Extracellular matrix.

Figure 7:
Distribution of genes by functional category: Figure 5 vs Figure 6

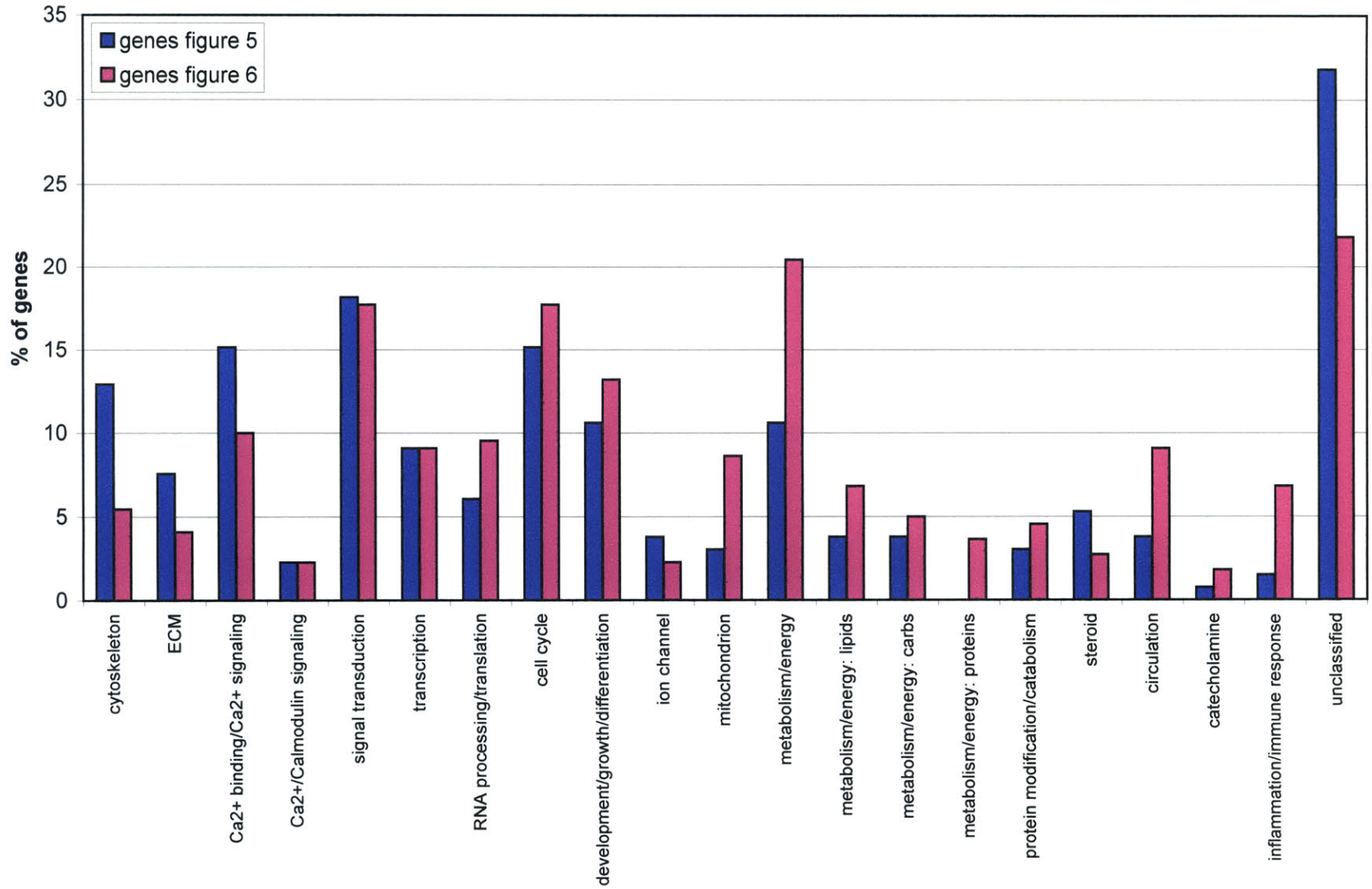

Figure 8 A:
Distribution of genes by functional category: Genes upregulated from NF to F, in Figure 5 vs Figure 6

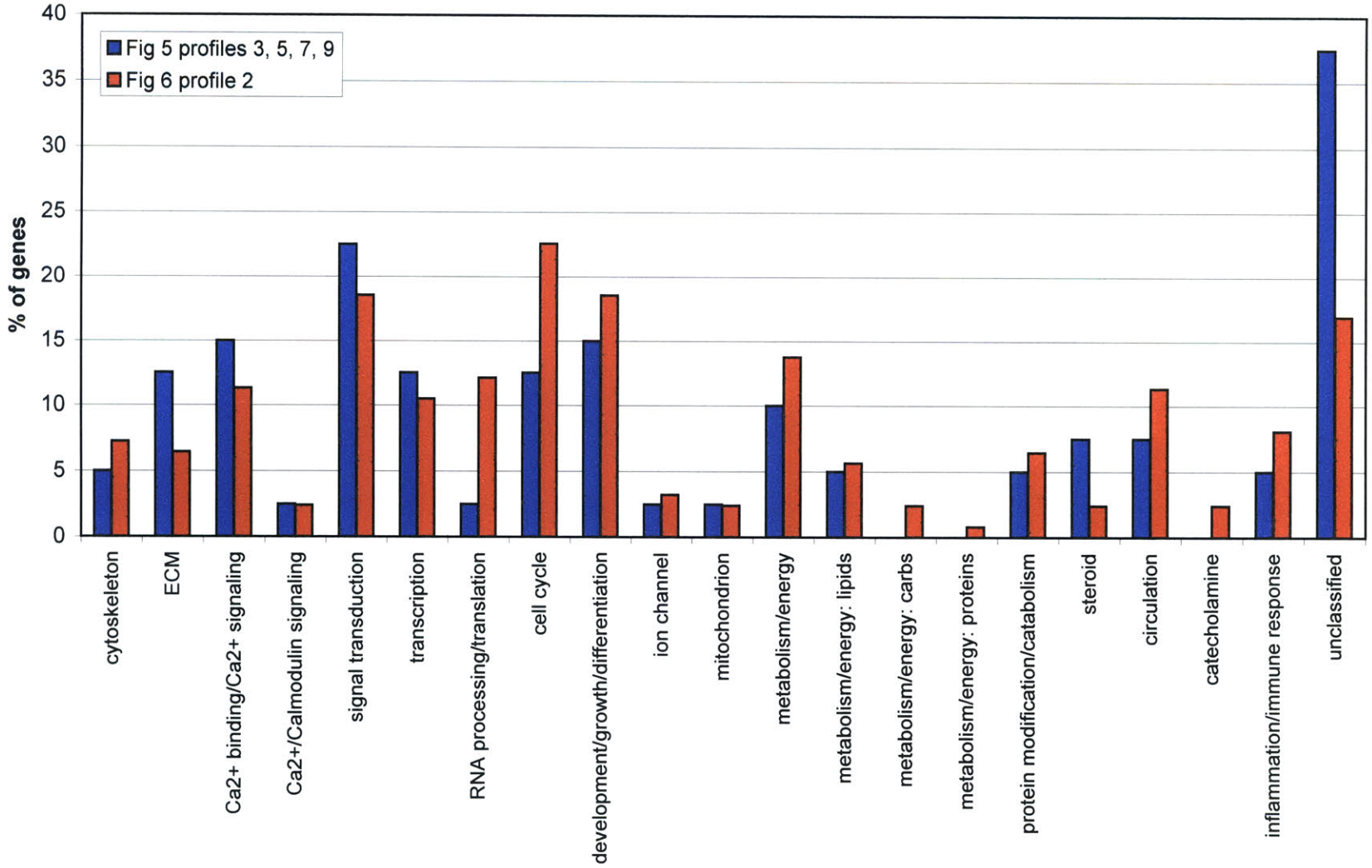

Figure 8 B:
Distribution of genes by functional category: Genes downregulated from NF to F, in Figure 5 vs Figure 6

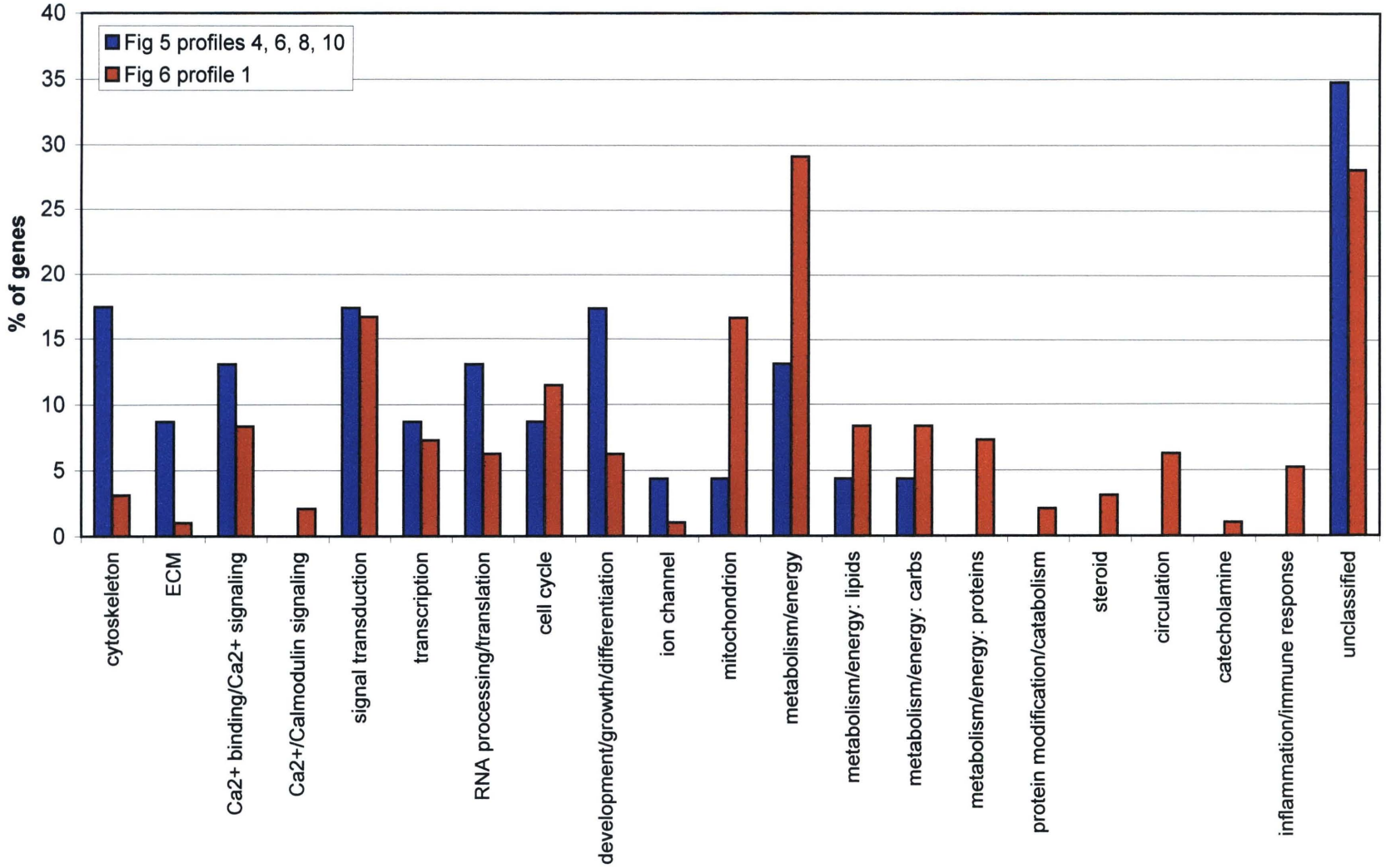

Figure 9 A:
Distribution of genes by functional category: Genes upregulated from F to FS in Figure 5, vs upregulated from NF to F in Figure 6

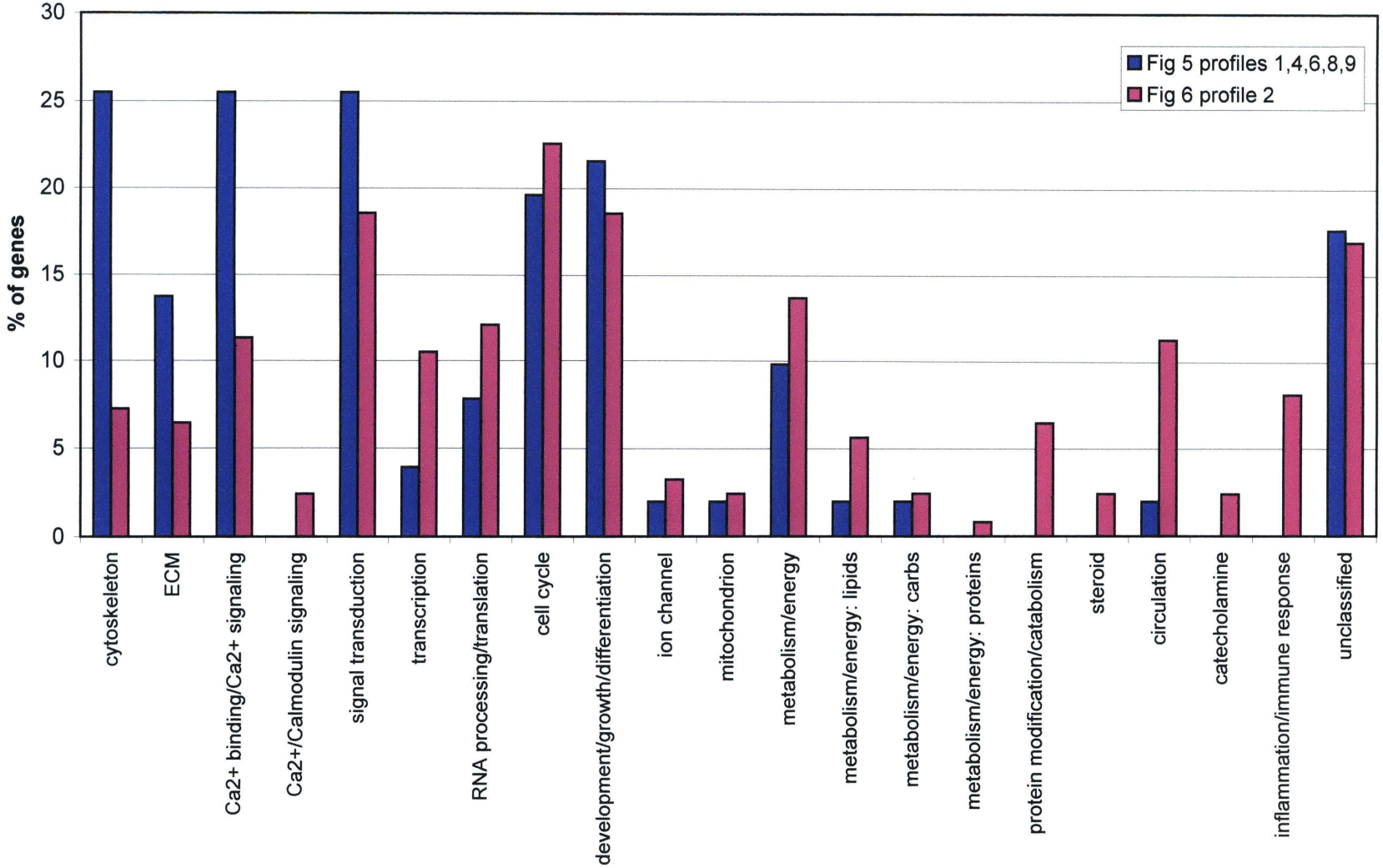

Figure 9 B:
Distribution of genes by functional category: Genes downregulated from F to FS in Figure 5, vs downregulated from NF to F in Figure 6

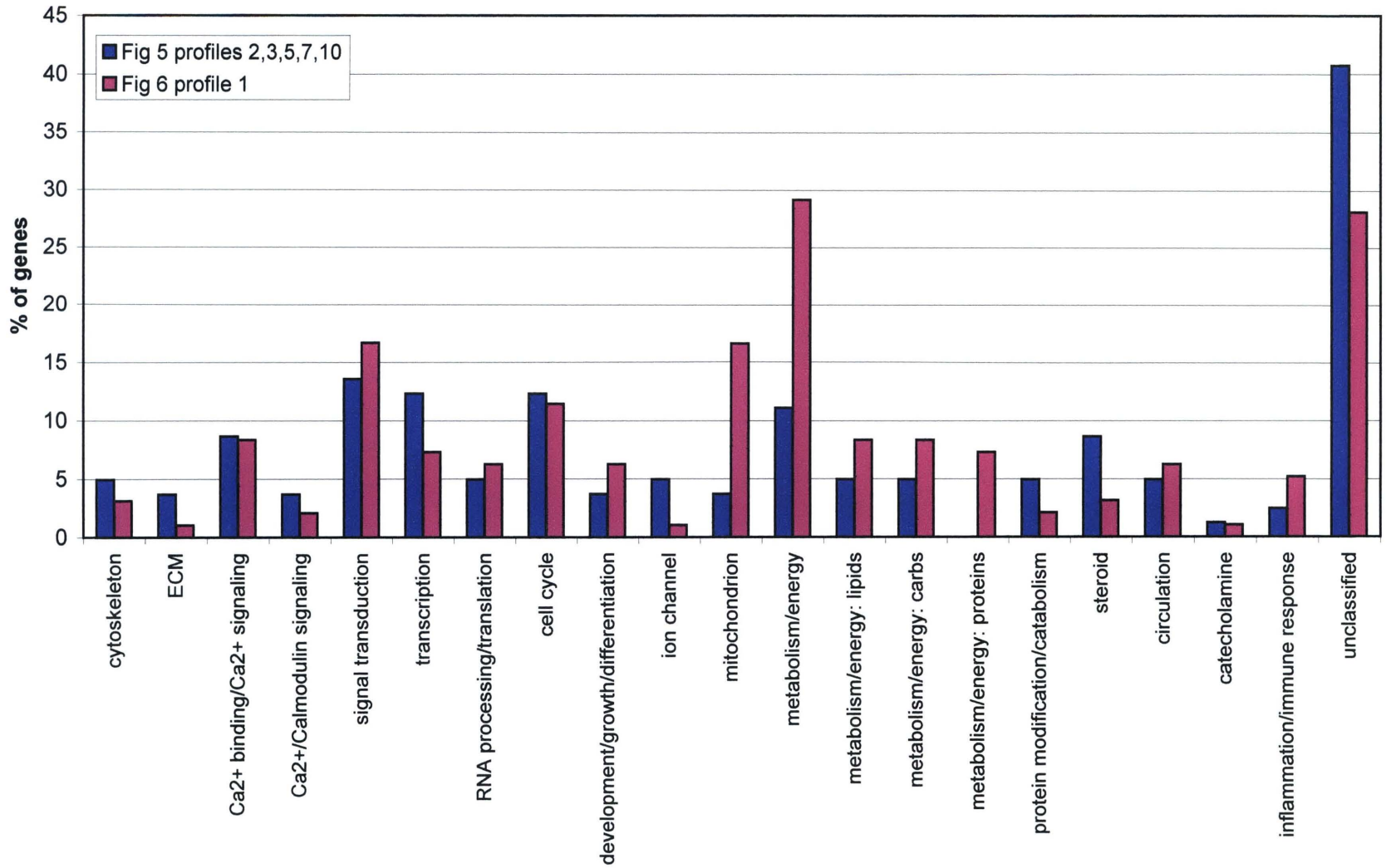

Figure 10:
Distribution of genes by functional category: upregulated vs downregulated Genes from F to FS in Figure 5

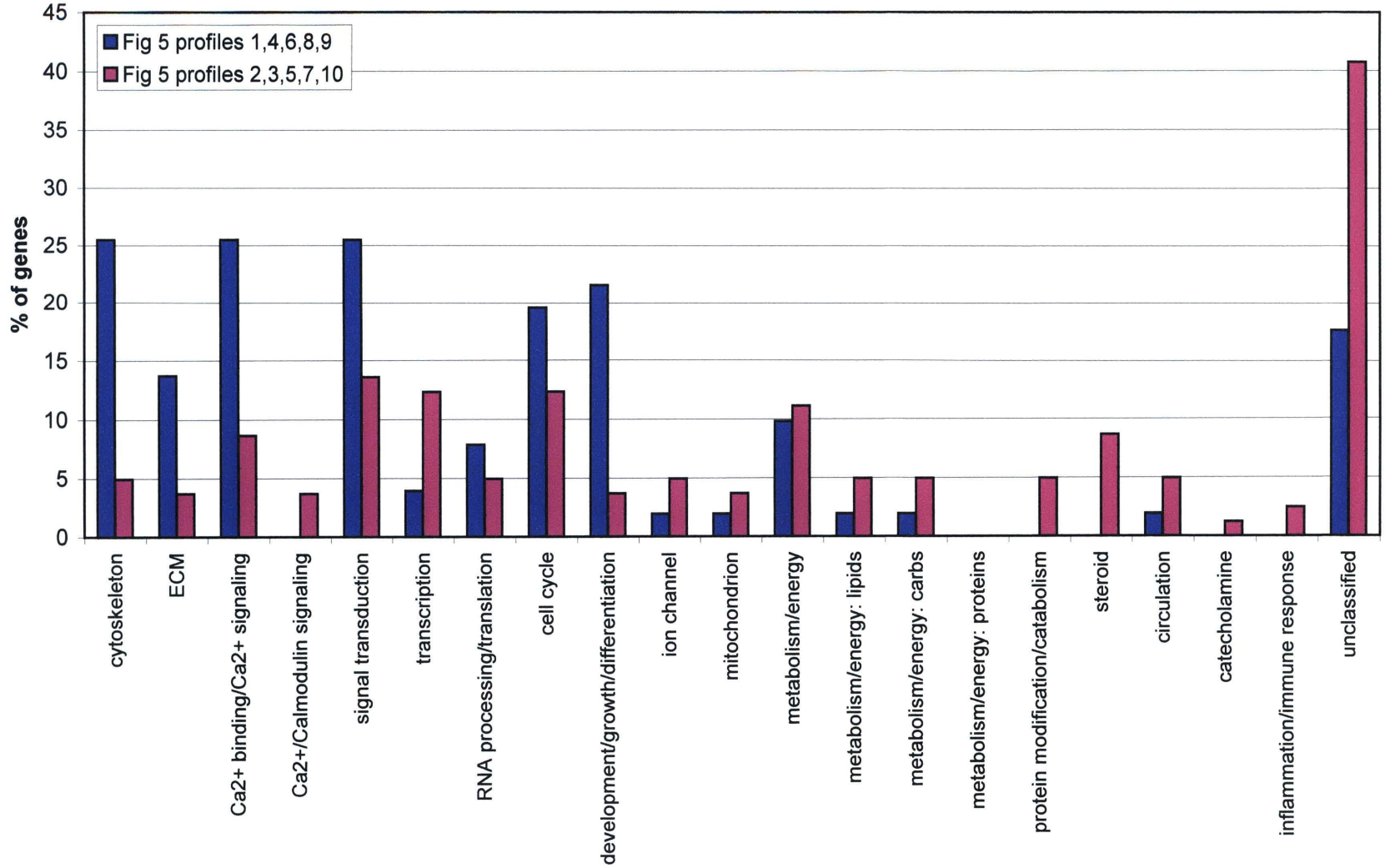

Figure 11 A:
Distribution of genes by functional category: Figure 5, profile 1 vs 2

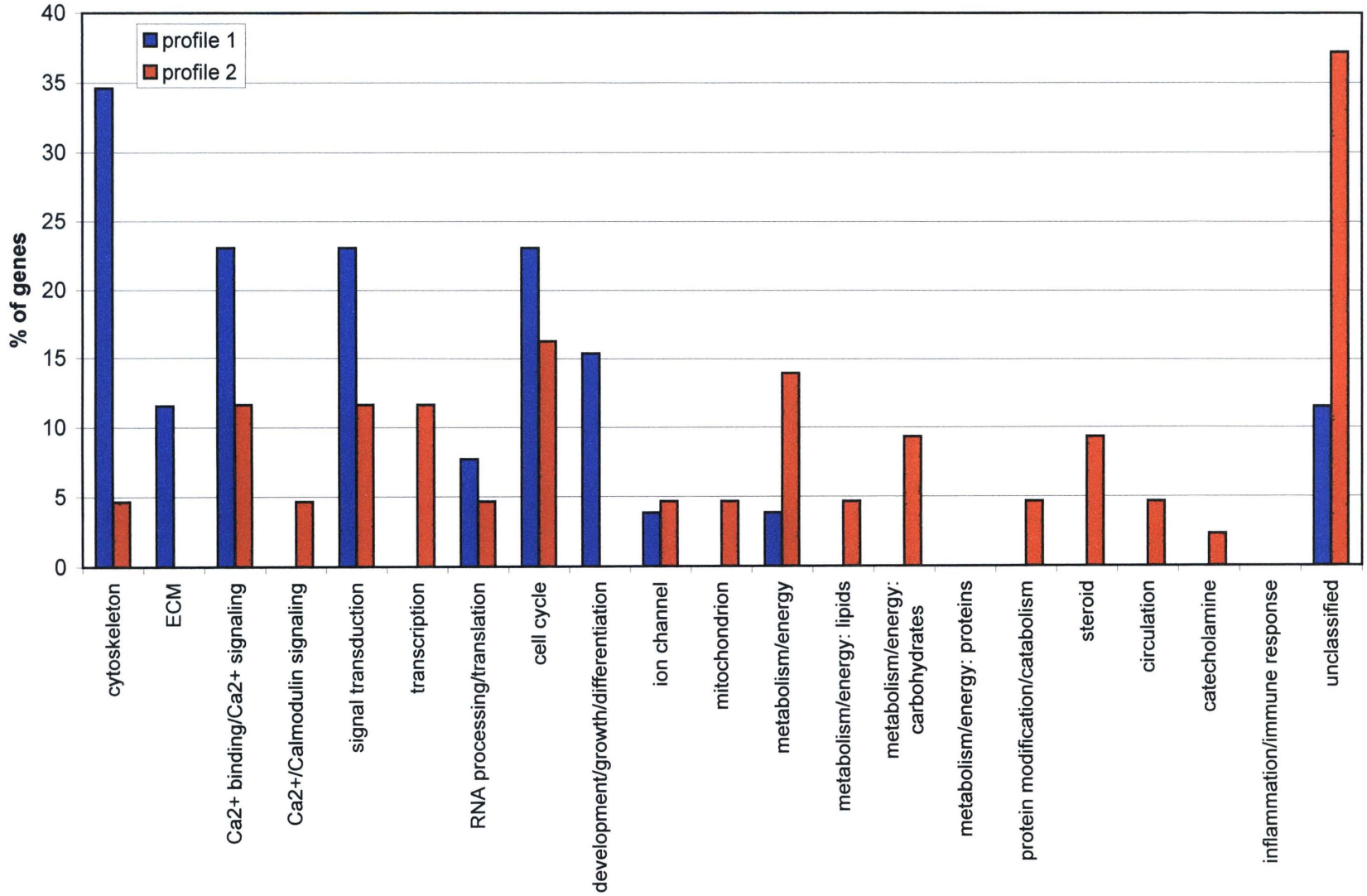

Figure 11 B:
Distribution of genes by functional category: Figure 5, profile 3 vs 4

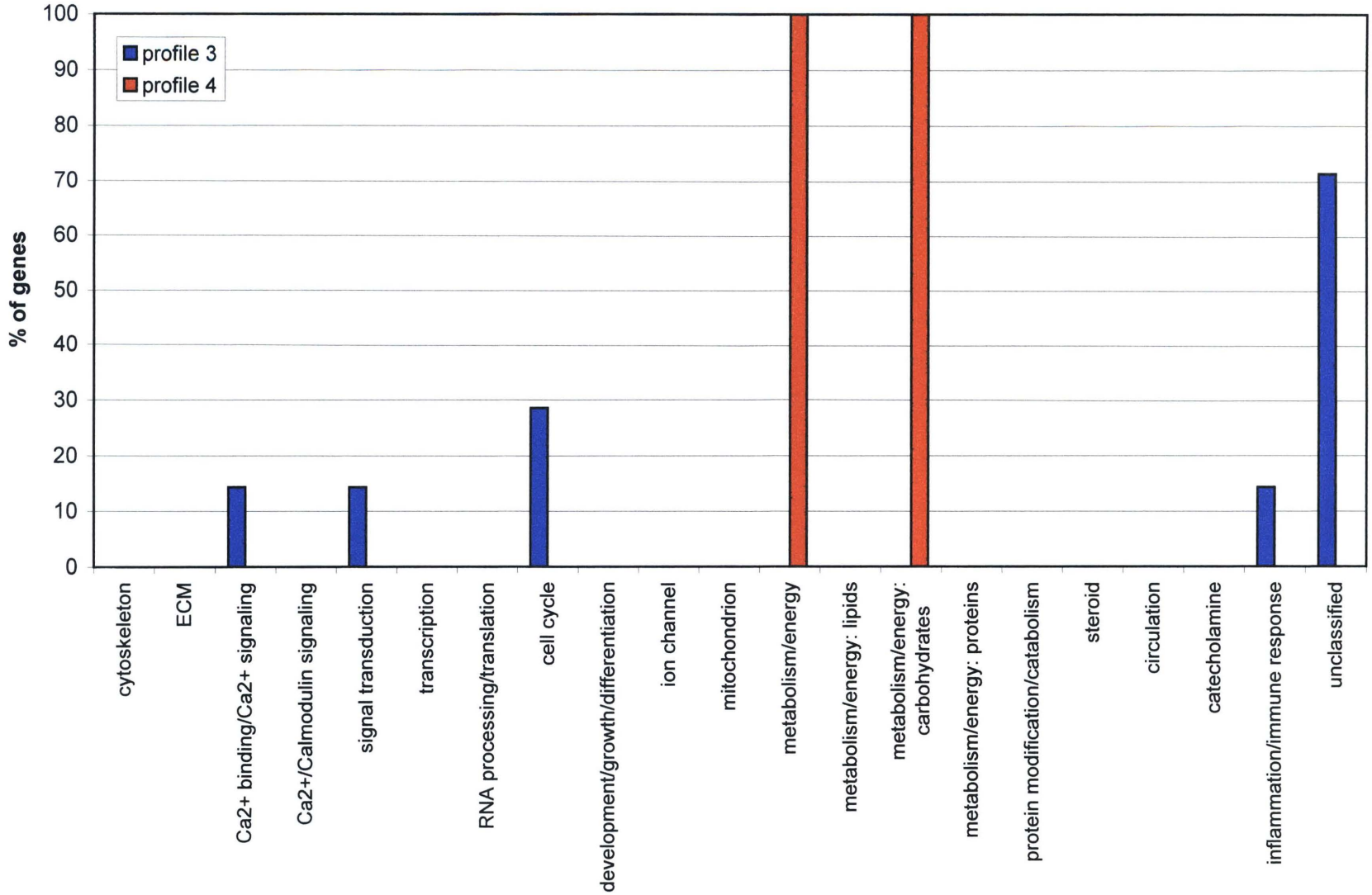

Figure 11 C:
Distribution of genes by functional category: Figure 5, profile 5 vs 6

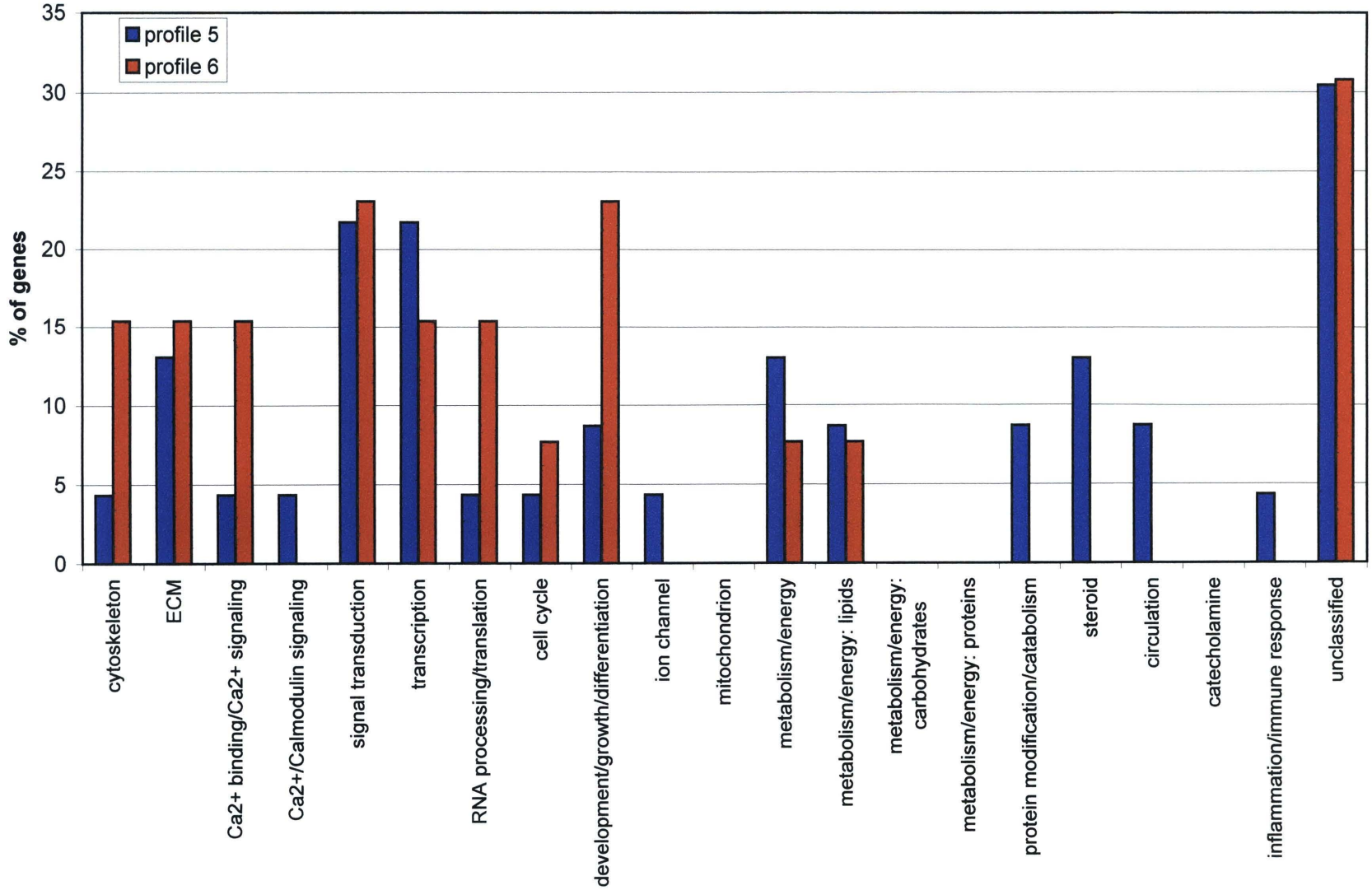

Figure 11 D:
Distribution of genes by functional category: Figure 5, profile 7 vs 8

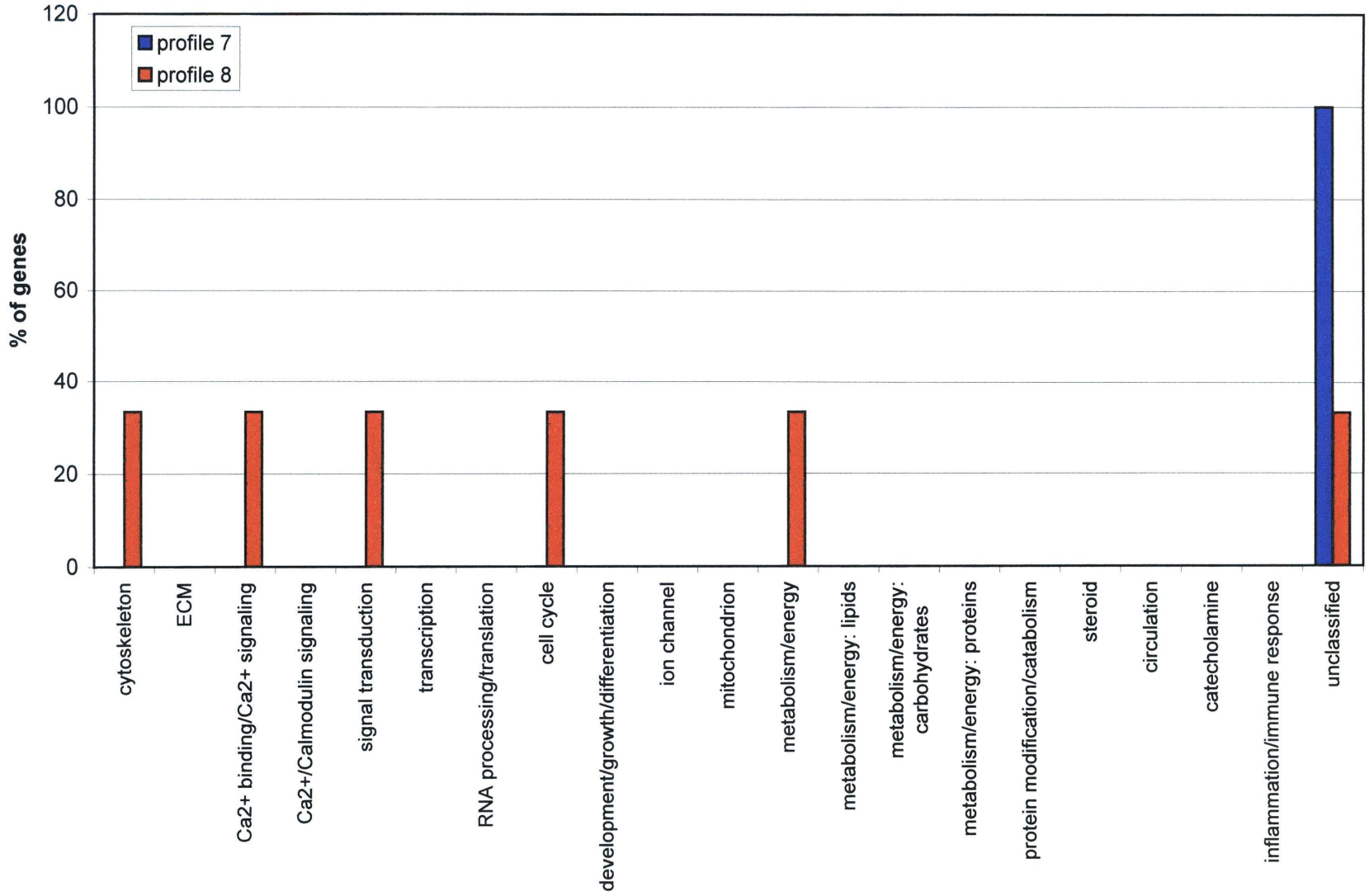

Figure 11 E:
Distribution of genes by functional category: Figure 5, profile 9 vs 10

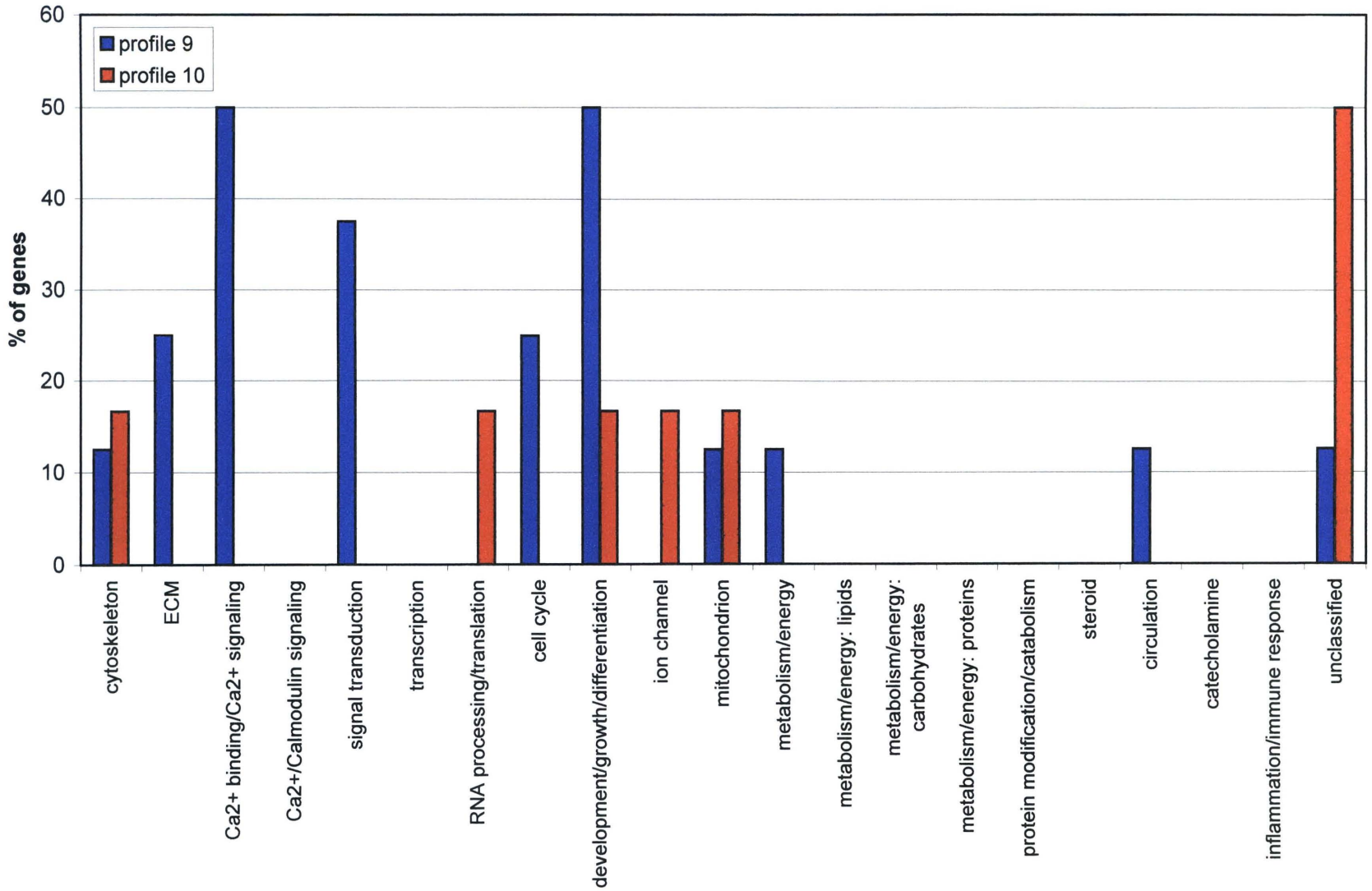

Figure 12:
Distribution of genes by functional category: Figure 6, profile 1 vs 2

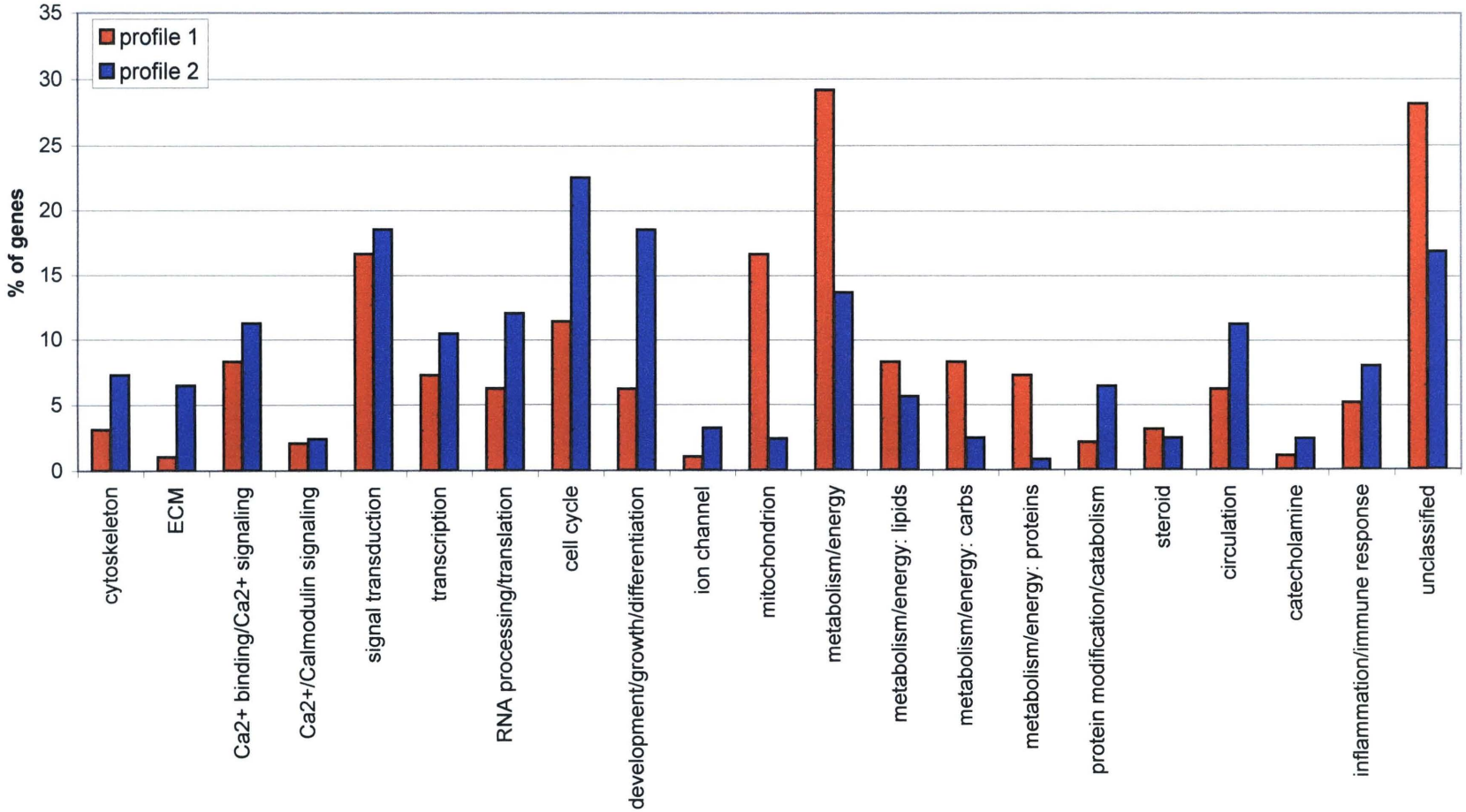

Figure 13 A:
Distribution of genes by functional category: Figure 5, profiles 1 and 2 vs 3 and 4, vs 5 and 6, vs 7 and 8, vs 9 and 10

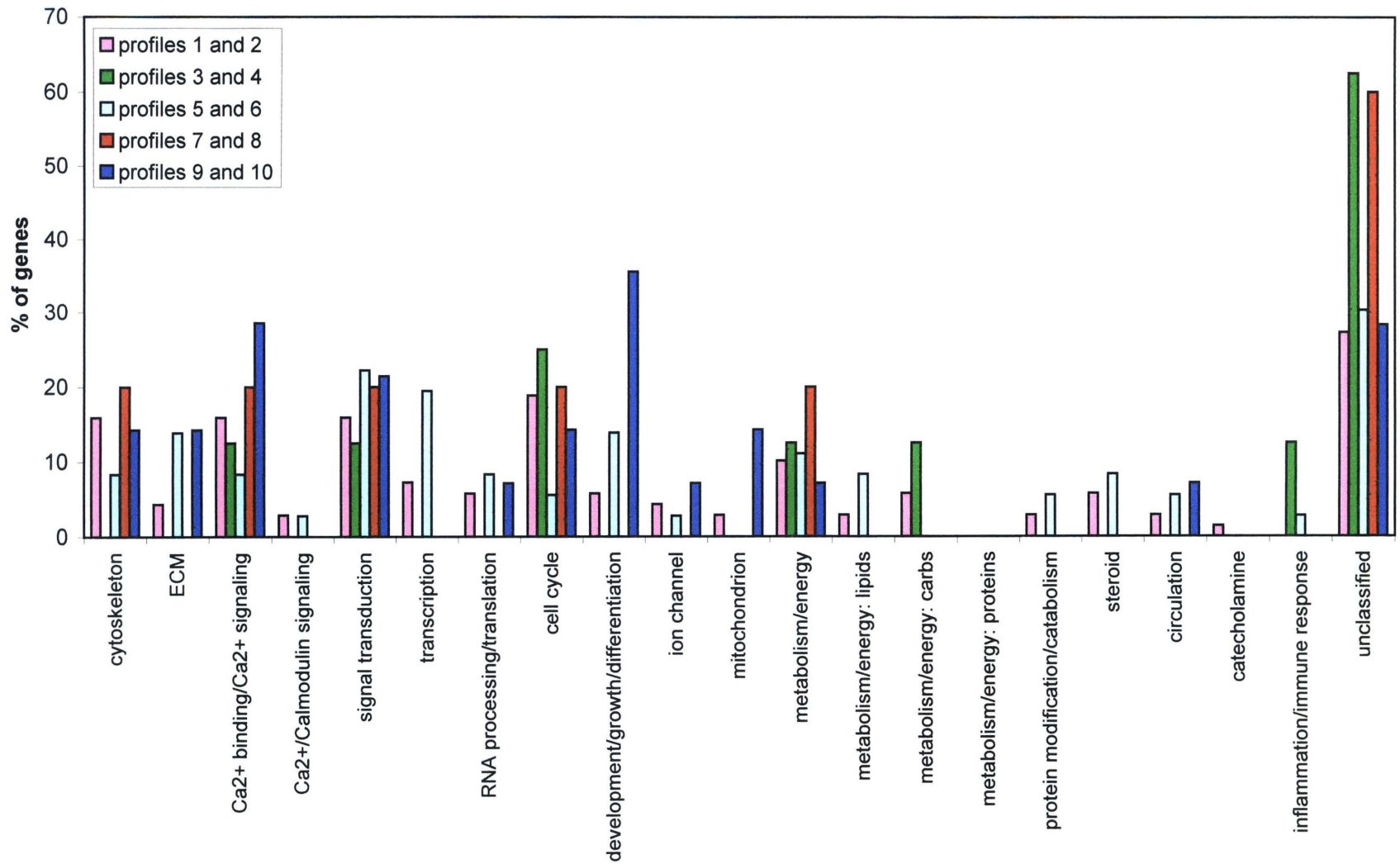

Figure 13 B:
Distribution of genes by functional category: Figure 5, profiles 1 and 2

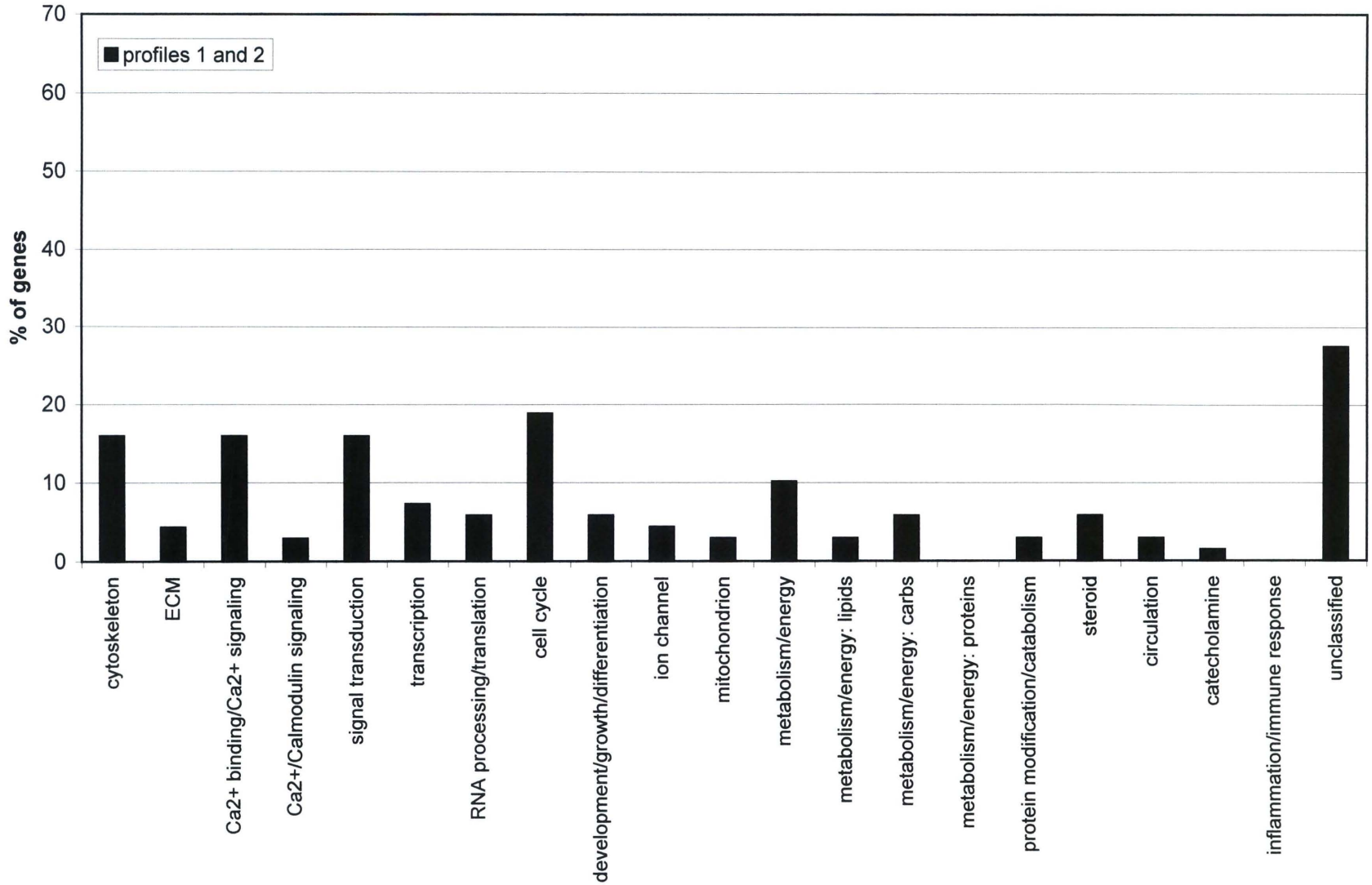

Figure 13 C:
Distribution of genes by functional category: Figure 5, profiles 3 and 4

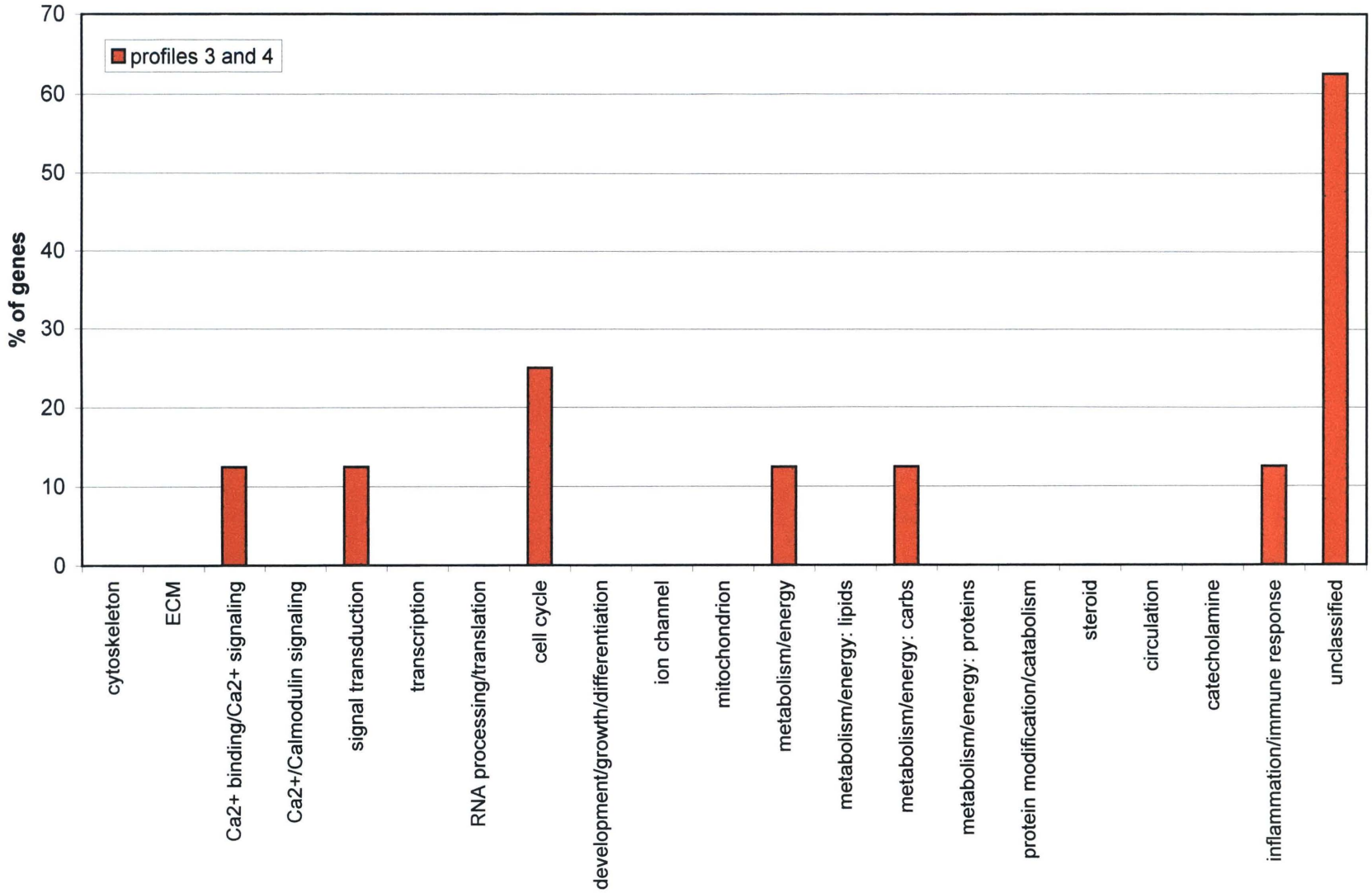

Figure 13 D:
Distribution of genes by functional category: Figure 5, profiles 5 and 6

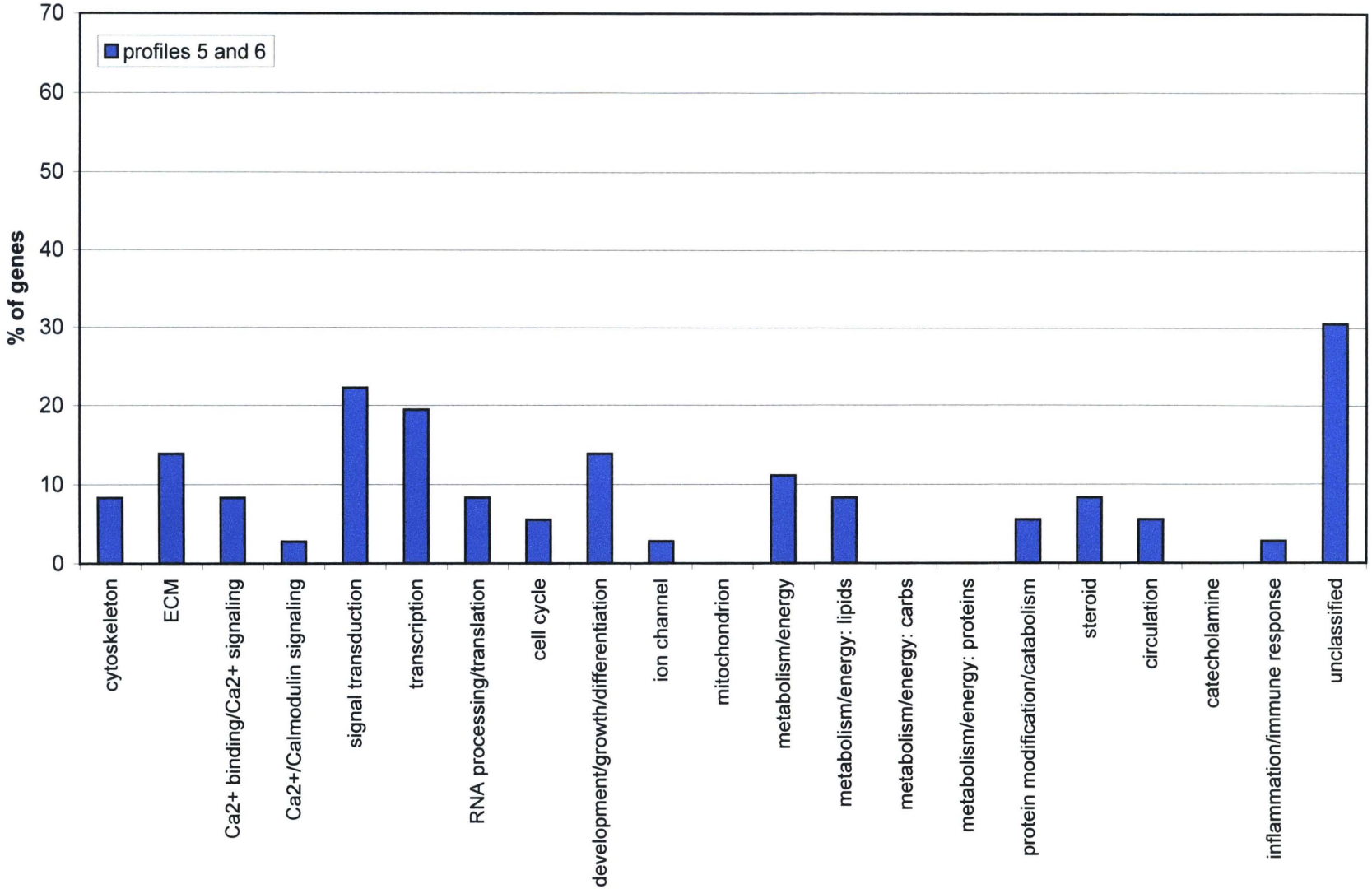

Figure 13 E:
Distribution of genes by functional category: Figure 5, profiles 7 and 8

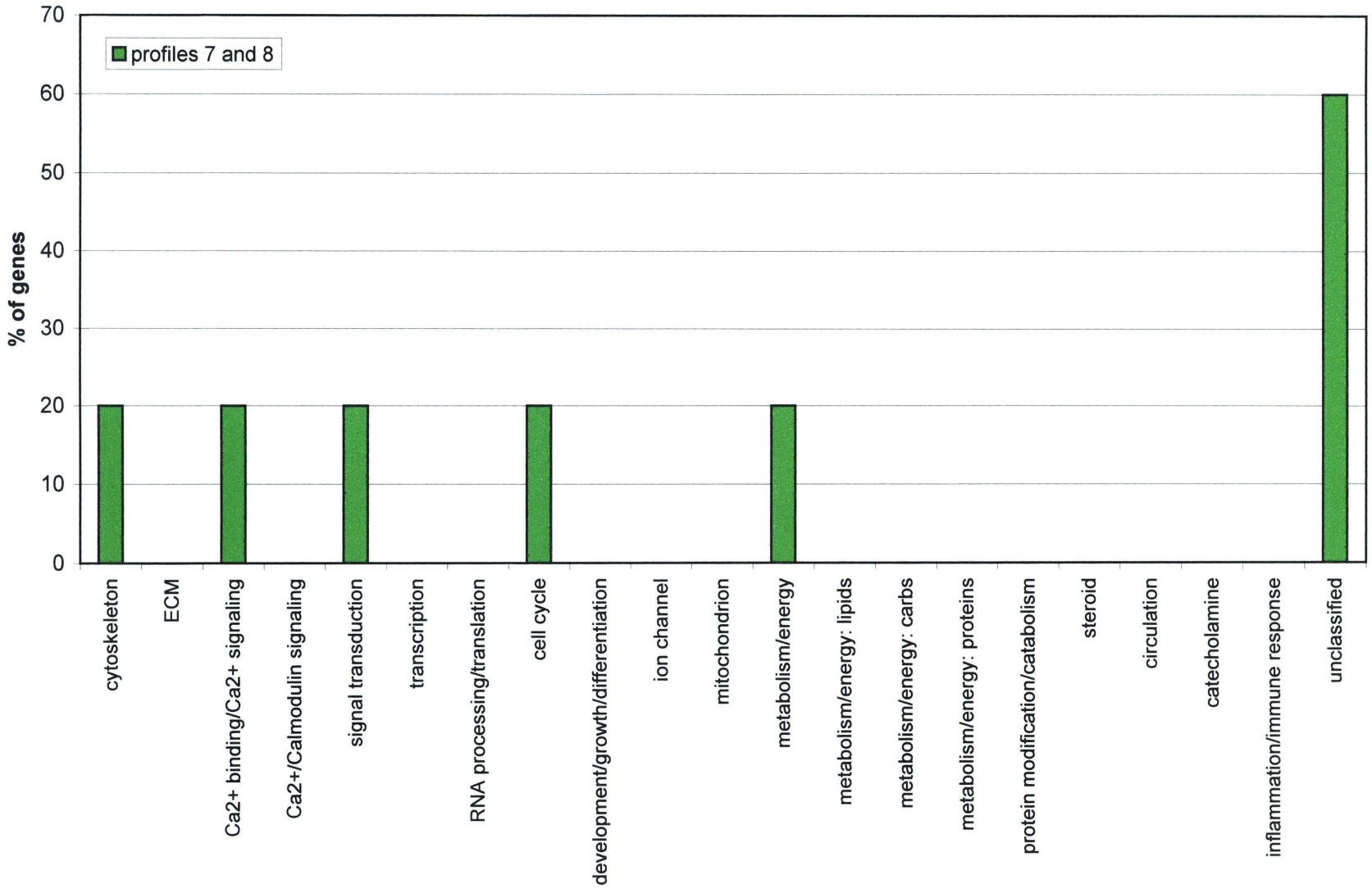

figure 13 F:
Distribution of genes by functional category: Figure 5, profiles 9 and 10

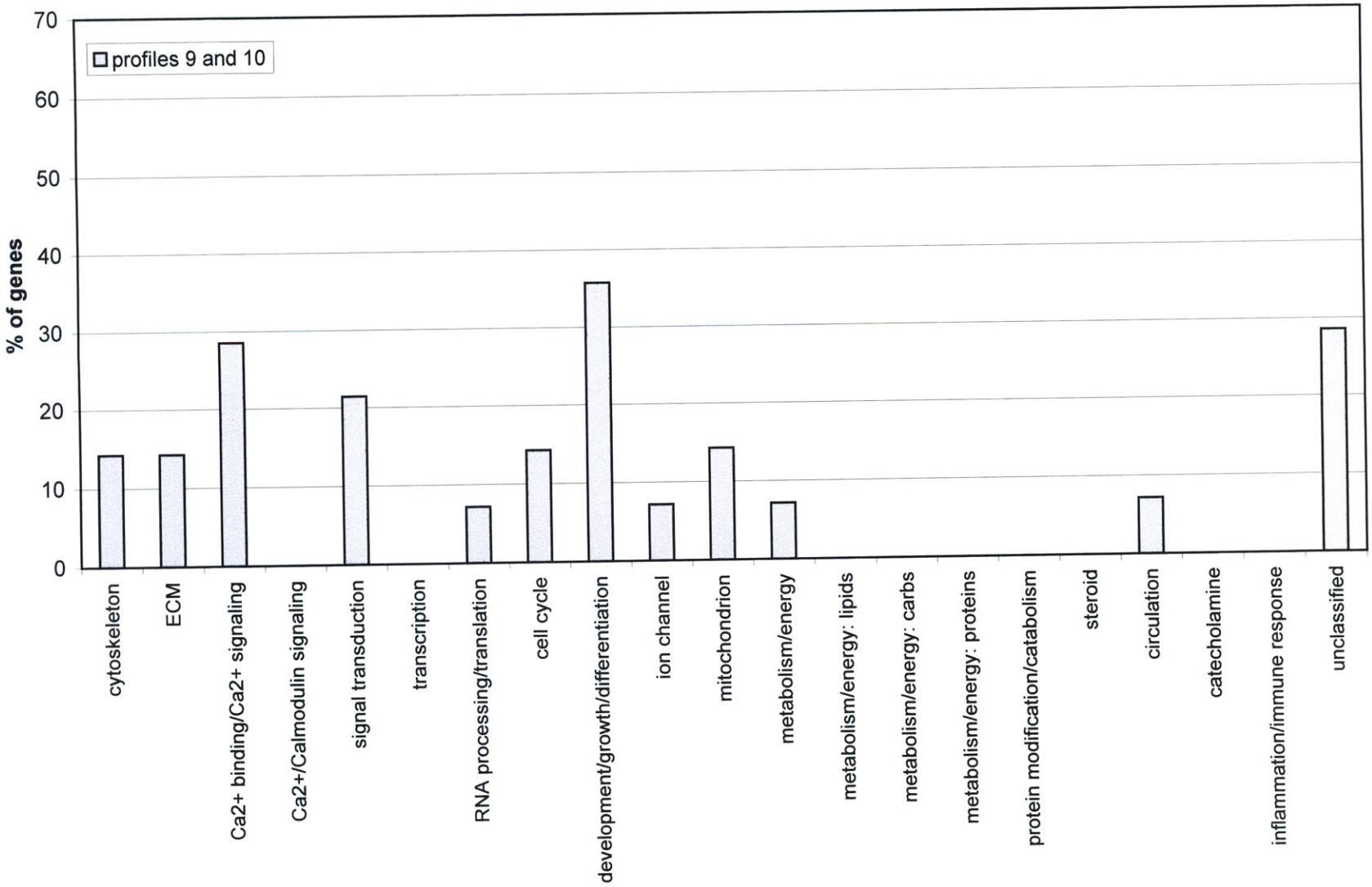

Figure 14:
Quantitative Reverse transcriptase PCR (QRT-PCR) validates microarray data.
Gene expression levels obtained from QRT-PCR experiments track the changes recorded in the microarray experiments, thus validating the microarray results.

Figure 14 A:
beta-Enolase: QRT-PCR validates microarray data

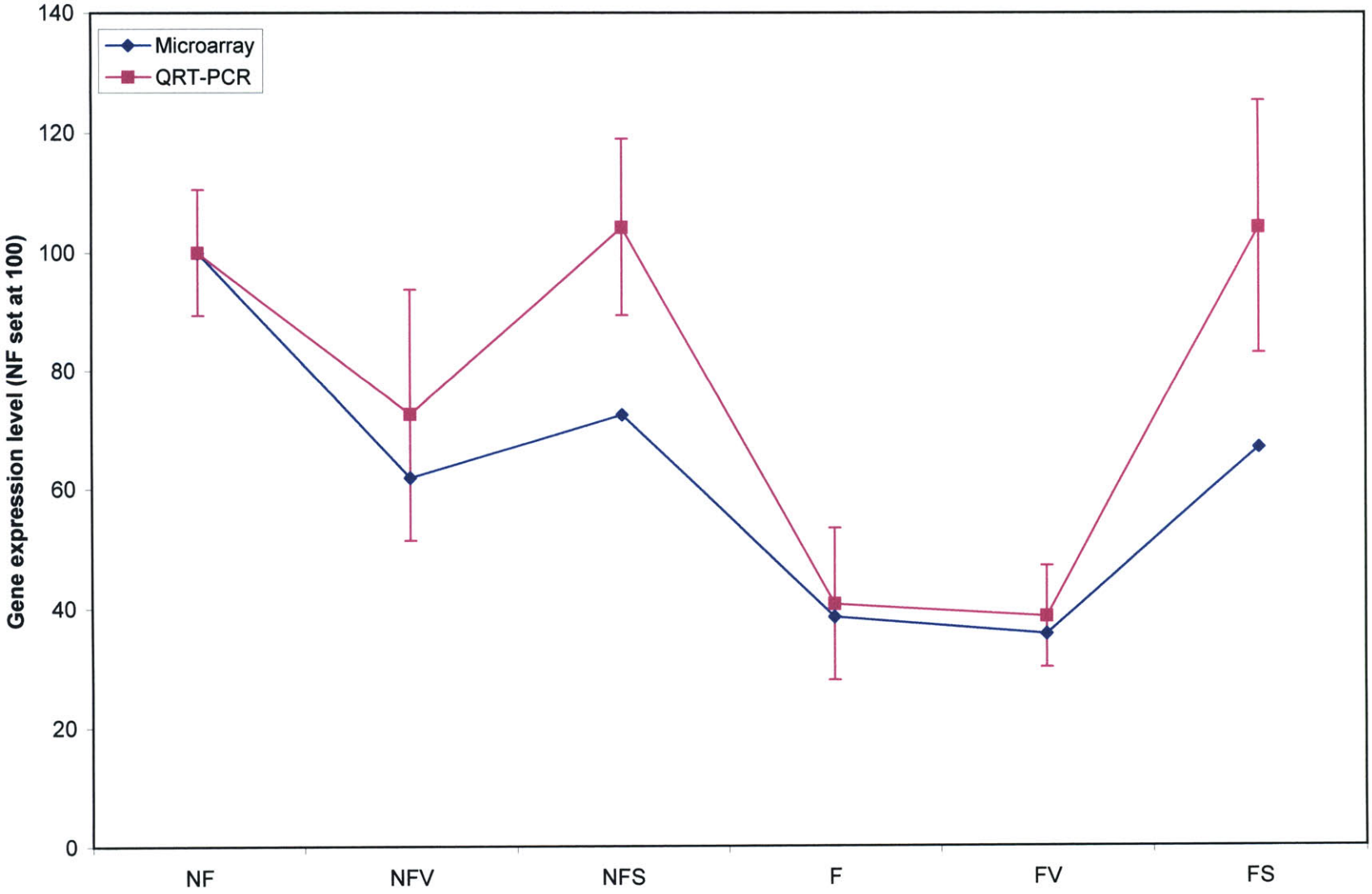

Figure 14 B:
Na channel: QRT-PCR validates microarray data

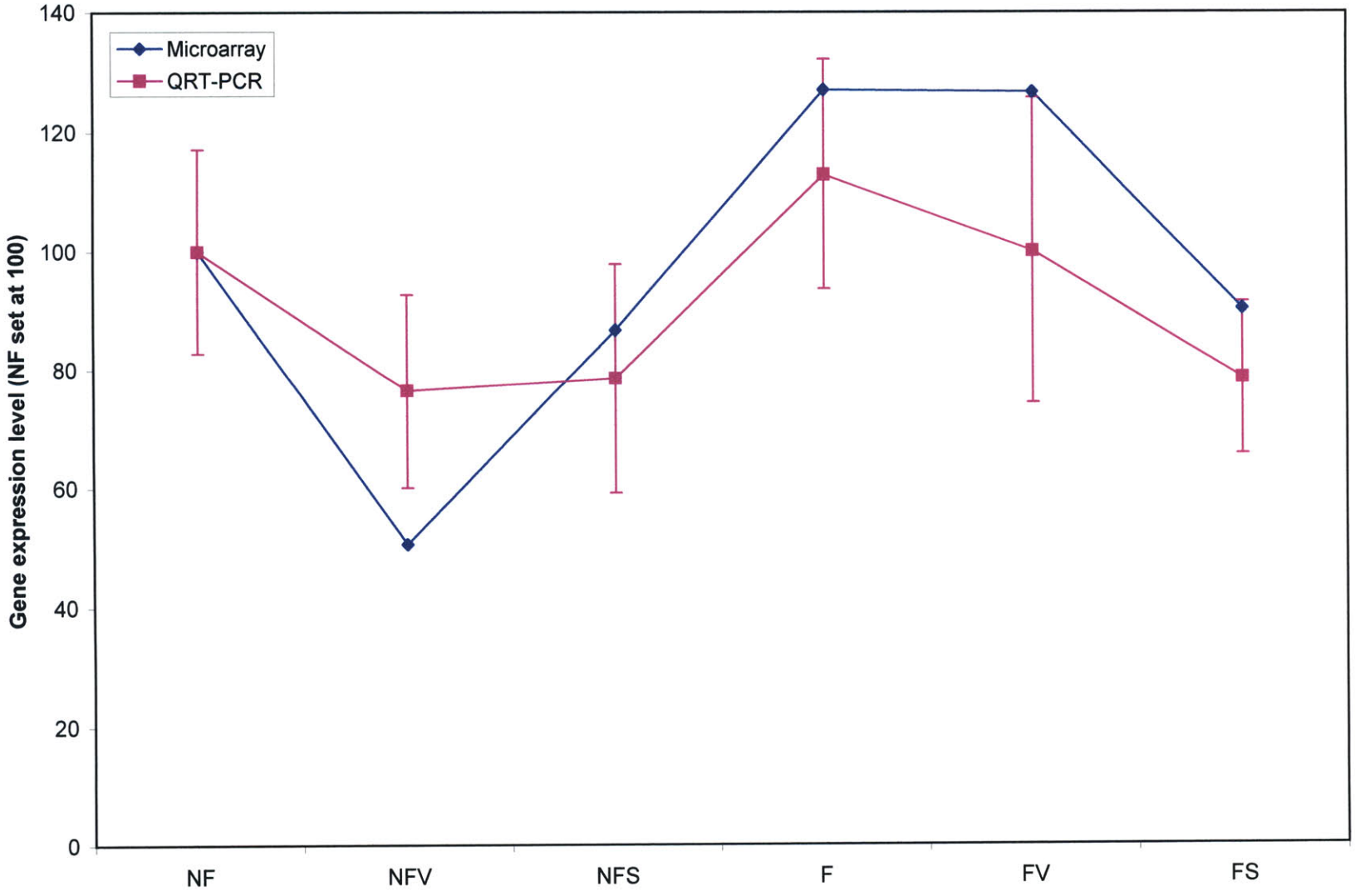

Figure 14 C:
Atrial Myosin Light Chain 1: QRT-PCR validates microarray data

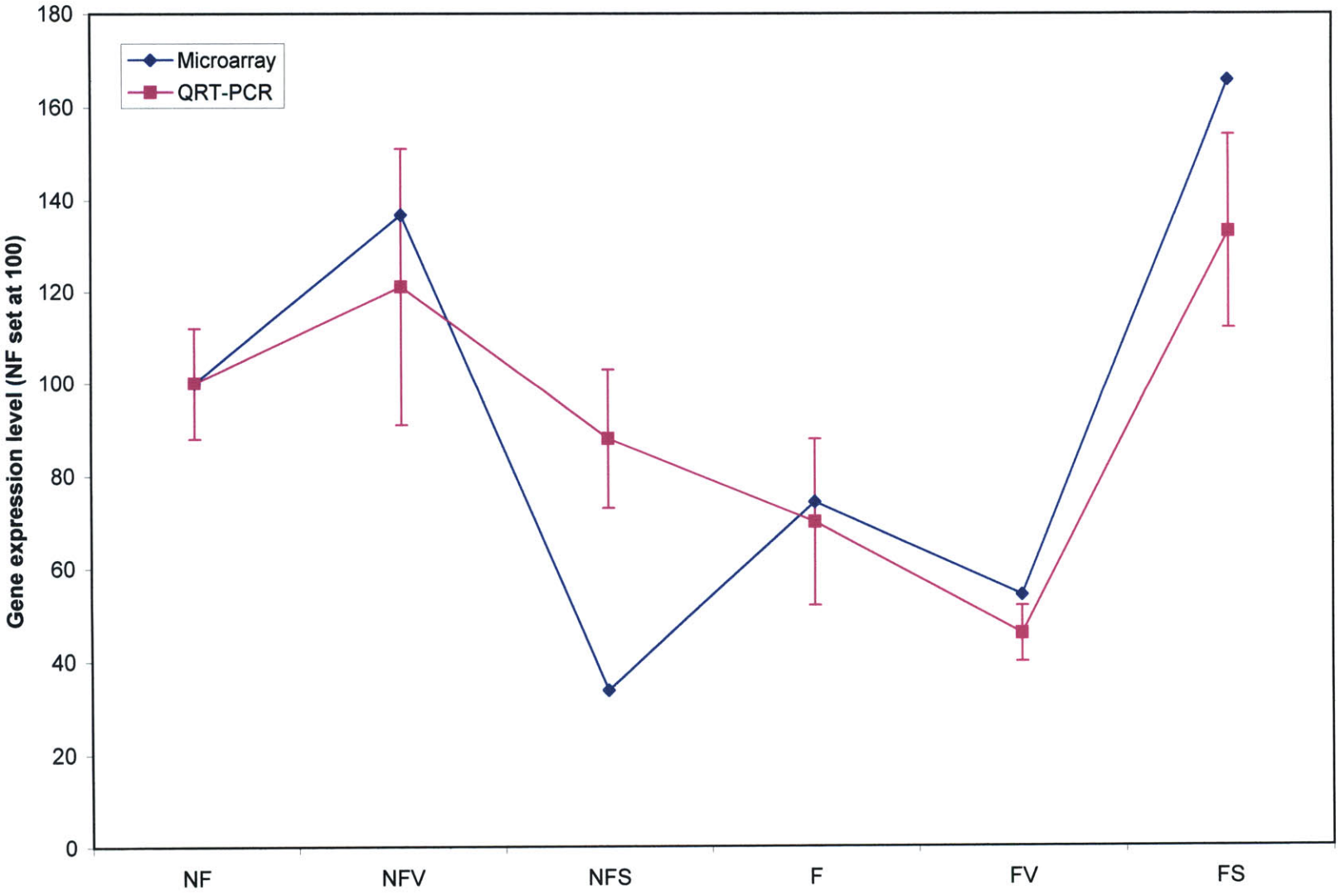

Figure 14 D:
Connexin 43: QRT-PCR validates microarray data

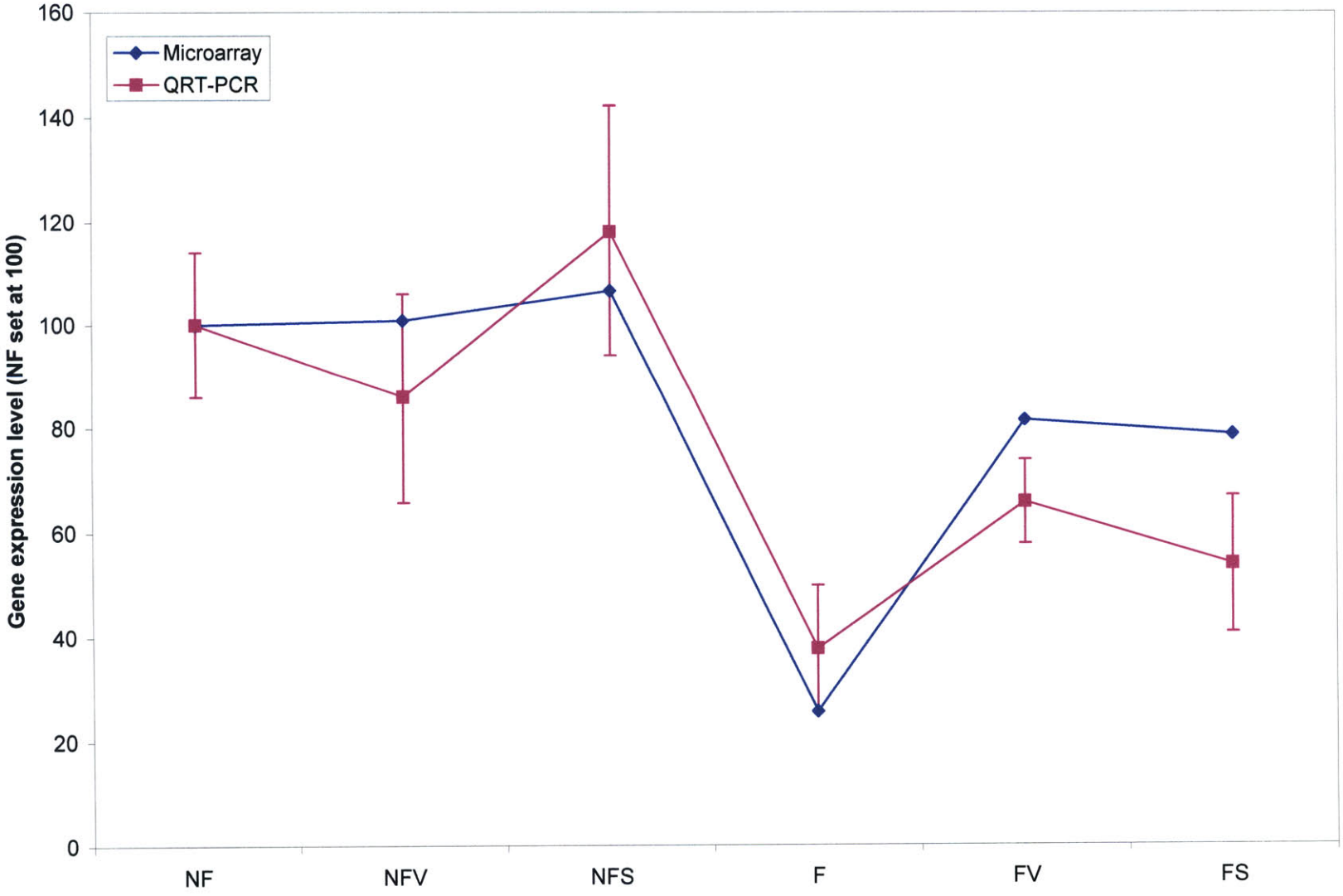

Figure 14 E:
Tensin: QRT-PCR validates microarray data

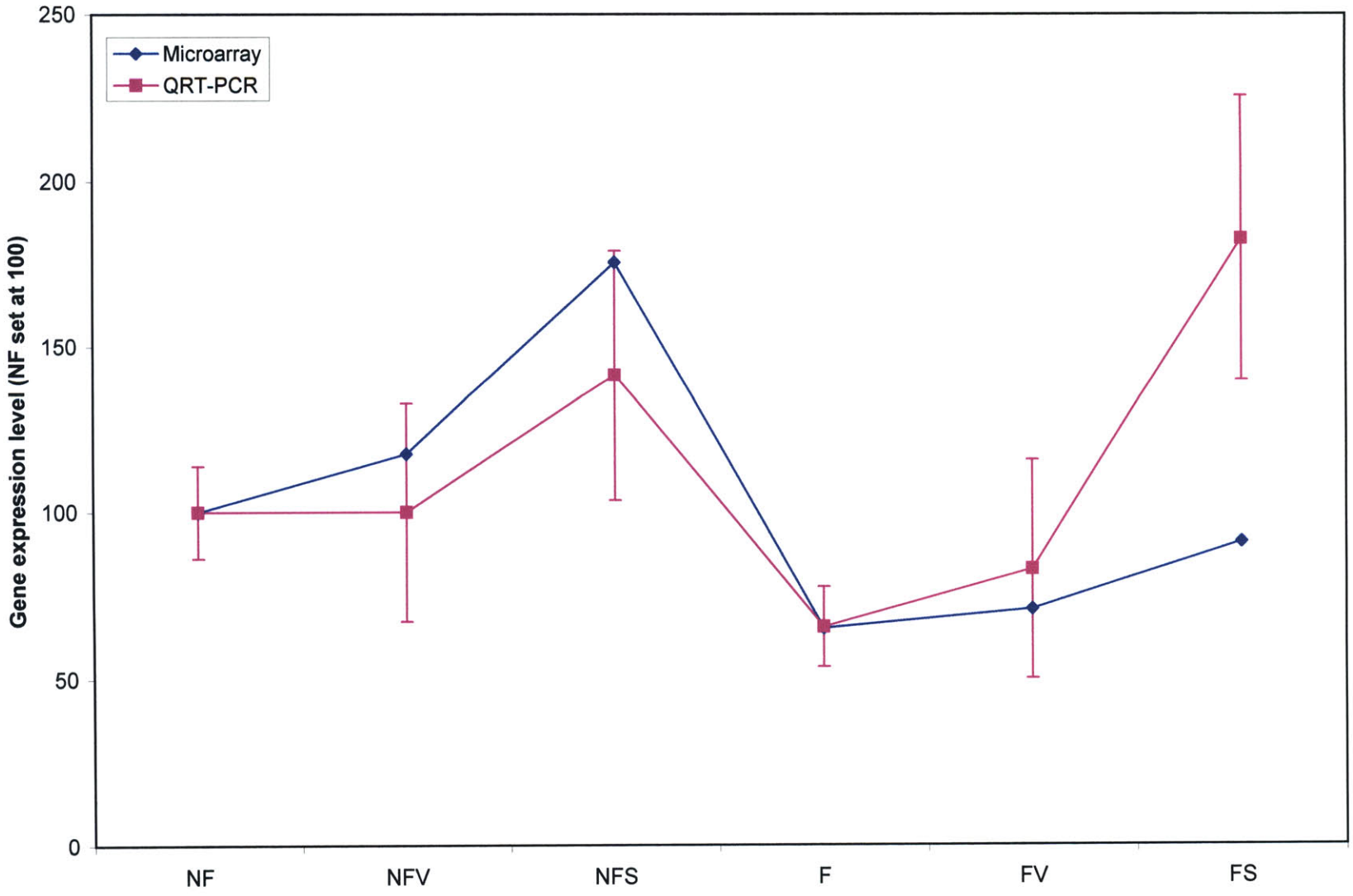

Figure 14 F:
Rev-ErbA-beta: QRT-PCR validates microarray data

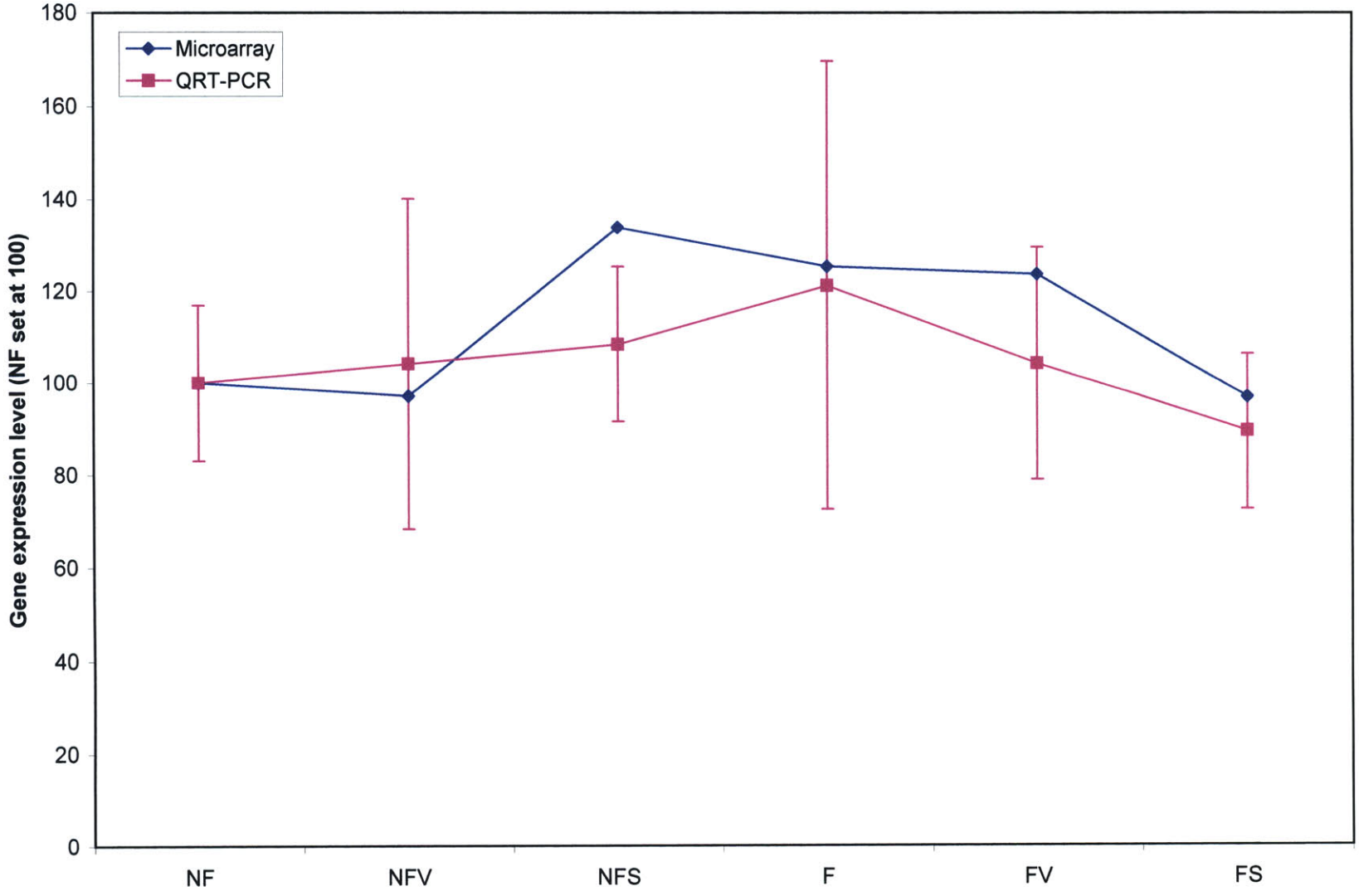

Figure 14 G:
GSK 3-beta: QRT-PCR validates microarray data

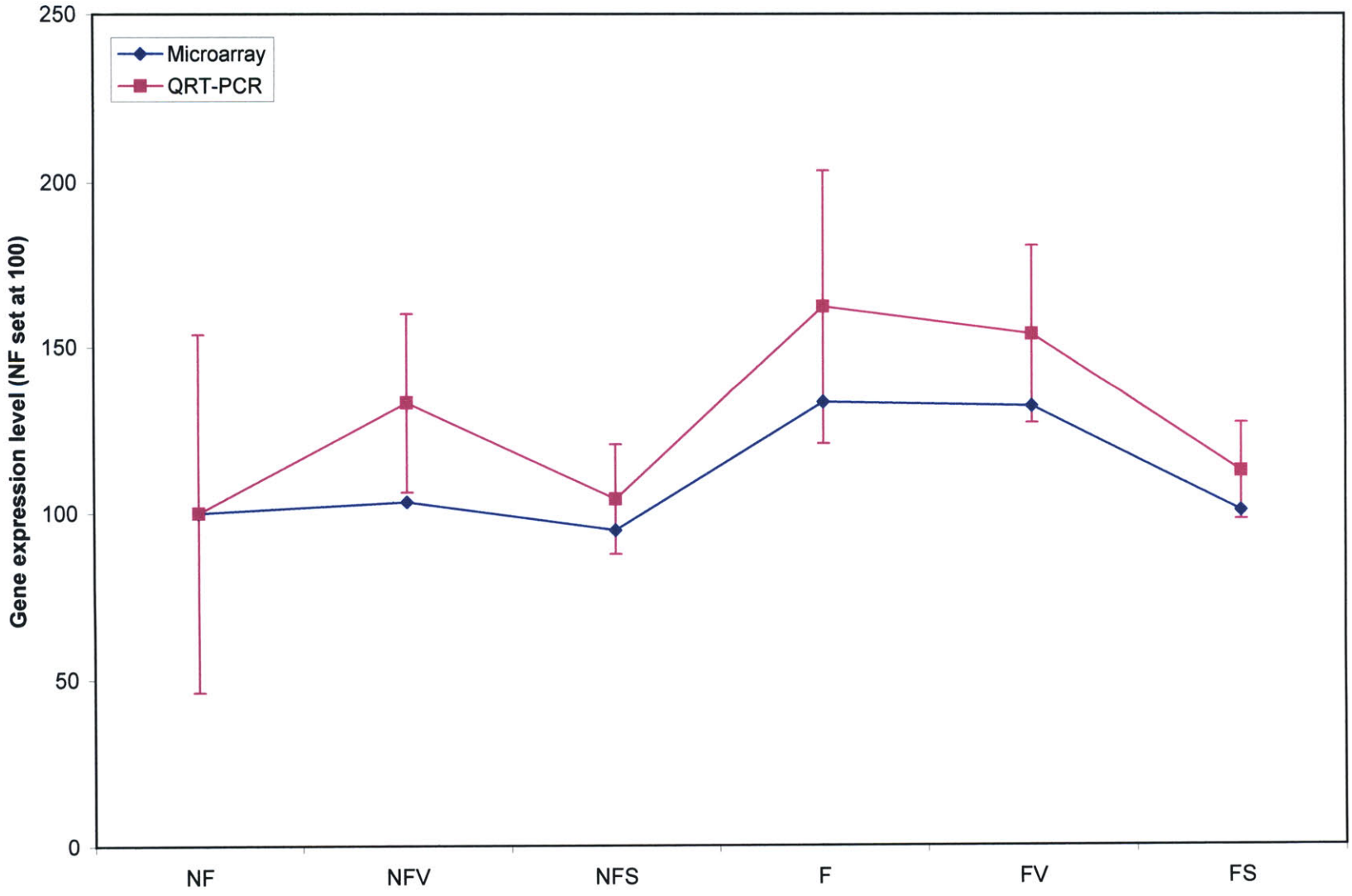

Figure 14 H:
Rev-ErbA-alpha: QRT-PCR validates microarray data

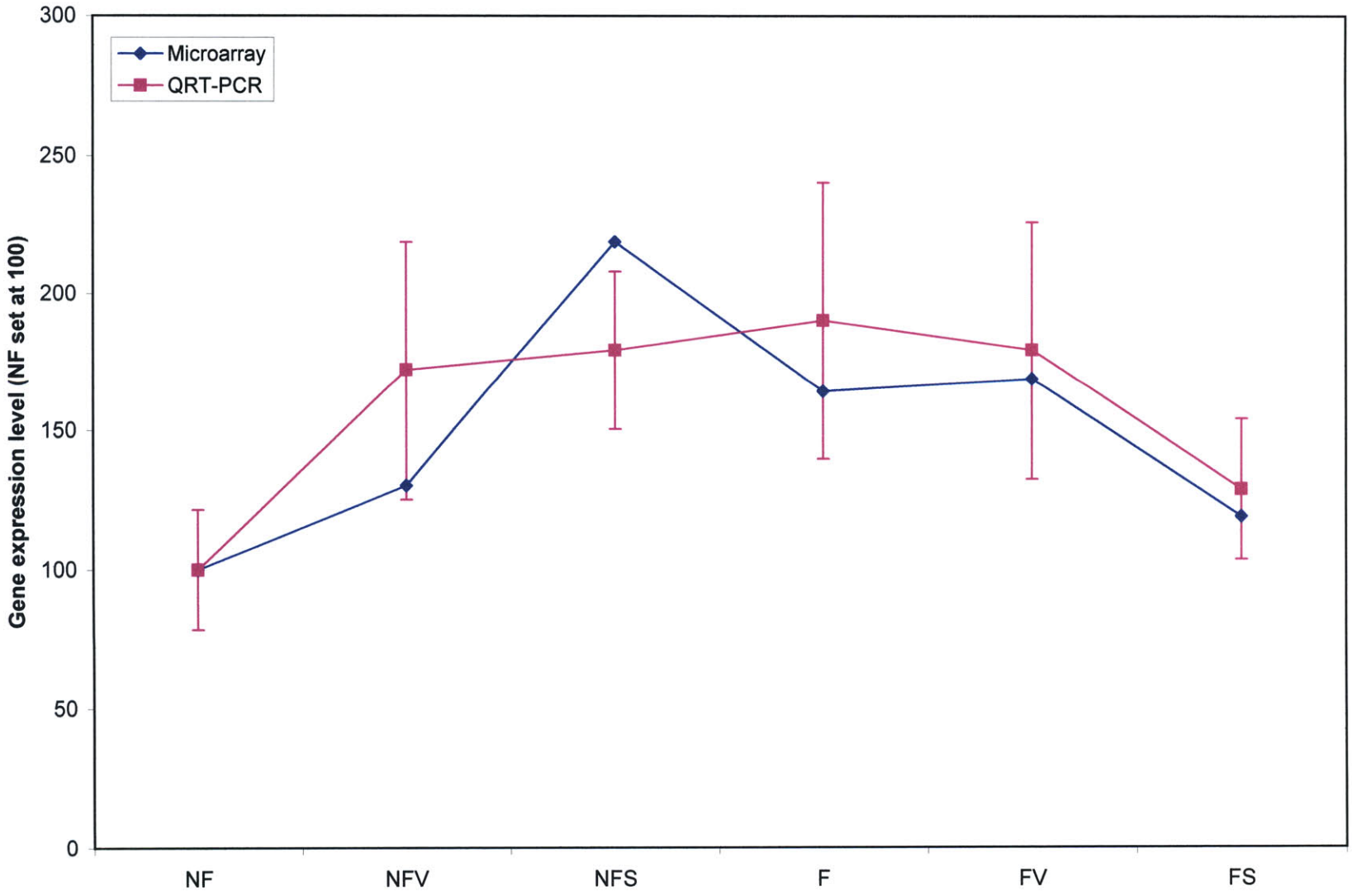

Tables

Table 1:
This is a list of all the 473 candidate gene targets of SERCA2a. The candidate gene probability of being a SERCA2a target is noted in the last column. Those genes correspond to the genes depicted in Figure 5A. The genes in the highest probability category were depicted in Figure 5D. The different fold changes that were used in the analysis are also found in the table. Genes where the fold change FS/FV > 2 or < 0.5, AND where FS/F > 2 or < 0.5, were shaded in gray, and may be important targets of SERCA2a in addition to the genes in the Highest probability category.

Table 1.1
Genes corresponding to Figure 5, Profile 1

Probe Set	Accession #	Gene	Function	FV/F	FS/FV	FS/F	F/NF	FV/NF	FS/NF	Probability
AF085693_at	AF085693	Git1: G protein-coupled receptor kinase-interactor 1	signal transduction/G protein coupled/GTPase activation	0.90	1.33	1.20	1.08	0.98	1.30	highest
rc_AA800737_at	AA800737	similar to PKP4: plakophilin 4	cell adhesion/cytoskeleton	0.90	1.36	1.22	1.11	0.99	1.35	highest
rc_H31847_at	H31847	Dncli1: dynein, cytoplasmic, light intermediate chain 1	GTPase signal transduction/motor activity/cytoskeleton	0.86	1.42	1.22	1.02	0.88	1.25	highest
rc_AA817892_at	AA817892	Gnb2: guanine nucleotide binding protein, beta polypeptide 2	G Protein/signal transduction/GTPase	1.02	1.20	1.23	1.16	1.19	1.43	highest
AF034582_at	AF034582	VAP1: vesicle associated protein	intracellular trafficking	0.98	1.27	1.25	1.02	1.01	1.27	highest
M83196_at	M83196	Mtap1a: microtubule-associated protein 1 A	cytoskeletal/development	0.90	1.40	1.27	1.18	1.07	1.50	highest
D16237_at	D16237	Cdc25b: cell division cycle 25B	cell cycle/tyrosine phosphatase	0.99	1.28	1.27	1.19	1.18	1.51	highest
X16002cds_s_at	X16002	Kcna4: potassium voltage gated channel, shaker related subfamily, member 4	K channel voltage gated/regulation of EC coupling	1.05	1.24	1.31	0.94	0.99	1.23	highest
X52619_at	X52619	Rpl28: ribosomal protein L28	ribosome	1.07	1.22	1.31	0.97	1.04	1.27	highest
X06801cds_f_at	X06801	Vascular alpha-actin	cytoskeleton	1.09	1.22	1.32	1.07	1.17	1.42	highest
S77858_s_at	S77858	Non-muscle myosin alkali light chain	myosin/Ca-binding/cytoskeleton/motor	1.05	1.26	1.33	1.20	1.26	1.60	highest
rc_AA866293_at	AA866293	unknown	unknown	0.97	1.38	1.33	0.93	0.90	1.24	highest
M17526_at	M17526	Gnao: guanine nucleotide binding protein, alpha o	G protein/GTPase/Ca-signaling/cytoskeletal rearrangement	1.08	1.24	1.34	1.01	1.09	1.35	highest
rc_AA875523_i_at	AA875523	similar to MYL6: myosin, light polypeptide 6, alkali, smooth muscle and non-muscle	myosin/Ca-binding/muscle contraction/cytoskeleton/motor	1.11	1.23	1.36	1.13	1.26	1.54	highest
M58758_at	M58758	Atp6n1a: ATPase, H+ transporting, lysosomal noncatalytic accessory protein 1a	proton transport/receptor medicated endocytosis	1.01	1.36	1.38	0.89	0.91	1.23	highest
D16309_at	D16309	Ccnd3: Cyclin D3	cell cycle	1.19	1.20	1.42	0.94	1.12	1.34	highest
M55015cds_s_at	M55015	Ncl: Nucleolin	ribosome synthesis/cell cycle	1.17	1.23	1.44	0.87	1.02	1.25	highest
S69383_at	S69383	Alox12: arachidonate 12-lipoxygenase	signal transduction/cell cycle	0.96	1.56	1.51	1.10	1.06	1.65	highest
M57664_g_at	M57664	Ckb: creatine kinase, brain	energy homeostasis/creatine kinase	1.03	1.50	1.54	0.90	0.93	1.39	highest

M17526_g_at	M17526	Gnao: guanine nucleotide binding protein, alpha o	G protein/Ca-signaling	1.11	1.40	1.56	1.13	1.26	1.77 highest
X78949_at	X78949	P4HA1: procollagen-proline, 2-oxoglutarate 4-dioxygenase (proline 4-hydroxylase), alpha polypeptide I	collagen synthesis/ECM	1.20	1.39	1.66	1.03	1.23	1.71 highest
U08136_at	U08136			1.23	1.20	1.47	0.88	1.08	1.30 high
U36482_at	U36482			1.29	1.21	1.56	0.90	1.16	1.40 high
AJ006971_at	AJ006971			1.31	1.20	1.57	0.89	1.16	1.39 high
rc_AA893235_at	AA893235			1.32	1.29	1.70	0.90	1.18	1.53 high
M89646_at	M89646			1.34	1.29	1.73	0.86	1.15	1.48 high
AJ010351_s_at	AJ010351			1.38	1.30	1.80	0.88	1.22	1.59 high
L25527_at	L25527			1.30	1.38	1.80	1.13	1.47	2.03 high
L02529_at	L02529			1.52	1.29	1.96	0.85	1.29	1.67 high
S54008_i_at	S54008			1.36	1.52	2.07	0.94	1.28	1.94 high
M80804_s_at	M80804			1.35	1.66	2.24	1.06	1.43	2.37 high
rc_AA891242_at	AA891242	similar to MYL7: myosin, light polypeptide 7, regulatory	myosin/Ca-binding/muscle contraction/muscle development/cytoskeleton	0.65	4.13	2.67	1.01	0.66	2.71 high
rc_AA891242_g_at	AA891242	similar to MYL7: myosin, light polypeptide 7, regulatory	myosin/Ca-binding/muscle contraction/muscle development/cytoskeleton	0.51	6.82	3.49	0.87	0.45	3.05 high
M24852_at	M24852	PCP4: Purkinje cell protein 4	Ca-binding/development	1.37	3.96	5.40	1.12	1.53	6.07 high
rc_AI137583_at	AI137583			1.60	0.77	1.23	1.17	1.86	1.43 lower
U82612cds_at	U82612			2.97	0.42	1.24	1.00	2.96	1.23 lower
rc_AA817854_s_at	AA817854			1.65	0.76	1.25	1.01	1.66	1.26 lower
M81183Exon_UTR_g_at	M81183			1.89	0.67	1.26	1.00	1.90	1.26 lower
D00698_s_at	D00698			1.79	0.72	1.30	0.98	1.76	1.27 lower
L11007_at	L11007			1.59	0.82	1.31	0.94	1.49	1.23 lower
AB005540_at	AB005540			1.67	0.79	1.33	1.01	1.69	1.34 lower
AJ000557cds_s_at	AJ000557			1.62	0.82	1.33	0.91	1.47	1.20 lower
rc_AI231213_g_at	AI231213			1.73	0.77	1.33	1.12	1.94	1.49 lower
X03015_at	X03015			1.85	0.74	1.36	1.07	1.97	1.45 lower
rc_AA893579_at	AA893579			2.20	0.63	1.38	1.00	2.20	1.38 lower
rc_AA799711_at	AA799711			1.69	0.83	1.40	0.86	1.46	1.20 lower
rc_AI059508_s_at	AI059508			1.92	0.74	1.42	0.96	1.84	1.36 lower
S59158_at	S59158			2.00	0.71	1.42	1.13	2.26	1.61 lower
U09401_s_at	U09401			6.39	0.22	1.43	1.00	6.39	1.43 lower

U21662_at	U21662			1.99	0.73	1.46	1.10	2.18	1.60 lower
rc_AI231778_at	AI231778			1.84	0.80	1.48	0.88	1.62	1.30 lower
AB017596_at	AB017596			2.07	0.71	1.48	0.86	1.78	1.27 lower
U77829mRNA_s_at	U77829			1.94	0.77	1.49	0.98	1.91	1.46 lower
rc_AI070295_g_at	AI070295			2.77	0.55	1.52	0.98	2.71	1.49 lower
rc_AA899253_at	AA899253			1.91	0.80	1.52	0.87	1.66	1.32 lower
J05132_s_at	J05132			1.92	0.79	1.53	1.11	2.14	1.70 lower
Y12009_at	Y12009			2.15	0.76	1.62	1.08	2.31	1.74 lower
S77494_s_at	S77494			3.37	0.49	1.64	1.19	4.01	1.95 lower
rc_AA866454_at	AA866454			3.02	0.55	1.66	1.00	3.01	1.66 lower
L32591mRNA_g_at	L32591			2.33	0.72	1.67	0.90	2.10	1.51 lower
rc_AA926129_at	AA926129			2.31	0.76	1.76	1.15	2.65	2.01 lower
L07114_at	L07114			2.41	0.75	1.80	1.14	2.76	2.06 lower
M10072mRNA_s_at	M10072			2.48	0.75	1.85	0.96	2.37	1.77 lower
rc_AA875620_at	AA875620			2.32	0.80	1.85	0.85	1.96	1.57 lower
AF087943_s_at	AF087943			2.68	0.70	1.87	0.91	2.43	1.70 lower
L32591mRNA_at	L32591			2.64	0.74	1.96	0.86	2.26	1.68 lower
rc_AA859827_at	AA859827			2.76	0.71	1.97	0.87	2.41	1.72 lower
rc_AA891725_at	AA891725			2.62	0.79	2.07	0.90	2.35	1.86 lower
AJ223184_at	AJ223184			3.73	0.57	2.14	1.14	4.24	2.43 lower
X04139_s_at	X04139			2.73	0.83	2.25	1.19	3.24	2.67 lower
K03039mRNA_s_at	K03039			2.99	0.75	2.26	1.00	2.99	2.26 lower
M34253_at	M34253			3.03	0.76	2.31	1.19	3.62	2.76 lower
U82612cds_g_at	U82612	fn-1: fibronectin	cell adhesion/cell migration/ECM/cell cycle/development	5.27	0.46	2.40	0.85	4.46	2.03 lower
L00191cds#1_s_at	L00191			4.44	0.56	2.50	0.94	4.19	2.35 lower
M34253_g_at	M34253			3.68	0.75	2.77	0.96	3.52	2.65 lower
X83537_at	X83537			3.86	0.77	2.95	0.96	3.71	2.84 lower
M32062_g_at	M32062			3.81	0.80	3.04	1.07	4.09	3.26 lower
rc_AA891944_at	AA891944			4.09	0.76	3.09	0.93	3.81	2.88 lower
J05495_at	J05495			3.97	0.81	3.20	0.85	3.37	2.72 lower
S66184_s_at	S66184	lysyl oxidase	collagen and elastin crosslinking/ECM/tumor suppressor	10.17	0.37	3.77	1.00	10.17	3.77 lower
U17035_s_at	U17035			5.39	0.76	4.08	1.15	6.21	4.71 lower

Table 1.2
Genes corresponding to Figure 5, profile 2

Probe Set	Accession #	Gene	Function	FV/F	FS/FV	FS/F	F/NF	FV/NF	FS/NF	Probability
rc_AA799465_at	AA799465	unknown	unknown	0.84	0.63	0.53	1.19	1.00	0.63	highest
rc_AI233225_at	AI233225	Gucy1b3: guanylate cyclase 1, soluble, beta 3	cGMP biosynthesis/nitric oxide signal transduction/vasodilation/circulation	0.84	0.70	0.58	1.16	0.97	0.68	highest
M77184_i_at	M77184	PTHR1: parathyroid hormone receptor 1	Ca metabolism/Ca signaling/cell cycle/G protein-coupled receptor	1.10	0.55	0.61	0.96	1.07	0.59	highest
rc_AI639331_at	AI639331	unknown	unknown	0.93	0.66	0.61	0.99	0.92	0.61	highest
rc_AI009268_at	AI009268	Camk2d: calcium/calmodulin-dependent protein kinase II, delta	Ca-binding/serine/threonine protein kinase/Ca-Calmodulin signal transduction	0.88	0.73	0.64	1.10	0.96	0.71	highest
rc_AA859896_at	AA859896	Marcks: myristoylated alanine rich protein kinase C substrate	actin crosslinking/cell cycle/binds to Ca Calmodulin/cytoskeleton	0.96	0.68	0.65	1.20	1.16	0.78	highest
X72757_at	X72757	Cox6a1: cytochrome c oxidase, subunit VIa, polypeptide 1	energy production/mitochondrion	0.99	0.67	0.66	1.17	1.16	0.78	highest
X75785_at	X75785	Sycp3: Synaptonemal complex protein 3	cell cycle	0.84	0.80	0.67	1.19	1.00	0.80	highest
rc_AI638958_at	AI638958	unknown	unknown	1.04	0.66	0.69	1.03	1.07	0.71	highest
rc_H31610_at	H31610	unknown	unknown	0.92	0.75	0.69	1.10	1.02	0.76	highest
X89705cds_at	X89705	Olr1606: olfactory receptor gene Olr1606	signal transduction/ 7 transmembrane receptor	0.86	0.81	0.69	1.08	0.93	0.75	highest
rc_AI639272_at	AI639272	unknown	unknown	0.88	0.79	0.70	1.08	0.95	0.76	highest
rc_AA956941_at	AA956941	Tcf4: transcription factor 4	transcription factor/cell cycle	0.85	0.82	0.70	1.13	0.96	0.79	highest
rc_AA892797_at	AA892797	Pgk1: phosphoglycerate kinase 1	glycolysis/energy production	0.96	0.74	0.71	1.03	0.99	0.73	highest
rc_AA894297_at	AA894297	unknown	unknown	0.99	0.74	0.73	1.02	1.01	0.74	highest
rc_AA874912_at	AA874912	similar to MOSPD1: motile sperm domain containing 1	unknown	0.97	0.75	0.73	0.96	0.93	0.70	highest
rc_AA874857_at	AA874857	similar to PURB: purine-rich element binding protein B	transcription factor/DNA replication/cell cycle	0.92	0.80	0.73	1.06	0.97	0.78	highest
rc_AA799751_at	AA799751	unknown	unknown	0.95	0.77	0.74	0.92	0.87	0.68	highest
AJ224680_at	AJ224680	Cngb1: cyclic nucleotide-gated channel beta subunit 1	Potassium channel cAMP gated	0.98	0.76	0.74	0.98	0.97	0.73	highest
X89703cds_at	X89703	unknown	unknown	1.04	0.71	0.74	1.10	1.14	0.81	highest
Y00766_g_at	Y00766	Scn3a: Sodium channel, voltage-gated, type III, alpha polypeptide	Na channel voltage gated/Ca-binding	0.92	0.81	0.75	0.90	0.83	0.67	highest

rc_AI009111_at	AI009111	Psma1: proteasome (prosome, macropain) subunit, alpha type 1	protein catabolism	0.92	0.82	0.75	0.98	0.90	0.73 highest
rc_AI639209_at	AI639209	unknown	unknown	0.94	0.79	0.75	0.97	0.92	0.73 highest
rc_AI236145_at	AI236145	Hsd17b7: hydroxysteroid dehydrogenase 17 beta, type 7	steroid/androgen biosynthesis	0.98	0.77	0.75	1.01	0.99	0.76 highest
rc_AA799538_at	AA799538	similar to SFRS2: splicing factor, arginine/serine-rich 2	RNA splicing	1.10	0.68	0.75	1.02	1.13	0.77 highest
rc_AA859994_at	AA859994	similar to E. coli Beta-galactosidase	carbohydrate metabolism	0.95	0.79	0.75	1.01	0.97	0.76 highest
rc_AI639106_at	AI639106	unknown	unknown	0.92	0.82	0.75	1.04	0.95	0.78 highest
M23264_at	M23264	Ar: androgen receptor	androgen activated transcription factor/cell cycle/signal transduction/receptor	1.03	0.74	0.76	0.94	0.97	0.71 highest
L12025_at	L12025	Taa1: tumor-associated antigen 1	unknown	0.97	0.78	0.76	0.96	0.93	0.73 highest
L29573_s_at	L29573	Slc6a2: solute carrier family 6 (neurotransmitter transporter,noradrenalin), member 2	norepinephrine transporter plasma membrane	0.98	0.78	0.76	1.04	1.02	0.79 highest
M13962mRNA#2_at	M13962	Gusb: Glucuronidase, beta	carbohydrate metabolism	1.04	0.73	0.76	0.92	0.96	0.70 highest
M29853_at	M29853	Cyp4b1: cytochrome P450, subfamily 4B, polypeptide 1	drug and lipid metabolism including steroids	0.97	0.79	0.76	0.90	0.87	0.69 highest
rc_AI227715_at	AI227715	Rbl2: retinoblastoma-like 2	transcritpion factor/cell cycle	0.96	0.80	0.77	0.89	0.85	0.68 highest
rc_AA892550_g_at	AA892550	similar to FBXO22: F-box only protein 22	ubiquitination	1.00	0.79	0.79	1.05	1.05	0.83 highest
rc_AA875496_at	AA875496	unknown	unknown	0.95	0.83	0.79	0.99	0.94	0.78 highest
rc_AA892504_at	AA892504	unknown	unknown	1.02	0.79	0.80	0.98	0.99	0.78 highest
U32314_g_at	U32314	Pc: Pyruvate carboxylase	lipid biosynthesis/gluconeogenesis/mitochondrion	0.99	0.82	0.81	0.84	0.83	0.68 highest
rc_AA849036_at	AA849036	Gucy1a3: guanylate cyclase 1, soluble, alpha 3	cGMP biosynthesis/nitric oxide signal transduction/vasodilation/circulation	0.99	0.83	0.82	0.99	0.98	0.81 highest
rc_AA894104_at	AA894104	unknown	unknown	1.04	0.79	0.82	1.01	1.04	0.83 highest
K01677_at	K01677	Eif5: eukaryotic initiation factor 5 (eIF-5)	translation initiation	1.16	0.71	0.83	0.92	1.07	0.76 highest
rc_AA891800_g_at	AA891800	unknown	unknown	1.01	0.82	0.83	0.86	0.87	0.72 highest
U10995_at	U10995	Nr2f1: nuclear receptor subfamily 2, group F, member 1	transcription factor/steroid hormone receptor/signal transduction	1.13	0.74	0.83	0.99	1.12	0.82 highest
rc_AI639523_at	AI639523	similar to SPTA1: spectrin, alpha, erythrocytic 1 (elliptocytosis 2)	Ca-binding/actin cytoskeleton	0.81	0.16	0.13	1.12	0.91	0.15 high

L19112_g_at	L19112	0.67	0.82	0.55	1.06	0.71	0.58	high
J00777_at	J00777	0.72	0.77	0.55	1.00	0.72	0.56	high
L28818cds_at	L28818	0.73	0.82	0.60	1.14	0.84	0.68	high
rc_AA892400_at	AA892400	0.83	0.73	0.60	1.08	0.89	0.64	high
U07619_at	U07619	0.78	0.78	0.61	1.09	0.85	0.66	high
rc_AA891721_at	AA891721	0.79	0.78	0.61	0.90	0.71	0.55	high
rc_AA892677_at	AA892677	0.75	0.82	0.61	1.09	0.81	0.67	high
U07683_at	U07683	0.76	0.83	0.63	1.07	0.81	0.67	high
D31838_at	D31838	0.79	0.81	0.63	1.18	0.93	0.75	high
rc_AI030089_at	AI030089	0.79	0.81	0.65	1.10	0.87	0.71	high
rc_AI639379_at	AI639379	0.83	0.80	0.66	1.00	0.82	0.66	high
L13445_at	L13445	1.23	0.63	0.77	0.85	1.05	0.66	high
rc_AI639470_g_at	AI639470	0.52	1.35	0.70	1.18	0.61	0.82	lower

Table 1.3
Genes corresponding to Figure 5, Profile 3

Probe Set	Accession #	Gene	Function	FV/F	FS/FV	FS/F	F/NF	FV/NF	FS/NF	Probability
rc_AI014135_at	AI014135	unknown	unknown	1.10	0.64	0.71	2.80	3.07	1.98	highest
X05472cds#2_at	X05472	unknown	unknown	0.97	0.78	0.76	1.75	1.70	1.33	highest
rc_AI014135_g_at	AI014135	unknown	unknown	1.10	0.70	0.77	2.27	2.48	1.74	highest
rc_AI171962_s_at	AI171962	Anxa1: annexin 1	Ca-binding/inhibits phospholipase A2 signal transduction/anti-inflammatory/cell cycle	0.96	0.81	0.78	2.22	2.14	1.73	highest
AF030091UTR#1_g_at	AF030091	Ccnl: cyclin L	cell cycle	0.96	0.83	0.80	2.03	1.95	1.62	highest
rc_AA799992_at	AA799992	similar to C11orf17: chromosome 11 open reading frame 17	unknown	1.00	0.80	0.80	2.39	2.39	1.92	highest
U17254_g_at	U17254			0.36	0.57	0.20	6.99	2.50	1.41	high
rc_AA800750_f_at	AA800750	unknown	unknown	0.82	0.40	0.32	4.53	3.70	1.46	high
rc_AI178971_at	AI178971			0.55	0.78	0.43	3.00	1.64	1.28	high
M24067_at	M24067			0.61	0.79	0.48	2.87	1.75	1.38	high
AF055714UTR#1_at	AF055714			0.79	0.66	0.53	3.72	2.95	1.96	high
D17309_at	D17309			0.76	0.76	0.58	2.27	1.73	1.31	high
rc_AA874848_s_at	AA874848			1.24	0.59	0.74	1.84	2.29	1.35	high
M18416_at	M18416			0.09	1.74	0.15	20.71	1.81	3.14	lower
AF023087_s_at	AF023087			0.17	1.22	0.21	15.31	2.68	3.27	lower
S74351_s_at	S74351			0.18	1.22	0.22	7.48	1.38	1.68	lower
rc_AA891041_at	AA891041			0.19	1.28	0.25	12.72	2.43	3.12	lower
rc_AA944156_s_at	AA944156			0.24	1.25	0.31	4.12	1.01	1.26	lower
X54686cds_at	X54686			0.29	1.33	0.39	13.73	3.99	5.32	lower
X96437mRNA_g_at	X96437			0.49	1.33	0.66	2.27	1.12	1.49	lower
D86297_at	D86297			0.46	1.69	0.78	1.90	0.88	1.48	lower

Table 1.4
Genes corresponding to Figure 5, Profile 4

Probe Set	Accession #	Gene	Function	FV/F	FS/FV	FS/F	F/NF	FV/NF	FS/NF	Probability
rc_AA851223_at	AA851223	Eno3: enolase 3, beta	glycolysis/energy production	0.93	1.88	1.74	0.39	0.36	0.67	highest
AJ222724_at	AJ222724			1.29	1.21	1.56	0.49	0.64	0.77	high
D89070cds_s_at	D89070			1.28	1.35	1.72	0.46	0.59	0.79	high
rc_AI639162_at	AI639162			1.37	1.30	1.77	0.40	0.55	0.71	high
U61184_at	U61184			1.58	0.77	1.22	0.68	1.08	0.83	lower
rc_AA817846_at	AA817846			1.57	0.78	1.22	0.49	0.78	0.60	lower
U77931_at	U77931			1.58	0.78	1.24	0.62	0.98	0.77	lower
rc_AA799406_at	AA799406			1.74	0.72	1.24	0.52	0.91	0.65	lower
rc_AI044488_at	AI044488			1.92	0.66	1.26	0.63	1.21	0.79	lower
AB007689_at	AB007689			1.54	0.83	1.28	0.62	0.95	0.79	lower
U31815_s_at	U31815			1.68	0.76	1.28	0.64	1.07	0.82	lower
X66366_at	X66366			1.71	0.75	1.29	0.56	0.96	0.72	lower
AF034577_at	AF034577			2.25	0.58	1.30	0.51	1.16	0.67	lower
E03344cds_s_at	E03344			1.65	0.79	1.30	0.58	0.95	0.75	lower
U36773_g_at	U36773			1.85	0.71	1.31	0.52	0.97	0.68	lower
rc_H33528_at	H33528			1.70	0.77	1.32	0.60	1.02	0.79	lower
rc_AI030286_s_at	AI030286			1.97	0.67	1.33	0.50	0.99	0.67	lower
U83895_at	U83895			1.63	0.83	1.36	0.53	0.86	0.72	lower
AF056333_s_at	AF056333			2.34	0.59	1.37	0.48	1.11	0.65	lower
U35775_g_at	U35775			1.77	0.79	1.39	0.59	1.04	0.82	lower
D14425_s_at	D14425			1.90	0.74	1.40	0.50	0.95	0.70	lower
rc_AA892339_at	AA892339			1.78	0.80	1.43	0.50	0.89	0.71	lower
M31809_at	M31809			1.88	0.76	1.43	0.52	0.97	0.74	lower
rc_AA800763_at	AA800763			1.83	0.79	1.44	0.52	0.96	0.75	lower
rc_AA800768_at	AA800768			1.73	0.83	1.44	0.47	0.81	0.68	lower
M93401_at	M93401			1.80	0.81	1.45	0.49	0.88	0.71	lower
rc_AA892500_at	AA892500			1.91	0.76	1.46	0.55	1.04	0.80	lower
AF055286_g_at	AF055286			1.83	0.80	1.47	0.37	0.68	0.54	lower
L29090cds_at	L29090			1.78	0.83	1.47	0.45	0.81	0.67	lower
L13406_s_at	L13406			1.86	0.79	1.47	0.43	0.81	0.64	lower
rc_AA859982_at	AA859982			2.05	0.72	1.48	0.53	1.09	0.78	lower
AF055286_at	AF055286			2.00	0.75	1.49	0.44	0.88	0.66	lower

X13167cds_s_at	X13167	2.17	0.72	1.57	0.52	1.13	0.81 lower
rc_AA925887_at	AA925887	1.98	0.80	1.57	0.37	0.73	0.58 lower
rc_AA893172_at	AA893172	2.59	0.61	1.57	0.38	0.99	0.60 lower
D25233cds_at	D25233	2.58	0.63	1.61	0.46	1.19	0.75 lower
M24104_at	M24104	2.48	0.67	1.67	0.46	1.15	0.78 lower
rc_AI233261_i_at	AI233261	2.39	0.73	1.75	0.40	0.94	0.69 lower
rc_AA800912_g_at	AA800912	2.43	0.72	1.76	0.42	1.02	0.74 lower
X99337cds_s_at	X99337	2.46	0.74	1.82	0.45	1.11	0.83 lower
AF075382_at	AF075382	2.35	0.80	1.87	0.39	0.91	0.73 lower
rc_AA799637_g_at	AA799637	2.79	0.70	1.95	0.33	0.93	0.65 lower
D84487_at	D84487	2.63	0.76	2.01	0.35	0.92	0.70 lower
S90449_at	S90449	2.77	0.83	2.29	0.35	0.96	0.79 lower
rc_AA893242_g_at	AA893242	3.36	0.68	2.30	0.25	0.82	0.56 lower
Y12517cds_at	Y12517	3.19	0.77	2.44	0.25	0.81	0.62 lower
U95157_at	U95157	3.51	0.77	2.70	0.29	1.01	0.78 lower
L13407_i_at	L13407	4.35	0.68	2.97	0.18	0.76	0.52 lower

Table 1.5
Genes corresponding to Figure 5, Profile 5

Probe Set	Accession #	Gene	Function	FV/F	FS/FV	FS/F	F/NF	FV/NF	FS/NF	Probability
S68245_g_at	S68245	Ca4: carbonic anhydrase 4	respiration/acid-base balance	0.91	0.64	0.58	1.46	1.33	0.85	highest
X07636_at	X07636	Asgr2: asialoglycoprotein receptor 2	cell surface receptor signal transduction	0.85	0.73	0.62	1.55	1.32	0.97	highest
AF104362_at	AF104362	Omd: osteomodulin (osteoadherin)	ECM/cell adhesion	0.90	0.71	0.64	1.47	1.33	0.94	highest
rc_AI639475_at	AI639475	unknown	unknown	0.86	0.76	0.65	1.35	1.16	0.87	highest
rc_AA892228_at	AA892228	similar to CUGBP1: CUG triplet repeat, RNA binding protein 1	mRNA processing/RNA interference/development	0.84	0.82	0.69	1.37	1.15	0.94	highest
rc_AA925248_at	AA925248	Scn6a: sodium channel, voltage-gated, type 6, alpha polypeptide	Na channel voltage gated	1.00	0.71	0.71	1.27	1.27	0.90	highest
rc_AA799472_at	AA799472	unknown	unknown	0.86	0.83	0.71	1.46	1.26	1.04	highest
AB003726_at	AB003726	Homer1: homer, neuronal immediate early gene, 1	regulates glutamate receptors	0.96	0.75	0.72	1.32	1.27	0.95	highest
rc_AI639060_at	AI639060	unknown	unknown	0.98	0.74	0.72	1.38	1.35	1.00	highest
M25804_at	M25804	Nr1d1: nuclear receptor subfamily 1, group D, member 1	transcription factor/steroid hormone receptor/myoblast differentiation/development/triglyceride metabolism/atherosclerosis	1.03	0.71	0.73	1.64	1.69	1.19	highest
rc_AA858578_at	AA858578	unknown	unknown	0.92	0.80	0.74	1.56	1.44	1.16	highest
rc_AA859545_at	AA859545	unknown	unknown	0.91	0.82	0.75	1.28	1.16	0.96	highest
D12769_g_at	D12769	Klf9: Kruppel-like factor 9	transcription factor	0.97	0.77	0.75	1.24	1.20	0.92	highest
X73653_at	X73653	Gsk3b: glycogen synthase kinase 3 beta	serine/threonine kinase/energy metabolism/development/cell cycle/signal transduction	0.99	0.76	0.76	1.33	1.32	1.01	highest
AB008538_at	AB008538	Alcam: activated leukocyte cell adhesion molecule	signal transduction/cell adhesion/immune response	1.07	0.71	0.76	1.23	1.32	0.93	highest
rc_AA892637_at	AA892637	similar to GRP58: glucose regulated protein, 58kDa	protein modification/signal transduction	0.92	0.83	0.76	1.33	1.23	1.02	highest
U20796_at	U20796	Nr1d2: nuclear receptor subfamily 1, group D, member 2	transcription factor/steroid hormone receptor	0.99	0.78	0.77	1.25	1.24	0.97	highest
rc_AA799526_at	AA799526	unknown	unknown	0.95	0.82	0.78	1.26	1.21	0.99	highest
M23697_at	M23697	Plat: Plasminogen activator, tissue	blood coagulation/protease/cell migration/tissue remodeling/extracellular	1.03	0.76	0.79	1.50	1.55	1.19	highest
rc_AI639245_at	AI639245	unknown	unknown	1.06	0.76	0.81	1.30	1.38	1.05	highest

rc_AI072435_at	AI072435	Nsep1: nuclease sensitive element binding protein 1	transcription factor/cell cycle	0.99	0.82	0.81	1.28	1.26	1.04 highest
U47110_at	U47110	Cask: calcium/calmodulin-dependent serine protein kinase	Ca-Calmodulin binding/signal transduction/actin cytoskeleton/serine-threonine kinase	1.16	0.72	0.83	1.26	1.46	1.04 highest
rc_AA799459_at	AA799459			0.56	0.73	0.41	2.08	1.17	0.86 high
rc_AA800784_at	AA800784			0.69	0.66	0.46	2.38	1.65	1.10 high
L26292_g_at	L26292			0.67	0.73	0.49	2.16	1.45	1.05 high
rc_AA893260_at	AA893260			0.83	0.73	0.61	1.64	1.37	1.00 high
AF096835_at	AF096835			0.74	0.83	0.61	1.40	1.03	0.85 high
U17697_s_at	U17697	Cyp51: cytochrome P450, subfamily 51	cholesterol/steroid biosynthesis	0.76	0.81	0.62	1.46	1.11	0.90 high
AF031657mRNA_at	AF031657	zinc-finger protein 94 (Zfp94) gene	transcription factor	0.75	0.83	0.62	1.43	1.07	0.89 high
U75404UTR#1_s_at	U75404			0.82	0.79	0.64	1.31	1.07	0.84 high
rc_AA866443_at	AA866443			1.29	0.54	0.70	1.23	1.59	0.86 high
rc_AI639412_at	AI639412			1.22	0.63	0.77	1.38	1.69	1.07 high
rc_AA893846_at	AA893846			1.47	0.54	0.79	1.22	1.80	0.97 high
U17254_at	U17254			0.12	1.26	0.15	7.62	0.92	1.16 lower
rc_AA891943_at	AA891943			0.65	1.26	0.82	1.27	0.82	1.03 lower
rc_AA875633_at	AA875633			0.68	1.21	0.82	1.25	0.85	1.03 lower

Table 1.6
Genes corresponding to Figure 5, Profile 6

Probe Set	Accession #	Gene	Function	FV/F	FS/FV	FS/F	F/NF	FV/NF	FS/NF	Probability
rc_AA892560_at	AA892560	unknown	unknown	0.97	1.25	1.20	0.81	0.78	0.97	highest
rc_AI639507_at	AI639507	unknown	unknown	0.95	1.30	1.23	0.71	0.67	0.87	highest
rc_AI105044_at	AI105044	similar to POLR3K: polymerase (RNA) III (DNA directed) polypeptide K, 12.3 kDa	subunit of RNA polymerase III /synthesis of tRNA and small ribosomal RNA	0.92	1.33	1.23	0.83	0.76	1.02	highest
U46034_at	U46034	Mmp11: Matrix metalloproteinase 11 (stromelysin 3)	breakdown of ECM/remodelling/metastasis/development/Ca-binding	1.02	1.26	1.29	0.82	0.84	1.06	highest
D30040_at	D30040	Akt1: v-akt murine thymoma viral oncogene homolog 1	anti-apoptosis/cell cycle/signal transduction/serine-threonine kinase/G protein coupled receptor	1.09	1.21	1.32	0.71	0.78	0.94	highest
rc_AA874934_at	AA874934	Doc2a	Ca-binding/Ca-dependent exocytosis	1.12	1.22	1.36	0.81	0.90	1.10	highest
U26310_at	U26310	Tns: tensin	focal adhesions/SH2 signal transduction/crosslinks actin cytoskeleton	1.09	1.28	1.40	0.65	0.71	0.91	highest
U30485mRNA_s_at	U30485	aspartyl-tRNA synthetase (DRS1)	tRNA synthesis	1.12	1.28	1.43	0.66	0.74	0.94	highest
rc_AA875132_at	AA875132	TPM1: tropomyosin 1 (alpha)	cytoskeleton/regulation of muscle contraction and heart rate/muscle development/contractile apparatus	1.03	1.41	1.45	0.75	0.77	1.08	highest
L19341_at	L19341	Acvr1: activin type I receptor	TGF-B/growth and differentiation factor/receptor serine-threonine kinase/signal transduction	1.06	1.41	1.50	0.73	0.78	1.10	highest
AF080568_at	AF080568	Pcyt2: phosphate cytidylyltransferase 2, ethanolamine	phospholipid biosynthesis	1.15	1.32	1.52	0.71	0.82	1.08	highest
rc_AI234969_s_at	AI234969			1.23	1.22	1.50	0.65	0.79	0.97	high
AF014009_at	AF014009			1.29	1.20	1.55	0.71	0.91	1.09	high
X65296cds_s_at	X65296			1.24	1.30	1.61	0.61	0.76	0.99	high
AF027571_s_at	AF027571			1.32	1.25	1.65	0.56	0.73	0.92	high
X55298_at	X55298			1.36	1.21	1.65	0.70	0.95	1.15	high
L01115_at	L01115			1.35	1.30	1.76	0.53	0.72	0.93	high
rc_AI145680_s_at	AI145680			1.51	1.20	1.82	0.59	0.90	1.08	high
X74402_at	X74402			1.56	1.21	1.90	0.58	0.91	1.11	high
rc_AA799497_g_at	AA799497			1.61	1.29	2.07	0.54	0.87	1.13	high

S50461_s_at	S50461			1.71	1.24	2.13	0.55	0.94	1.17 high
Z15123exon#5_s_at	Z15123			1.24	1.72	2.13	0.46	0.57	0.99 high
rc_AI008131_s_at	AI008131			1.31	1.82	2.37	0.39	0.50	0.91 high
Y08138_at	Y08138			2.17	1.26	2.74	0.37	0.81	1.02 high
M74494_g_at	M74494			2.35	1.23	2.88	0.41	0.96	1.18 high
X06827_g_at	X06827			2.72	1.30	3.53	0.31	0.85	1.10 high
rc_AA892146_f_at	AA892146	unknown	unknown	1.40	2.79	3.90	0.29	0.40	1.12 high
M91234_f_at	M91234	VL30 element (virus-like 30S)	unknown	1.34	3.28	4.41	0.25	0.33	1.09 high
M20131cds_s_at	M20131			1.62	0.75	1.21	0.81	1.31	0.98 lower
U39320_at	U39320			1.75	0.69	1.21	0.73	1.27	0.88 lower
U27201_at	U27201			1.47	0.83	1.22	0.78	1.15	0.95 lower
S62096_s_at	S62096			1.82	0.67	1.22	0.70	1.28	0.86 lower
rc_AA892813_s_at	AA892813			1.72	0.71	1.22	0.70	1.21	0.86 lower
E13890cds_s_at	E13890			1.51	0.81	1.23	0.82	1.24	1.01 lower
U76997_at	U76997			1.57	0.79	1.23	0.80	1.26	0.99 lower
S35751_f_at	S35751			1.86	0.66	1.23	0.75	1.40	0.93 lower
Z34004exon_at	Z34004			1.53	0.81	1.23	0.74	1.13	0.91 lower
rc_AI013472_at	AI013472			1.53	0.81	1.23	0.71	1.08	0.87 lower
rc_H31955_at	H31955			1.76	0.71	1.25	0.75	1.32	0.94 lower
rc_AA866240_i_at	AA866240			1.55	0.81	1.25	0.71	1.10	0.88 lower
U87306_at	U87306			1.55	0.81	1.26	0.76	1.17	0.95 lower
rc_AA866444_s_at	AA866444			1.51	0.83	1.26	0.79	1.20	1.00 lower
S79214cds_s_at	S79214			1.65	0.77	1.26	0.81	1.33	1.02 lower
U40188_at	U40188			1.59	0.80	1.27	0.78	1.24	0.99 lower
rc_AA800053_at	AA800053			1.59	0.80	1.27	0.71	1.12	0.90 lower
X62950mRNA_f_at	X62950			2.27	0.56	1.28	0.69	1.56	0.88 lower
D83598_at	D83598			1.57	0.82	1.28	0.83	1.29	1.06 lower
rc_AI180288_s_at	AI180288			1.60	0.80	1.28	0.80	1.29	1.03 lower
M83567_s_at	M83567			1.74	0.74	1.28	0.69	1.19	0.88 lower
rc_AA998683_at	AA998683			1.57	0.83	1.29	0.83	1.30	1.07 lower
U50842_at	U50842			1.71	0.76	1.29	0.75	1.28	0.97 lower
M94557_s_at	M94557			1.82	0.71	1.30	0.71	1.30	0.93 lower
D15069_s_at	D15069			2.07	0.63	1.30	0.81	1.67	1.05 lower
rc_AA819643_at	AA819643			1.61	0.81	1.30	0.70	1.13	0.91 lower
U78090_s_at	U78090			1.61	0.82	1.32	0.73	1.18	0.96 lower
D14421_at	D14421			1.62	0.82	1.32	0.71	1.15	0.94 lower
rc_AI235492_at	AI235492			1.62	0.82	1.33	0.70	1.13	0.94 lower

rc_AA893980_at	AA893980	1.77	0.77	1.36	0.77	1.37	1.05 lower
rc_AA892598_g_at	AA892598	1.70	0.80	1.36	0.73	1.24	0.99 lower
rc_AA891803_at	AA891803	1.70	0.82	1.39	0.60	1.02	0.84 lower
rc_AA893870_g_at	AA893870	1.90	0.74	1.41	0.80	1.51	1.12 lower
rc_AI009141_at	AI009141	1.92	0.74	1.43	0.62	1.19	0.88 lower
L19180_g_at	L19180	1.74	0.83	1.44	0.64	1.11	0.92 lower
J03025_at	J03025	1.92	0.75	1.45	0.60	1.14	0.86 lower
rc_AA892394_g_at	AA892394	1.77	0.82	1.46	0.64	1.14	0.94 lower
S79213_at	S79213	1.78	0.82	1.46	0.66	1.18	0.96 lower
U77697_at	U77697	1.89	0.77	1.46	0.81	1.54	1.19 lower
U97146_at	U97146	1.90	0.77	1.46	0.72	1.36	1.05 lower
X61296cds#2_f_at	X61296	2.10	0.70	1.47	0.69	1.44	1.01 lower
D25543_at	D25543	1.80	0.82	1.47	0.68	1.22	0.99 lower
rc_AA894312_at	AA894312	2.02	0.73	1.47	0.79	1.59	1.16 lower
U09229_at	U09229	1.80	0.82	1.47	0.69	1.24	1.01 lower
rc_AI229637_at	AI229637	1.98	0.75	1.48	0.79	1.56	1.17 lower
AB017655_s_at	AB017655	1.83	0.81	1.49	0.65	1.18	0.96 lower
AB017912_g_at	AB017912	1.88	0.80	1.50	0.80	1.51	1.20 lower
rc_AA858626_at	AA858626	1.89	0.81	1.54	0.73	1.38	1.12 lower
Z14118cds_g_at	Z14118	2.08	0.74	1.54	0.72	1.49	1.10 lower
U32575_at	U32575	2.01	0.78	1.57	0.62	1.25	0.98 lower
AA686579_at	AA686579	2.23	0.72	1.60	0.65	1.45	1.04 lower
U90888_at	U90888	2.50	0.65	1.63	0.62	1.54	1.00 lower
U15550_at	U15550	2.50	0.65	1.63	0.66	1.64	1.07 lower
AF059678_s_at	AF059678	2.13	0.77	1.63	0.56	1.20	0.92 lower
J02998_at	J02998	2.16	0.76	1.64	0.63	1.36	1.04 lower
rc_AI639343_at	AI639343	2.58	0.64	1.65	0.52	1.33	0.85 lower
U64030_at	U64030	2.01	0.82	1.65	0.61	1.23	1.01 lower
U87971_g_at	U87971	2.26	0.74	1.68	0.70	1.59	1.18 lower
rc_AA875506_at	AA875506	2.31	0.74	1.70	0.66	1.51	1.11 lower
U91847_s_at	U91847	2.09	0.82	1.71	0.61	1.27	1.04 lower
U42755_at	U42755	2.17	0.81	1.76	0.48	1.04	0.85 lower
D10754_at	D10754	2.24	0.80	1.78	0.55	1.23	0.98 lower
S56464mRNA_at	S56464	2.27	0.78	1.78	0.59	1.34	1.05 lower
L15354_s_at	L15354	2.61	0.69	1.80	0.58	1.51	1.04 lower
S81497_s_at	S81497	2.33	0.80	1.86	0.57	1.33	1.06 lower
U13895_s_at	U13895	2.68	0.70	1.87	0.45	1.21	0.84 lower

AF084205_at	AF084205	2.29	0.82	1.88	0.58	1.32	1.09 lower
rc_AI014091_at	AI014091	2.54	0.74	1.88	0.62	1.57	1.17 lower
D10938exon_s_at	D10938	2.37	0.80	1.91	0.54	1.28	1.03 lower
rc_AA800908_at	AA800908	2.38	0.80	1.91	0.48	1.14	0.91 lower
Y09333_g_at	Y09333	2.43	0.82	2.00	0.44	1.08	0.89 lower
AF087839mRNA#2_f_at	AF087839	2.85	0.70	2.01	0.50	1.42	1.00 lower
M58287_s_at	M58287	2.61	0.79	2.05	0.45	1.18	0.93 lower
AF021935_at	AF021935	2.55	0.81	2.07	0.51	1.30	1.05 lower
L04760_at	L04760	2.77	0.80	2.21	0.44	1.23	0.98 lower
rc_AI233365_at	AI233365	3.03	0.80	2.43	0.45	1.36	1.09 lower
rc_AI231354_at	AI231354	3.40	0.74	2.52	0.37	1.27	0.94 lower
J03481mRNA_at	J03481	3.15	0.81	2.56	0.35	1.11	0.90 lower
AF099093_g_at	AF099093	3.31	0.81	2.68	0.33	1.09	0.88 lower
AJ007632_s_at	AJ007632	3.65	0.75	2.74	0.37	1.35	1.02 lower
U31599_at	U31599	3.91	0.74	2.88	0.39	1.54	1.14 lower
AF061242_s_at	AF061242	3.61	0.82	2.95	0.31	1.10	0.90 lower
Y09333_at	Y09333	6.61	0.79	5.21	0.17	1.11	0.87 lower

Table 1.7
Genes corresponding to Figure 5, Profile 7

Probe Set	Accession #	Gene	Function	FV/F	FS/FV	FS/F	F/NF	FV/NF	FS/NF	Probability
AF031430_at	AF031430	Stx7: syntaxin 7	intracellular protein transport	1.11	0.58	0.64	1.25	1.39	0.81	highest
rc_AA800708_at	AA800708	unknown	unknown	0.87	0.77	0.67	1.24	1.08	0.83	highest
rc_AI169756_s_at	AI169756			0.22	0.80	0.18	4.33	0.97	0.78	high
rc_AI639394_at	AI639394			0.68	0.73	0.50	1.47	1.00	0.73	high
J03179_g_at	J03179			0.66	0.82	0.54	1.47	0.97	0.80	high
rc_AI638984_at	AI638984			0.74	0.74	0.54	1.23	0.90	0.67	high
AF000901_s_at	AF000901			0.83	0.70	0.58	1.36	1.13	0.79	high
rc_AA893043_at	AA893043			0.76	0.77	0.59	1.31	1.00	0.78	high
rc_AI228675_at	AI228675			0.75	0.79	0.59	1.26	0.94	0.75	high
J02589mRNA#2_at	J02589			0.78	0.79	0.62	1.26	0.98	0.77	high
U34843_g_at	U34843			0.82	0.76	0.62	1.23	1.01	0.77	high
U90312_at	U90312			0.80	0.80	0.64	1.24	0.99	0.79	high
rc_AA894086_g_at	AA894086			0.79	0.81	0.64	1.24	0.98	0.79	high
AF082834_s_at	AF082834			0.51	1.22	0.62	1.24	0.63	0.76	lower

Table 1.8
Genes corresponding to Figure 5, Profile 8

Probe Set	Accession #	Gene	Function	FV/F	FS/FV	FS/F	F/NF	FV/NF	FS/NF	Probability
rc_AI011376_at	AI011376			1.36	1.24	1.69	0.77	1.05	1.30	high
U83883_at	U83883			1.45	1.23	1.78	0.68	0.98	1.21	high
S53987_at	S53987			1.42	1.39	1.97	0.67	0.95	1.32	high
M65251_s_at	M65251			1.71	1.22	2.09	0.72	1.24	1.51	high
rc_AA875500_at	AA875500			1.28	1.69	2.17	0.81	1.03	1.75	high
X51531cds_g_at	X51531	atrial myosin light chain 1	myosin/Ca-binding/muscle contraction/cytoskeleton/heart	0.73	3.06	2.23	0.74	0.54	1.66	high
L26525_at	L26525			1.62	1.38	2.24	0.56	0.91	1.25	high
D26154cds_at	D26154			1.86	1.21	2.25	0.63	1.18	1.42	high
rc_AI008836_s_at	AI008836			1.87	1.23	2.29	0.76	1.43	1.75	high
M96601_at	M96601			2.17	1.22	2.64	0.64	1.40	1.70	high
M86870_at	M86870			3.32	1.22	4.04	0.33	1.10	1.34	high
rc_AA894027_at	AA894027			5.77	1.58	9.09	0.21	1.22	1.92	high
X62951mRNA_s_at	X62951	RNPBUS19, pBUS19	unknown	1.76	6.42	11.28	0.15	0.26	1.64	high
rc_AI230228_at	AI230228			1.90	0.77	1.47	0.82	1.56	1.20	lower
rc_AA892630_at	AA892630			2.13	0.77	1.63	0.75	1.59	1.22	lower
D13623_g_at	D13623			2.14	0.78	1.67	0.81	1.72	1.35	lower
rc_AA800930_at	AA800930			2.06	0.83	1.71	0.75	1.54	1.28	lower
U06434_at	U06434			2.39	0.72	1.73	0.79	1.89	1.36	lower
AF065387_g_at	AF065387			2.45	0.73	1.79	0.76	1.87	1.36	lower
S56937_s_at	S56937			2.76	0.65	1.80	0.71	1.97	1.28	lower
S68135_s_at	S68135			2.88	0.63	1.81	0.70	2.03	1.28	lower
Y09507_at	Y09507			2.39	0.78	1.86	0.76	1.81	1.41	lower
rc_AA925762_at	AA925762			3.14	0.61	1.90	0.74	2.33	1.41	lower
rc_AI179610_at	AI179610			3.84	0.50	1.92	0.66	2.52	1.26	lower
D30649mRNA_s_at	D30649			2.63	0.76	1.99	0.83	2.17	1.65	lower
AF087944mRNA_s_at	AF087944			2.80	0.74	2.07	0.72	2.01	1.48	lower
U13396_g_at	U13396			2.75	0.76	2.10	0.70	1.92	1.46	lower
X83579_at	X83579			2.88	0.75	2.15	0.72	2.09	1.55	lower
M92059_s_at	M92059			3.55	0.62	2.19	0.77	2.72	1.68	lower
AF052596_at	AF052596			2.84	0.79	2.25	0.53	1.52	1.21	lower
rc_AI231354_g_at	AI231354			3.13	0.74	2.31	0.53	1.66	1.22	lower

U93306_at	U93306			3.80	0.61	2.33	0.53	2.02	1.24 lower
D42145_at	D42145			3.04	0.80	2.44	0.53	1.61	1.29 lower
AB006881mRNA_at	AB006881			3.01	0.82	2.47	0.50	1.51	1.24 lower
rc_AI104012_at	AI104012			3.32	0.81	2.69	0.52	1.74	1.41 lower
AF100470_at	AF100470			3.42	0.82	2.79	0.48	1.64	1.34 lower
X64403_at	X64403			3.67	0.76	2.80	0.49	1.78	1.36 lower
U31599_g_at	U31599			3.80	0.75	2.86	0.46	1.76	1.33 lower
M14656_at	M14656			3.95	0.81	3.21	0.74	2.91	2.36 lower
M10094_g_at	M10094			6.26	0.65	4.07	0.42	2.63	1.71 lower
X53054_at	X53054			6.94	0.61	4.24	0.81	5.62	3.43 lower
M31038_at	M31038			7.18	0.77	5.52	0.57	4.07	3.13 lower
Z78279_g_at	Z78279			9.32	0.65	6.08	0.66	6.13	4.00 lower
M80367_at	M80367			10.24	0.75	7.70	0.78	8.02	6.03 lower
J02722cds_at	J02722	Hmox1: Heme oxygenase	heme catabolism/cell cycle/signal transduction/cell survival	21.27	0.40	8.54	0.18	3.89	1.56 lower

Table 1.9
Genes corresponding to Figure 5, Profile 9

Probe Set	Accession #	Gene	Function	FV/F	FS/FV	FS/F	F/NF	FV/NF	FS/NF	Probability
S65355_at	S65355	Ednrb: endothelin receptor type B	signal transduction/G protein coupled receptor/Ca-signaling/vasoactive/cell cycle/development/ECM	0.93	1.32	1.23	1.23	1.14	1.51	highest
AB005143_s_at	AB005143	Ucp2: Uncoupling protein 2, mitochondrial	energy homeostasis/mitochondrial/Ca	1.03	1.25	1.29	1.29	1.33	1.66	highest
X14221_at	X14221	Sftpc: Surfactant, pulmonary-associated protein C	lung surfactant for gas exchange	0.93	1.43	1.33	1.43	1.33	1.90	highest
L23128_g_at	L23128	RT1-N1: RT1 class Ib gene, H2-TL-like, grc region	MHC Class I/growth control/development	1.06	1.43	1.51	1.33	1.40	2.01	highest
X89963_at	X89963	Thbs4: thrombospondin 4	cell adhesion/cell motility/Ca-binding/development	1.10	1.40	1.54	1.61	1.78	2.48	highest
U44948_at	U44948	Csrp2: cysteine rich protein 2	myoblast differentiation/development/signal transduction	1.15	1.57	1.81	1.61	1.84	2.90	highest
X51529_at	X51529	Pla2g2a: phospholipase A2, group IIA (platelets, synovial fluid)	Ca-binding/Ca-dependant phospholipase A2 signaling activity/cell cycle	1.15	1.77	2.05	1.74	2.01	3.57	highest
X53858_at	X53858			0.80	1.65	1.33	1.33	1.07	1.77	high
M84488_at	M84488			1.35	1.45	1.96	2.63	3.56	5.17	high
L18948_at	L18948			1.40	1.70	2.39	5.01	7.03	11.95	high
D64045_s_at	D64045			1.55	1.84	2.84	1.65	2.55	4.68	high
rc_AA957003_at	AA957003			1.76	1.72	3.02	1.43	2.51	4.33	high
U42719_at	U42719			2.17	1.40	3.03	1.45	3.15	4.41	high
U09256_at	U09256			1.49	0.81	1.21	1.23	1.84	1.49	lower
U77038_g_at	U77038			1.58	0.78	1.24	1.24	1.97	1.54	lower
X52711_at	X52711			1.66	0.76	1.27	1.28	2.13	1.63	lower
M98820_at	M98820			1.67	0.76	1.27	1.69	2.82	2.15	lower
D85189_at	D85189			1.90	0.68	1.29	1.22	2.32	1.58	lower
S82383_s_at	S82383			1.58	0.83	1.31	1.60	2.52	2.09	lower
AJ005394_at	AJ005394			1.58	0.83	1.31	1.25	1.97	1.64	lower
M58364_at	M58364			1.67	0.79	1.32	1.24	2.07	1.64	lower
S79676_s_at	S79676			1.97	0.68	1.34	1.25	2.46	1.68	lower
X17053cds_s_at	X17053			1.80	0.76	1.37	1.61	2.90	2.21	lower

AF029240_at	AF029240			1.87	0.74	1.37	1.30	2.42	1.78	lower
rc_AI237535_s_at	AI237535			1.75	0.82	1.44	1.27	2.24	1.84	lower
rc_AI070295_at	AI070295			2.17	0.67	1.46	1.27	2.76	1.86	lower
rc_AA799861_g_at	AA799861			2.94	0.51	1.50	1.96	5.78	2.94	lower
rc_AA799861_at	AA799861			2.66	0.57	1.50	2.85	7.58	4.29	lower
U28938_at	U28938			1.84	0.82	1.51	1.33	2.44	2.00	lower
X17053mRNA_s_at	X17053			2.03	0.75	1.52	2.46	4.99	3.74	lower
rc_AA875531_s_at	AA875531			2.25	0.69	1.54	1.58	3.55	2.44	lower
X06916_at	X06916			1.91	0.83	1.58	2.20	4.20	3.49	lower
U57362_at	U57362			2.86	0.56	1.60	1.68	4.81	2.69	lower
rc_AI639103_s_at	AI639103			2.16	0.77	1.66	1.85	4.00	3.07	lower
S76779_s_at	S76779			2.30	0.73	1.68	1.36	3.14	2.29	lower
rc_AI179399_at	AI179399			2.66	0.66	1.75	1.33	3.54	2.33	lower
U14647_at	U14647			2.47	0.82	2.03	1.21	2.98	2.45	lower
J02962_at	J02962			2.64	0.78	2.06	1.46	3.85	3.01	lower
X05834_at	X05834			3.33	0.64	2.15	1.82	6.07	3.91	lower
rc_AI231472_s_at	AI231472			3.19	0.70	2.24	1.84	5.87	4.13	lower
rc_AA894029_at	AA894029			2.87	0.80	2.30	1.27	3.64	2.92	lower
U10894_s_at	U10894			3.01	0.76	2.30	1.52	4.57	3.49	lower
AF050214_at	AF050214			4.20	0.59	2.46	1.45	6.10	3.57	lower
AJ222813_s_at	AJ222813			3.24	0.79	2.56	1.52	4.94	3.90	lower
X57523_g_at	X57523			4.74	0.67	3.18	1.57	7.42	4.98	lower
rc_AI169327_g_at	AI169327			4.97	0.74	3.67	2.52	12.55	9.26	lower
rc_AA894092_at	AA894092			7.02	0.56	3.90	4.79	33.63	18.70	lower
Z78279_at	Z78279	Col1a1: collagen, type 1, alpha 1	collagen/ECM	10.89	0.49	5.29	1.46	15.90	7.73	lower
M98049_s_at	M98049			9.54	0.66	6.26	3.30	31.45	20.64	lower

Table 1.10
Genes corresponding to Figure 5, Profile 10

Probe Set	Accession #	Gene	Function	FV/F	FS/FV	FS/F	F/NF	FV/NF	FS/NF	Probability
rc_AA891839_at	AA891839	unknown	unknown	0.84	0.70	0.59	0.76	0.64	0.45	highest
rc_AI233219_at	AI233219	Esm1: endothelial cell-specific molecule 1	growth factor	0.89	0.78	0.70	0.75	0.67	0.52	highest
U14950_at	U14950	Dlgh1: discs, large homolog 1 (Drosophila)	cytoskeleton/guanylate kinase	0.97	0.74	0.72	0.76	0.74	0.55	highest
rc_AI638988_at	AI638988	unknown	unknown	1.00	0.77	0.77	0.79	0.79	0.61	highest
rc_AA892863_at	AA892863	similar to hs MTCH2: mitochondrial carrier homolog 2 (C. elegans)	transport	1.09	0.74	0.81	0.80	0.87	0.65	highest
rc_AA799656_at	AA799656	similar to MRPS31: mitochondrial ribosomal protein S31	ribosome/mitochondrion	1.03	0.79	0.82	0.83	0.86	0.68	highest
U92564_g_at	U92564			1.61	0.50	0.80	0.74	1.19	0.59	high

Table 2:
This is a list of all the 226 candidate gene for encoding natural adaptive responses to aortic banding that are needed for clinical non-failure. Those genes correspond to the genes depicted in Figure 6. The different fold changes that were used in the analysis are also found in the table. Genes were ordered according to F/NF fold change. Genes were this fold change is < 0.5 or > 2 are shaded in gray.

Table 2.1
Genes corresponding to Figure 6, Profile 1

Probe Set	Accession #	Gene	Function	FV/F	FS/FV	FS/F	F/NF	FV/NF	FS/NF
rc_AA818982_at	AA818982	Tmpo: thymopoietin	DNA binding/transcription/cell cycle	1.14	0.88	1.00	0.51	0.58	0.51
rc_AA799883_at	AA799883	unknown	unknown	1.05	0.97	1.02	0.57	0.60	0.58
rc_AA893160_at	AA893160	unknown	unknown	0.97	1.12	1.09	0.57	0.56	0.63
J02827_at	J02827	Bckdha: branched chain keto acid dehydrogenase subunit E1, alpha polypeptide	keto acid metabolism/energy production/mitochondrion	1.14	0.88	1.00	0.58	0.66	0.58
AB009999_g_at	AB009999	Cds1: CDP-diacylglycerol synthase (phosphatidate cytidylyltransferase) 1	lipid metabolism/signal transduction/Ca-signaling/mitochondrion+ER	1.08	1.04	1.12	0.61	0.66	0.68
Z49858_at	Z49858	TM4SF11: transmembrane 4 superfamily member 11 (plasmolipin)	ion channel	1.06	0.84	0.89	0.62	0.66	0.56
AF062740_g_at	AF062740	PDP1: pyruvate dehydrogenase phosphatase isoenzyme 1	signal transduction/carbohydrate metabolism/energy production	1.18	1.00	1.18	0.63	0.75	0.75
X06889cds_at	X06889	RAB3A: RAB3A, member RAS oncogene family	GTPase signal transduction/oncogene	1.02	1.02	1.04	0.64	0.65	0.66
M84719_at	M84719	Fmo1: flavin containing monooxygenase 1	oxidation of amino-trimethylamine	1.12	1.07	1.19	0.66	0.74	0.78
rc_AA859508_at	AA859508	unknown	unknown	1.14	0.92	1.05	0.66	0.75	0.69
AJ001320_at	AJ001320	Mpdz: multiple PDZ domain protein	unknown	1.09	0.95	1.04	0.66	0.72	0.69
rc_AA891499_at	AA891499	unknown	unknown	1.10	1.06	1.16	0.66	0.73	0.77
rc_AA892280_at	AA892280	unknown	unknown	1.13	1.02	1.15	0.66	0.75	0.76
rc_AA891962_at	AA891962	unknown	unknown	1.16	0.94	1.09	0.67	0.77	0.73
D82074_at	D82074	NEUROD1: neurogenic differentiation 1	transcription factor/differentiation/insulin transcription/development	1.12	0.86	0.96	0.67	0.74	0.64
rc_AA891069_at	AA891069	similar to SRPK2: SFRS protein kinase 2	serine-threonine kinase/signal transduction	1.17	1.00	1.16	0.67	0.78	0.78
L15618_at	L15618	CSNK2A1: casein kinase 2, alpha 1 polypeptide	serine-threonine kinase/signal transduction/cell cycle	1.04	1.05	1.09	0.68	0.70	0.74
rc_AA859975_at	AA859975	SLC25A11: solute carrier family 25 (mitochondrial carrier; oxoglutarate carrier), member 11	oxoglutarate carrier/energy production/mitochondrion	1.16	1.02	1.18	0.68	0.79	0.80
rc_AI231547_at	AI231547	Fkbp4: FK506 binding protein 4	protein folding/steroid receptor trafficking/immunoregulation/Hsp binding/cell cycle	1.05	1.11	1.17	0.68	0.72	0.80
U22830_at	U22830	P2RY1: purinergic receptor P2Y, G-protein coupled, 1	signal transduction/G-protein receptor for ATP-ADP/Ca-signaling/platelets	0.96	0.98	0.94	0.69	0.66	0.64
rc_AA799421_at	AA799421	PRKCE: protein kinase C, epsilon	signal transduction/apoptosis/kinase	1.17	0.84	0.98	0.69	0.81	0.68

rc_AA800036_at	AA800036	similar to SCHIP1: schwannomin interacting protein 1	cytoskeleton	1.14	1.03	1.18	0.69	0.79	0.82
rc_AA892799_s_at	AA892799	similar to GRHPR: glyoxylate reductase/hydroxypyruvate reductase	metabolism/energy production	1.08	0.92	1.00	0.70	0.75	0.70
U68417_at	U68417	BCAT2: branched chain aminotransferase 2, mitochondrial	amino acid metabolism/mitochondrion	1.15	0.95	1.09	0.70	0.80	0.76
rc_AI639155_at	AI639155	similar to C20orf36: chromosome 20 open reading frame 36	protein modification	1.13	0.99	1.12	0.71	0.80	0.79
rc_AA875023_at	AA875023	unknown	unknown	1.07	0.94	1.00	0.71	0.75	0.71
U10357_at	U10357	PDK2: pyruvate dehydrogenase kinase, isoenzyme 2	signal transduction/glucose metabolism/energy production/mitochondrion	1.19	0.94	1.13	0.71	0.85	0.80
rc_AI102838_s_at	AI102838	IVD: isovaleryl Coenzyme A dehydrogenase	amino acid catabolism/energy production/mitochondrion	1.19	0.97	1.16	0.71	0.85	0.82
rc_AA800120_at	AA800120	SLC25A20: solute carrier family 25 (carnitine/acylcarnitine translocase), member 20	fatty acid transport for oxidation/energy production/mitochondrion	1.13	0.99	1.12	0.71	0.80	0.80
rc_AA892271_at	AA892271	unknown	unknown	1.18	0.88	1.03	0.72	0.84	0.74
rc_AI228548_at	AI228548	S100A1: S100 calcium binding protein A1	Ca-binding/Ca-induced Ca release/cell cycle/intracellular signaling	1.11	0.87	0.96	0.72	0.80	0.69
rc_AA891037_g_at	AA891037	similar to RPL3L: ribosomal protein L3-like	ribosome/specific to heart and muscle	1.04	0.96	1.00	0.73	0.75	0.73
rc_H31982_at	H31982	similar to ELAVL1: ELAV (embryonic lethal, abnormal vision, Drosophila)-like 1 (Hu antigen R)	mRNA catabolism/cell cycle/renin production	1.13	0.97	1.10	0.73	0.83	0.80
D90109_at	D90109	ACSL1: acyl-CoA synthetase long-chain family member 1	fatty acid metabolism/energy production	1.05	0.96	1.01	0.73	0.77	0.74
U26356mRNA_s_at	U26356	S100A1: S100 calcium binding protein A1	Ca-binding/Ca-induced Ca release/cell cycle/intracellular signaling	1.03	1.07	1.11	0.74	0.76	0.82
rc_AA875428_at	AA875428	similar to TCTA: T-cell leukemia translocation altered gene	unknown	1.03	1.03	1.06	0.74	0.76	0.78
rc_AI044900_s_at	AI044900	ACSL1: acyl-CoA synthetase long-chain family member 1	fatty acid metabolism/energy production	1.08	1.00	1.08	0.74	0.80	0.80
rc_AA892821_at	AA892821	AKR7A2: aldo-keto reductase family 7, member A2 (aflatoxin aldehyde reductase)	carbohydrate metabolism/detoxification/energy production	1.05	0.97	1.02	0.74	0.78	0.75
L00370cds_s_at	L00370	embryonic skeletal muscle myosin heavy chain gene	myosin/cytoskeleton/muscle/development	1.00	1.00	1.00	0.74	0.74	0.74
rc_AA859788_at	AA859788	similar to MRPS11: mitochondrial ribosomal protein S11	ribosome/mitochondrion	1.13	0.99	1.11	0.74	0.84	0.83
rc_AA800275_at	AA800275	unknown	unknown	1.10	0.88	0.97	0.75	0.82	0.73
U16802_at	U16802	CADPS: Ca2+-dependent activator protein for secretion	Ca-binding/exocytosis	1.09	0.90	0.98	0.75	0.81	0.74

D28561_s_at	D28561	SLC2A4: solute carrier family 2 (facilitated glucose transporter), member 4	glucose transporter/insulin	0.97	1.00	0.98	0.75	0.73	0.73
rc_AA859468_at	AA859468	similar to SHB: SHB (Src homology 2 domain containing) adaptor protein B	SH3/SH2 adaptor protein/intracellular signaling cascade/cell cycle	1.06	1.02	1.08	0.75	0.80	0.81
D26439_at	D26439	CD1D: CD1D antigen, d polypeptide	antigen presentation/immune response	1.04	1.00	1.04	0.75	0.78	0.78
V01216_at	V01216	Orm1: orosomucoid 1	acute phase reactant/inflammatroy response	1.00	1.02	1.02	0.75	0.75	0.77
rc_AA891521_at	AA891521	unknown	unknown	1.01	1.06	1.07	0.75	0.76	0.81
rc_AA892808_at	AA892808	IDH3G: isocitrate dehydrogenase 3 (NAD+) gamma	aa metabolism/rate limiting step of TCA/energy production/mitochondrion	1.03	0.98	1.00	0.76	0.77	0.76
D13376_at	D13376	Ak1: adenylate kinase 1	ATP metabolism/cell cycle/protein kinase	1.14	0.96	1.10	0.76	0.87	0.83
rc_AA892547_at	AA892547	unknown	unknown	1.19	0.89	1.06	0.76	0.90	0.81
AB012234_g_at	AB012234	NFIX: nuclear factor I/X (CCAAT-binding transcription factor)	transcription factor/DNA replication	1.10	0.96	1.06	0.76	0.84	0.81
rc_AI232256_at	AI232256	CYB5-M: cytochrome b5 outer mitochondrial membrane precursor	steroid biosynthesis/mitochondria	1.03	1.01	1.03	0.76	0.79	0.79
rc_AA799779_g_at	AA799779	GNPAT: glyceronephosphate O-acyltransferase	fatty acid metabolism/development	1.10	0.88	0.96	0.77	0.84	0.73
rc_AI012275_at	AI012275	C5orf12: chromosome 5 open reading frame 12	unknown	1.16	0.88	1.02	0.77	0.89	0.78
AB015724_at	AB015724	CGI-63: nuclear receptor binding factor 1	transcription factor/energy production	1.06	0.88	0.93	0.77	0.81	0.71
J05571_s_at	J05571	MAT2A: methionine adenosyltransferase II, alpha	one carbon compound metabolism	1.01	0.96	0.97	0.77	0.78	0.74
X05341_at	X05341	Acaa2: acetyl-Coenzyme A acyltransferase 2 (mitochondrial 3-oxoacyl-Coenzyme A thiolase)	fatty acid catabolism/energy production/mitochondria	1.05	1.00	1.05	0.77	0.81	0.80
X16554_at	X16554	PRPS1: phosphoribosyl pyrophosphate synthetase 1	amino acid and nucleotide metabolism	1.13	0.90	1.01	0.77	0.87	0.78
AF035943_at	AF035943	UCP3: uncoupling protein 3 (mitochondrial, proton carrier)	energy production/mitochondrion	1.16	0.91	1.05	0.77	0.90	0.81
rc_AA799531_at	AA799531	similar to NS3TP1: HCV NS3-transactivated protein 1	amino acid metabolism	1.12	0.85	0.95	0.77	0.87	0.74
rc_AA875129_at	AA875129	similar to ELP4: elongation protein 4 homolog (S. cerevisiae)	translation	1.04	1.03	1.07	0.78	0.80	0.83
rc_AA891800_at	AA891800	unknown	unknown	0.96	0.97	0.94	0.78	0.75	0.73
rc_AI638960_g_at	AI638960	unknown	unknown	1.05	0.91	0.95	0.78	0.82	0.74
rc_AA799804_at	AA799804	unknown	unknown	1.12	0.95	1.07	0.78	0.87	0.83
L20427_at	L20427	Coq3: coenzyme q (ubiquinone) biosynthetic enzyme 3	one carbon compound metabolism	1.16	0.86	0.99	0.78	0.90	0.77
rc_AA891790_at	AA891790	unknown	unknown	1.04	0.91	0.95	0.79	0.82	0.75
rc_AA891524_at	AA891524	unknown	unknown	1.08	0.90	0.97	0.79	0.85	0.76

J03190_g_at	J03190	Alas1: aminolevulinic acid synthase 1	heme biosynthesis/mitochondrion	0.85	1.18	1.01	0.79	0.67	0.80
rc_AA800745_at	AA800745	Alad: aminolevulinate, delta-, dehydratase	heme biosynthesis	1.09	0.89	0.98	0.79	0.86	0.77
rc_AA799594_at	AA799594	unknown	unknown	1.02	0.97	0.99	0.79	0.81	0.79
D37880_at	D37880	TYRO3: TYRO3 protein tyrosine kinase	signal transduction/receptor tyrosine kinase	0.97	1.01	0.98	0.79	0.77	0.78
U53486mRNA_s_at	U53486	corticotropin releasing factor receptor	response to stress/immune response/development/cell cycle/G protein coupled receptor/signal transduction	1.16	0.89	1.03	0.79	0.92	0.82
rc_AI639451_at	AI639451	unknown	unknown	0.91	1.03	0.93	0.80	0.72	0.75
M75148_at	M75148	KNS2: kinesin 2 60/70kDa	cytoskeleton/motor activity	0.90	1.09	0.97	0.80	0.72	0.78
X74227cds_at	X74227	ITPKB: inositol 1,4,5-trisphosphate 3-kinase B	signal transduction/Ca-Calmodulin binding/kinase/IP3	1.05	0.94	0.99	0.80	0.84	0.79
rc_AA800184_at	AA800184	unknown	unknown	1.11	0.86	0.95	0.80	0.89	0.76
rc_AA799464_at	AA799464	TIMM8B: translocase of inner mitochondrial membrane 8 homolog B (yeast)	protein translocase/mitochondrion	1.07	0.84	0.90	0.80	0.86	0.73
rc_AA800210_at	AA800210	CSNK2A1: casein kinase 2, alpha 1 polypeptide	serine-threonine kinase/signal transduction/cell cycle	1.13	0.89	1.01	0.81	0.91	0.81
X01785_at	X01785	MOX2: antigen identified by monoclonal antibody MRC OX-2	cell surface immunoglobulin/immune response	1.11	0.93	1.03	0.81	0.90	0.83
rc_AA799299_at	AA799299	similar to AK5: adenylate kinase 5	nucleotide metabolism/kinase	1.05	0.94	0.99	0.81	0.85	0.80
U95920_at	U95920	PCM1: pericentriolar material 1	transcription	1.05	0.97	1.02	0.81	0.85	0.83
M25888_at	M25888	PLP1: proteolipid protein 1 (Pelizaeus-Merzbacher disease, spastic paraplegia 2, uncomplicated)	myelination	0.94	0.95	0.90	0.81	0.76	0.73
rc_AA891311_at	AA891311	unknown	unknown	0.96	0.92	0.88	0.82	0.78	0.72
X14265_at	X14265	CALM3: calmodulin 3 (phosphorylase kinase, delta)	Ca-Camodulin binding/kinase/signal transduction	1.01	0.99	1.01	0.82	0.83	0.82
AF071204_g_at	AF071204	KITLG: KIT ligand	signal transduction/cell cycle/cell migration/development/hematopoesis/growth factor	1.03	0.95	0.98	0.82	0.84	0.80
J02749_at	J02749	ACAA1: acetyl-Coenzyme A acyltransferase 1 (peroxisomal 3-oxoacyl-Coenzyme A thiolase)	fatty acid metabolism/energy production	1.11	0.87	0.96	0.82	0.91	0.79
rc_AA875198_at	AA875198	unknown	unknown	1.06	0.91	0.96	0.82	0.87	0.79
rc_AA874955_s_at	AA874955	CLTB: clathrin, light polypeptide (Lcb)	Ca-binding/receptor-mediated endocytosis	0.92	0.96	0.88	0.82	0.75	0.72
M18467_at	M18467	GOT2: glutamic-oxaloacetic transaminase 2, mitochondrial (aspartate aminotransferase 2)	amino acid metabolism/mitochondrion	1.07	0.94	1.00	0.82	0.88	0.83
U08976_at	U08976	Ech1: enoyl coenzyme A hydratase 1	fatty acid catabolism/energy production/mitochondrion	1.04	0.97	1.01	0.82	0.86	0.83

M36074_at	M36074	NR3C2: nuclear receptor subfamily 3, group C, member 2	signal transduction/hypertension/mineralocorticoid steroid hormone receptor/sodium ion homeostasis/transcription factor	1.10	0.92	1.01	0.82	0.90	0.83
rc_AA891037_at	AA891037	similar to RPL3L: ribosomal protein L3-like	ribosome/muscle and heart	0.97	1.03	0.99	0.82	0.79	0.82
rc_AA957961_at	AA957961	D1S155E: NRAS-related gene	transcription factor/DNA binding/RNA binding/development	1.14	0.84	0.97	0.83	0.94	0.80
rc_AA799879_at	AA799879	SYNGR1: synaptogyrin 1	Ca-binding/synaptic vesicles exocytosis	0.91	1.07	0.98	0.83	0.75	0.81
rc_AA892380_at	AA892380	unknown	unknown	1.17	0.84	0.99	0.83	0.97	0.82
rc_AA891864_at	AA891864	similar to AGTPBP1: ATP/GTP binding protein 1	amino acid metabolism	1.16	0.85	0.99	0.83	0.97	0.83
rc_AA891802_at	AA891802	similar to Cyhr1: cysteine and histidine rich 1	unknown	0.96	0.97	0.94	0.83	0.80	0.78

Table 2.2
Genes corresponding to Figure 6, Profile 2

Probe Set	Accession #	Gene	Function	FV/F	FS/FV	FS/F	F/NF	FV/NF	FS/NF
rc_AA892578_at	AA892578	unknown	unknown	0.97	0.96	0.92	2.04	1.97	1.89
U53855_at	U53855	Ptgis: prostaglandin I2 synthase	vasodilator/inhibitor of platelet aggregation	0.93	1.10	1.02	1.99	1.85	2.03
rc_AA799992_g_at	AA799992	Similar to C11orf17	unknown	0.95	0.92	0.88	1.99	1.89	1.74
rc_AA799534_at	AA799534	unknown	unknown	1.03	0.93	0.96	1.98	2.04	1.90
rc_AA849769_g_at	AA849769	Fstl: follistatin-like	Ca-binding/autoantigen	0.89	1.09	0.97	1.96	1.74	1.89
rc_AI169104_at	AI169104	Similar to Platelet factor 4 precursor (PF-4) (CXCL4)	immune response/signaling/inhibitor of angiogenesis/platelet activation	1.03	0.92	0.95	1.92	1.97	1.82
X62952_at	X62952	VIM: vimentin	cytoskeleton	0.91	0.98	0.89	1.87	1.70	1.66
rc_AA799762_g_at	AA799762	similar to chromosome 20 open reading frame 149	unknown	1.06	0.97	1.03	1.83	1.94	1.88
J03627_at	J03627	S100A10: S100 calcium binding protein A10 (annexin II ligand, calpactin I, light polypeptide (p11))	Ca-binding/cell cycle/differentiation/interacts with K-channel	1.07	0.94	1.01	1.83	1.96	1.84
D00688_s_at	D00688	MAOA: monoamine oxidase A	catecholamine catabolism/mitochondrion	1.04	0.93	0.96	1.72	1.79	1.66
rc_AI136891_at	AI136891	ZFP36L1: zinc finger protein 36, C3H type-like 1	transcription factor/regulates response to growth factors	0.95	1.01	0.96	1.67	1.59	1.60
M58404_at	M58404	TMSB10: thymosin, beta 10	cytoskeleton	1.04	0.93	0.97	1.64	1.70	1.59
U42627_at	U42627	DUSP6: dual specificity phosphatase 6	cell-cycle/apoptosis/differentiation/serine-threonine phosphatase/targets MAP kinase/targeted by angiotensin II/signal trnasduction	0.91	1.07	0.97	1.64	1.49	1.59
Y13714_at	Y13714	SPARC: secreted protein, acidic, cysteine-rich (osteonectin)	Ca-binding/ECM synthesis/cell-shape/cell cycle/collagen-binding/angiogenesis	0.90	1.09	0.99	1.63	1.47	1.61
rc_AA893743_at	AA893743	Pkia: Protein kinase inhibitor, alpha	kinase inhibitor/signal transduction	0.91	0.97	0.89	1.62	1.48	1.44
L26268_at	L26268	BTG1: B-cell translocation gene 1, anti-proliferative	tumor suppressor/cell cycle/angiogenesis/myoblast differentiation/transcription factor	0.85	1.10	0.93	1.60	1.36	1.49
AF030091UTR#1_at	AF030091	CCNL1: cyclin L1	cell-cycle	1.03	0.92	0.95	1.59	1.64	1.52
L40362_f_at	L40362	RT1-Aw2: RT1 class Ib, locus Aw2	MHC class I /immune response/antigen presentation	1.07	0.97	1.04	1.59	1.70	1.65
D13417_g_at	D13417	HES1: hairy and enhancer of split 1, (Drosophila)	transcription factor/development	1.08	0.91	0.98	1.59	1.71	1.56
rc_AA800663_at	AA800663	similar to XPO7 exportin 7	nuclear transport	0.94	0.90	0.85	1.59	1.49	1.34
S45812_s_at	S45812	MAOA: monoamine oxidase A	catecholamine catabolism/mitochondrion	1.04	0.98	1.02	1.57	1.63	1.60

rc_AI234146_at	AI234146	CSRP1: cysteine and glycine-rich protein 1	transcription factor/differentiation/cell growth/development	0.94	1.02	0.96	1.56	1.46	1.50
rc_AA894259_at	AA894259	similar to 2010110M21Rik: RIKEN cDNA 2010110M21 gene	unknown	1.09	0.96	1.05	1.55	1.70	1.63
L23148_at	L23148	ID1: inhibitor of DNA binding 1, dominant negative helix-loop-helix protein	transcription factor/differentiation/cell growth/senescence/cell cycle	0.88	1.02	0.90	1.55	1.37	1.39
D00913_g_at	D00913	ICAM1: intercellular adhesion molecule 1 (CD54), human rhinovirus receptor	intercellular adhesion molecule/binds integrin	1.15	0.96	1.11	1.55	1.79	1.71
rc_AI639246_at	AI639246	similar to Xlkd1: extra cellular link domain-containing 1	receptor for cell adhesion	1.02	0.84	0.86	1.55	1.59	1.33
rc_AA799498_at	AA799498	NPPB: natriuretic peptide precursor B	receptor signal transduction/blood pressure/diuresis/natriuresis/vasoactive/negative regulation of cell growth and angiogenesis	0.89	1.20	1.06	1.55	1.38	1.65
U04835_at	U04835	Crem: cAMP responsive element modulator	transcription factor/signal transduction	0.91	1.13	1.03	1.52	1.37	1.56
X04979_at	X04979	APOE: apolipoprotein E	lipoprotein triglyceride catabolism	1.08	0.88	0.95	1.51	1.63	1.44
rc_AA859837_g_at	AA859837	GDA: guanine deaminase	nucleic acid metabolism/development	0.95	1.10	1.05	1.51	1.43	1.58
U72660_at	U72660	NINJ1: ninjurin 1	cell adhesion/development/tissue regeneration	1.17	0.85	1.00	1.50	1.75	1.50
Z24721_at	Z24721	SOD3: superoxide dismutase 3, extracellular	superoxide metabolism	1.03	1.15	1.18	1.50	1.54	1.77
AF041066_at	AF041066	ANG: angiogenin, ribonuclease, RNase A family, 5	potent angiogenesis factor/tRNA catabolism with decreased protein production	1.15	0.88	1.01	1.48	1.70	1.49
X01118_at	X01118	NPPA: natriuretic peptide precursor A	blood pressure regulation	0.98	1.08	1.07	1.47	1.45	1.57
rc_AA891940_at	AA891940	Similar to Potentail helicase MOV-10 (LOC310756)	RNA processing/development	0.84	1.08	0.91	1.47	1.24	1.34
X61295cds_s_at	X61295	L1 retroposon, ORF2 mRNA (partial)	unknown	0.94	0.92	0.86	1.46	1.38	1.27
AF087037_g_at	AF087037	Btg3: B-cell translocation gene 3	anti-proliferative/cell cycle	0.93	0.92	0.86	1.46	1.36	1.26
rc_AA892897_at	AA892897	PLOD2: procollagen-lysine, 2-oxoglutarate 5-dioxygenase (lysine hydroxylase) 2	collagen metabolism	1.07	0.89	0.95	1.45	1.55	1.38
D28560_g_at	D28560	ENPP2: ectonucleotide pyrophosphatase/phosphodiesterase 2 (autotaxin)	G protein coupled receptor signal transduction/nucleotide metabolism	1.03	0.84	0.86	1.44	1.49	1.25
J02780_at	J02780	TPM4: tropomyosin 4	cytoskeleton/muscle development	1.07	0.84	0.90	1.44	1.54	1.30
rc_AA891880_at	AA891880	Tricarboxylate carrier-like protein	cation transporter	0.91	0.97	0.89	1.44	1.31	1.28
X05566_i_at	X05566	Mrlcb: myosin regulatory light chain	myosin/Ca-binding/cytoskeleton	0.99	0.95	0.94	1.44	1.43	1.35
L25785_at	L25785	TSC22: transforming growth factor beta-stimulated protein TSC-22	transcription factor	1.00	1.12	1.11	1.43	1.43	1.59
X16145_at	X16145	FUCA1: fucosidase, alpha-L- 1, tissue	carbohydrate metabolism/glycosaminoglycan catabolism	1.01	0.92	0.93	1.43	1.45	1.33

rc_AA893611_s_at	AA893611	MXI1: MAX interacting protein 1	transcription factor/tumor suppressor/cell cycle	0.96	0.98	0.94	1.43	1.38	1.34
rc_AA799598_at	AA799598	Similar to pyruvate dehydrogenase	mitochondrion/glycolysis/energy production	0.95	0.99	0.94	1.42	1.35	1.33
rc_AI008888_at	AI008888	CSTB: cystatin B (stefin B)	protease inhibitor	1.07	1.05	1.12	1.42	1.52	1.59
rc_AA800790_at	AA800790	unknown	unknown	0.93	0.96	0.90	1.42	1.32	1.27
rc_AI011706_at	AI011706	similar to SFRS3: splicing factor, arginine/serine-rich 3	RNA processing	1.15	0.89	1.03	1.42	1.63	1.45
rc_AA799340_at	AA799340	TIMP2: tissue inhibitor of metalloproteinase 2	inhibitor of matrix metalloproteinases/ECM/cancer	1.08	0.95	1.03	1.42	1.53	1.45
AB000778_s_at	AB000778	PLD1: phospholipase D1, phophatidylcholine-specific	signal transduction/phospholipid metabolism/Ras signaling/Ca-signaling/myoblast migration	1.00	0.99	0.99	1.41	1.41	1.40
rc_AA800024_at	AA800024	similar to C6orf109: chromosome 6 open reading frame 109	unknown	1.13	0.96	1.09	1.41	1.60	1.53
U25264_at	U25264	SEPW1: selenoprotein W, 1	oxidoreductase/heart	0.87	0.99	0.86	1.41	1.22	1.21
rc_AI231292_g_at	AI231292	CST3: cystatin C (amyloid angiopathy and cerebral hemorrhage)	protease inhibitor	0.91	1.01	0.91	1.40	1.27	1.27
rc_AA799744_at	AA799744	unknown	unknown	0.84	1.05	0.88	1.39	1.16	1.22
M13100cds#2_s_at	M13100	Lre3: LINE retrotransposable element 3	unknown	0.92	1.04	0.96	1.39	1.28	1.33
AF068860_s_at	AF068860	Defb1: defensin beta 1	immune response	0.91	1.09	1.00	1.39	1.26	1.38
rc_AA892042_at	AA892042	similar to DDX3X: DEAD (Asp-Glu-Ala-Asp) box polypeptide 3, X-linked	RNA binding/RNA splicing/translation/development/cell growth/cell division	0.97	0.91	0.89	1.38	1.34	1.22
X07686cds_s_at	X07686	RNLB6: Rat L1Rn B6 repetitive DNA element	unknown	0.90	1.04	0.94	1.38	1.24	1.29
U53475_at	U53475	LOC51762: RAB-8b protein	RAS superfamily/GTPase signal transduction	0.99	1.07	1.06	1.37	1.35	1.44
L08814_at	L08814	SSRP1: structure specific recognition protein 1	transcription factor	1.00	0.97	0.97	1.36	1.36	1.32
rc_AA925556_at	AA925556	similar to CKIP-1: CK2 interacting protein 1; HQ0024c protein	unknown	1.10	0.94	1.04	1.36	1.50	1.41
rc_AA894101_at	AA894101	unknown	unknown	1.08	1.08	1.17	1.36	1.46	1.58
E13732cds_at	E13732	CC chemokine receptor	unknown	1.00	1.01	1.01	1.36	1.36	1.38
AF058791_at	AF058791	G10: maternal G10 transcript	transcription factor	0.93	1.03	0.96	1.35	1.26	1.30
rc_AA894345_at	AA894345	PEA15: phosphoprotein enriched in astrocytes 15	glucose transport/cell cycle	1.03	1.00	1.03	1.35	1.39	1.39
rc_AA893195_at	AA893195	unknown	unknown	0.99	1.14	1.12	1.34	1.32	1.50
rc_AA891222_at	AA891222	similar to SS18: synovial sarcoma translocation, chromosome 18	cell growth	1.12	0.89	1.00	1.34	1.50	1.34

L12383_at	L12383	ARF4: ADP-ribosylation factor 4	RAS superfamily/vesicular trafficking/activator of phospholipase D/ADP-ribosyltransferase/G protein GTPase signal transduction	1.12	0.89	0.99	1.34	1.49	1.33
rc_AA892520_g_at	AA892520	similar to VAT1: vesicle amine transport protein 1 homolog (T californica)	neurotransmitter vesicular transport	1.05	1.04	1.09	1.33	1.40	1.45
rc_AA894099_at	AA894099	VPS4A: vacuolar protein sorting 4A (yeast)	intracellular protein trafficking	0.94	1.00	0.94	1.33	1.25	1.25
rc_AA875225_g_at	AA875225	GNAI2: guanine nucleotide binding protein (G protein), alpha inhibiting activity polypeptide 2	G protein GTPase signal transduction	0.91	1.12	1.01	1.33	1.21	1.35
D25224_at	D25224	LAMR1: laminin receptor 1 (ribosomal protein SA, 67kDa)	cell adhesion to ECM/differentiation/metastasis/cell surface receptor signal transduction/ribosome	0.90	1.04	0.94	1.33	1.20	1.25
L11587_at	L11587	PTPRS: protein tyrosine phosphatase, receptor type, S	receptor tyrosine phosphatase/signal transduction/cell cycle/cell growth/differentiation/development/cell adhesion	0.88	1.04	0.91	1.33	1.16	1.21
rc_AI233749_at	AI233749	RPL30: ribosomal protein L30	ribosome	0.92	1.00	0.92	1.33	1.23	1.23
rc_AI169370_at	AI169370	TUBA8: tubulin, alpha 8	cytoskeleton microtubules	1.01	0.97	0.98	1.32	1.34	1.30
L38483_at	L38483	JAG1: jagged 1 (Alagille syndrome)	Ca-binding/cell cycle/myoblast differentiation/hematopoesis/angiogenesis/development	0.94	1.00	0.94	1.32	1.25	1.24
rc_AA800303_at	AA800303	similar to PLSCR3: phospholipid scramblase 3	Ca-binding/signal transduction	1.07	0.87	0.93	1.32	1.41	1.23
D21132_at	D21132	PITPNB: phosphotidylinositol transfer protein, beta	phospholipid transport	0.93	1.02	0.95	1.32	1.23	1.26
rc_AI231292_at	AI231292	CST3: cystatin C (amyloid angiopathy and cerebral hemorrhage)	protease inhibitor	1.04	1.03	1.07	1.32	1.36	1.41
rc_AI105448_at	AI105448	HSD11B1: hydroxysteroid (11-beta) dehydrogenase 1	steroid/cortisol metabolism	0.88	1.19	1.04	1.32	1.15	1.37
X14323cds_g_at	X14323	FCGRT: Fc fragment of IgG, receptor, transporter, alpha	immune response/receptor/IgG binding	0.94	1.01	0.95	1.31	1.24	1.25
X69903_at	X69903	IL4R: interleukin 4 receptor	immune response/receptor signal transduction	1.01	0.93	0.94	1.31	1.33	1.24
M86564_at	M86564	PTMA: prothymosin, alpha (gene sequence 28)	cell cycle/development/transcription	1.00	1.09	1.09	1.31	1.30	1.42
rc_AI232268_at	AI232268	Lrpap1: Low density lipoprotein receptor-related protein associated protein 1	Ca-binding/cell proliferation/receptor/protein folding/cell cycle/lipoprotein metabolism	1.01	0.92	0.93	1.31	1.32	1.22
X53377cds_s_at	X53377	Rps7: ribosomal protein S7	ribosome	1.17	0.96	1.13	1.30	1.53	1.47
rc_AI008888_g_at	AI008888	CSTB: cystatin B (stefin B)	protease inhibitor	1.05	0.98	1.03	1.30	1.36	1.34

rc_AA684631_at	AA684631	unknown	unknown	1.09	1.03	1.12	1.30	1.42	1.46
rc_AI176170_at	AI176170	FKBP1A: FK506 binding protein 1A, 12kDa	immune response/protein folding/interacts with Ca-release channels important for contraction-relaxation/signal transduction/cell cycle	1.00	0.99	0.99	1.29	1.30	1.28
rc_AI177054_at	AI177054	RALA: v-ral simian leukemia viral oncogene homolog A (ras related)	signal transduction/Ras family GTPase/cell cycle/Ca-Calmodulin binding	0.96	1.06	1.01	1.29	1.24	1.31
rc_AI176546_at	AI176546	HSPCA: heat shock 90kDa protein 1, alpha	signal transduction/heat shock protein/protein folding/cell cycle	1.04	1.07	1.11	1.29	1.34	1.44
L26268_g_at	L26268	BTG1: B-cell translocation gene 1, anti-proliferative	tumor suppressor/cell cycle/angiogenesis/myoblast differentiation/transcription factor	1.07	0.99	1.06	1.29	1.37	1.36
rc_AA859804_at	AA859804	similar to EIF4EL3: eukaryotic translation initiation factor 4E-like 3	translation initiation	1.10	0.90	1.00	1.28	1.42	1.28
M94919mRNA_f_at	M94919	beta globin gene	oxygen transport	1.01	1.05	1.06	1.28	1.29	1.35
X13933_s_at	X13933	Calm1: calmodulin 1	Ca-binding/affects K channel voltage gated/G protein coupled receptor signal transduction/signaling	1.05	1.09	1.14	1.28	1.34	1.46
rc_AA875665_g_at	AA875665	similar to RCN3: reticulocalbin 3, EF-hand calcium binding domain	Ca-binding/signal transduction	0.95	1.07	1.02	1.28	1.22	1.30
D78613_s_at	D78613	PTPRE: protein tyrosine phosphatase, receptor type, E	receptor tyrosine phosphatase/signal transduction/cell growth/differentiation/cell cycle/activation of K channel voltage gated/Ras signaling	0.90	1.08	0.97	1.28	1.15	1.24
rc_AI229655_at	AI229655	similar to hs CTDSP1: CTD (carboxy-terminal domain, RNA polymerase II, polypeptide A) small phosphatase 1	transcription	0.94	1.13	1.06	1.27	1.19	1.35
J04187_at	J04187	Cyp2a2: cytochrome P450, subfamily 2A, polypeptide 1	steroid metabolism	1.04	0.96	0.99	1.27	1.32	1.27
AF020618_g_at	AF020618	PPP1R15A: protein phosphatase 1, regulatory (inhibitor) subunit 15A	apoptosis/cell cycle	1.12	0.90	1.01	1.27	1.42	1.28
U31463_at	U31463	MYH9: myosin, heavy polypeptide 9, non-muscle	myosin/cytoskeleton/motor activity/Ca-Calmodulin binding	1.09	0.89	0.97	1.27	1.38	1.22
X06483cds_at	X06483	RPL32: ribosomal protein L32	ribosome	1.02	1.02	1.04	1.27	1.29	1.32
rc_AA875523_s_at	AA875523	similar to MLC1SA: myosin light chain 1 slow a	myosin/Ca-binding/muscle development/cytoskeleton	0.89	1.11	1.00	1.27	1.13	1.26
rc_AA946313_s_at	AA946313	SPARC: secreted protein, acidic, cysteine-rich (osteonectin)	Ca-binding/ECM synthesis/cell-shape/cell cycle/collagen-binding/angiogenesis	1.17	0.98	1.15	1.26	1.48	1.46
rc_AI176658_s_at	AI176658	HSPB1: heat shock 27kDa protein 1	heat shock protein/protein folding/cell cycle	1.17	1.01	1.18	1.26	1.47	1.49
L33869_at	L33869	Cp: ceruloplasmin	iron/copper homeostasis and transport	1.05	1.05	1.10	1.26	1.32	1.39

rc_AI227887_g_at	AI227887	CDC42: cell division cycle 42 (GTP binding protein, 25kDa)	signal transduction/cell cycle/cell morphology/actin polymerization/cytoskeleton	1.14	0.91	1.04	1.26	1.43	1.31
rc_AI171085_at	AI171085	RPL39: ribosomal protein L39	ribosome	0.90	1.07	0.96	1.26	1.13	1.21
D88666_at	D88666	PLA1A: phospholipase A1 member A	phospholipid metabolism	0.99	1.02	1.01	1.25	1.24	1.27
rc_AA800017_at	AA800017	unknown	unknown	1.10	0.93	1.03	1.25	1.38	1.28
U75929UTR#1_f_at	U75929	SPARC: secreted protein, acidic, cysteine-rich (osteonectin)	Ca-binding/ECM synthesis/cell-shape/cell cycle/collagen-binding/angiogenesis	1.00	1.11	1.11	1.25	1.25	1.39
X66369_at	X66369	RPL37: ribosomal protein L37	ribosome	0.87	1.15	0.99	1.25	1.08	1.24
U59184_at	U59184	BAX: BCL2-associated X protein	pro-apoptosis/cell cycle/development	1.07	0.91	0.97	1.24	1.33	1.20
M94918mRNA_f_at	M94918	Hbb: hemoglobin beta chain complex	oxygen transport	1.08	1.04	1.13	1.24	1.34	1.40
D29683_at	D29683	ECE1: endothelin converting enzyme 1	forms endothelin 1/vasoactive/blood pressure/cell cycle	1.10	1.05	1.16	1.24	1.36	1.43
rc_AI014087_at	AI014087	RPS26: ribosomal protein S26	ribosome	1.17	0.97	1.12	1.23	1.44	1.39
M27905_at	M27905	RPL21: ribosomal protein L21	ribosome	0.90	1.10	0.99	1.23	1.11	1.22
U24652_at	U24652	LNK: lymphocyte adaptor protein	immune response/signal transduction	0.94	1.06	1.00	1.23	1.16	1.23
rc_AI104389_g_at	AI104389	TH: tyrosine hydroxylase	catecholamine biosynthesis rate limiting enzyme/amino acid metabolism	1.03	1.00	1.04	1.23	1.27	1.27
rc_AA891729_at	AA891729	RPS27A: ribosomal protein S27a	ribosome	1.03	1.04	1.07	1.23	1.27	1.31
rc_AI228674_s_at	AI228674	PPIA: peptidylprolyl isomerase A (cyclophilin A)	protein folding/immune response/cell cycle	0.96	1.03	0.98	1.22	1.17	1.20
X56325mRNA_s_at	X56325	Hemoglobin, alpha 1	oxygen transport	0.92	1.10	1.01	1.22	1.12	1.23
X58200mRNA_at	X58200	RPL23: ribosomal protein L23	ribosome	1.13	1.01	1.14	1.22	1.37	1.39
rc_AA891828_g_at	AA891828	similar to RAD23A: RAD23 homolog A (S. cerevisiae)	DNA nucleotide excision-repair/ubiquitin mediated protein degradation	0.97	1.04	1.01	1.22	1.18	1.22
M34043_at	M34043	Tmsb4x: thymosin beta-4	cytoskeleton/immune response/development	1.02	1.10	1.12	1.21	1.24	1.36
rc_AA875552_at	AA875552	unknown	unknown	1.00	1.01	1.01	1.20	1.20	1.21
rc_AI639338_at	AI639338	unknown	unknown	1.05	1.03	1.08	1.20	1.26	1.30
M38566mRNA_s_at	M38566	CYP27A1: cytochrome P450, family 27, subfamily A, polypeptide 1	steroid metabolism/cholesterol homeostasis	1.12	0.91	1.02	1.20	1.35	1.22

VII Bibliography

1. Levy D, Kenchaiah S, Larson MG, et al. Long-term trends in the incidence of and survival with heart failure. N Engl J Med 2002;347(18):1397-402.

2. Frey N, Olson EN. Cardiac hypertrophy: the good, the bad, and the ugly. Annu Rev Physiol 2003;65:45-79.

3. Hwang JJ, Allen PD, Tseng GC, et al. Microarray gene expression profiles in dilated and hypertrophic cardiomyopathic end-stage heart failure. Physiol Genomics 2002;10(1):31-44.

4. Meyer M, Schillinger W, Pieske B, et al. Alterations of sarcoplasmic reticulum proteins in failing human dilated cardiomyopathy. Circulation 1995;92(4):778-84.

5. He TC, Zhou S, da Costa LT, Yu J, Kinzler KW, Vogelstein B. A simplified system for generating recombinant adenoviruses. Proc Natl Acad Sci U S A 1998;95(5):2509-14.

6. Del Monte F, Butler K, Boecker W, Gwathmey JK, Hajjar RJ. Novel technique of aortic banding followed by gene transfer during hypertrophy and heart failure. Physiol Genomics 2002;9(1):49-56.

7. del Monte F, Williams E, Lebeche D, et al. Improvement in survival and cardiac metabolism after gene transfer of sarcoplasmic reticulum Ca(2+)-ATPase in a rat model of heart failure. Circulation 2001;104(12):1424-9.

8. Hajjar RJ, Schmidt U, Matsui T, et al. Modulation of ventricular function through gene transfer in vivo. Proc Natl Acad Sci U S A 1998;95(9):5251-6.

9. Pfaffl MW. A new mathematical model for relative quantification in real-time RT-PCR. Nucleic Acids Res 2001;29(9):e45.

10. Eisen MB, Spellman PT, Brown PO, Botstein D. Cluster analysis and display of genome-wide expression patterns. Proc Natl Acad Sci U S A 1998;95(25):14863-8.

11. del Monte F, Harding SE, Schmidt U, et al. Restoration of contractile function in isolated cardiomyocytes from failing human hearts by gene transfer of SERCA2a. Circulation 1999;100(23):2308-11.

12. del Monte F, Harding SE, Dec GW, Gwathmey JK, Hajjar RJ. Targeting phospholamban by gene transfer in human heart failure. Circulation 2002;105(8):904-7.

13. Hajjar RJ, Kang JX, Gwathmey JK, Rosenzweig A. Physiological effects of adenoviral gene transfer of sarcoplasmic reticulum calcium ATPase in isolated rat myocytes. Circulation 1997;95(2):423-9.

14. Kadonaga JT. Regulation of RNA polymerase II transcription by sequence-specific DNA binding factors. Cell 2004;116(2):247-57.

15. McKenna NJ, O'Malley BW. Combinatorial control of gene expression by nuclear receptors and coregulators. Cell 2002;108(4):465-74.

16. Stewart CB. The powers and pitfalls of parsimony. Nature 1993;361(6413):603-7.

17. Haq S, Choukroun G, Kang ZB, et al. Glycogen synthase kinase-3beta is a negative regulator of cardiomyocyte hypertrophy. J Cell Biol 2000;151(1):117-30.

18. Haq S, Choukroun G, Lim H, et al. Differential activation of signal transduction pathways in human hearts with hypertrophy versus advanced heart failure. Circulation 2001;103(5):670-7.

19. Trencia A, Perfetti A, Cassese A, et al. Protein kinase B/Akt binds and phosphorylates PED/PEA-15, stabilizing its antiapoptotic action. Mol Cell Biol 2003;23(13):4511-21.

20. Rane MJ, Pan Y, Singh S, et al. Heat shock protein 27 controls apoptosis by regulating Akt activation. J Biol Chem 2003;278(30):27828-35.

21. Lo SH, Weisberg E, Chen LB. Tensin: a potential link between the cytoskeleton and signal transduction. Bioessays 1994;16(11):817-23.

22. Maruta H. [F-actin cappers]. Gan To Kagaku Ryoho 1997;24(11):1442-7.

23. Guan JL. Focal adhesion kinase in integrin signaling. Matrix Biol 1997;16(4):195-200.

24. Schafer DA, Cooper JA. Control of actin assembly at filament ends. Annu Rev Cell Dev Biol 1995;11:497-518.

25. Thierfelder L, Watkins H, MacRae C, et al. Alpha-tropomyosin and cardiac troponin T mutations cause familial hypertrophic cardiomyopathy: a disease of the sarcomere. Cell 1994;77(5):701-12.

26. ten Dijke P, Ichijo H, Franzen P, et al. Activin receptor-like kinases: a novel subclass of cell-surface receptors with predicted serine/threonine kinase activity. Oncogene 1993;8(10):2879-87.

27. Tanaka M, Ozaki S, Osakada F, Mori K, Okubo M, Nakao K. Cloning of follistatin-related protein as a novel autoantigen in systemic rheumatic diseases. Int Immunol 1998;10(9):1305-14.

28. Matsuda A, Suzuki Y, Honda G, et al. Large-scale identification and characterization of human genes that activate NF-kappaB and MAPK signaling pathways. Oncogene 2003;22(21):3307-18.

29. Abraham NG, Kushida T, McClung J, et al. Heme oxygenase-1 attenuates glucose-mediated cell growth arrest and apoptosis in human microvessel endothelial cells. Circ Res 2003;93(6):507-14.

30. Wang J, Lu S, Moenne-Loccoz P, Ortiz de Montellano PR. Interaction of nitric oxide with human heme oxygenase-1. J Biol Chem 2003;278(4):2341-7.

31. Li Volti G, Wang J, Traganos F, Kappas A, Abraham NG. Differential effect of heme oxygenase-1 in endothelial and smooth muscle cell cycle progression. Biochem Biophys Res Commun 2002;296(5):1077-82.

32. Herrmann S, Schmidt-Petersen K, Pfeifer J, et al. A polymorphism in the endothelin-A receptor gene predicts survival in patients with idiopathic dilated cardiomyopathy. Eur Heart J 2001;22(20):1948-53.

33. Porteri E, Rizzoni D, Guelfi D, et al. Role of ET(A) receptors in the vasoconstriction induced by endothelin-1 in subcutaneous small arteries of normotensive subjects and hypertensive patients. Blood Press 2002;11(1):6-12.

34. Carrasquillo MM, McCallion AS, Puffenberger EG, Kashuk CS, Nouri N, Chakravarti A. Genome-wide association study and mouse model identify interaction between RET and EDNRB pathways in Hirschsprung disease. Nat Genet 2002;32(2):237-44.

35. Rosano L, Spinella F, Di Castro V, et al. Endothelin receptor blockade inhibits molecular effectors of Kaposi's sarcoma cell invasion and tumor growth in vivo. Am J Pathol 2003;163(2):753-62.

36. Teshima Y, Akao M, Jones SP, Marban E. Uncoupling protein-2 overexpression inhibits mitochondrial death pathway in cardiomyocytes. Circ Res 2003;93(3):192-200.

37. Mattiasson G, Shamloo M, Gido G, et al. Uncoupling protein-2 prevents neuronal death and diminishes brain dysfunction after stroke and brain trauma. Nat Med 2003;9(8):1062-8.

38. Kiewitz R, Acklin C, Schafer BW, et al. Ca2+ -dependent interaction of S100A1 with the sarcoplasmic reticulum Ca2+ -ATPase2a and phospholamban in the human heart. Biochem Biophys Res Commun 2003;306(2):550-7.

39. Most P, Boerries M, Eicher C, et al. Extracellular S100A1 protein inhibits apoptosis in ventricular cardiomyocytes via activation of the extracellular signal-regulated protein kinase 1/2 (ERK1/2). J Biol Chem 2003;278(48):48404-12.

40. Most P, Remppis A, Weber C, et al. The C terminus (amino acids 75-94) and the linker region (amino acids 42-54) of the Ca2+-binding protein S100A1 differentially enhance sarcoplasmic Ca2+ release in murine skinned skeletal muscle fibers. J Biol Chem 2003;278(29):26356-64.

41. Razeghi P, Young ME, Ying J, et al. Downregulation of metabolic gene expression in failing human heart before and after mechanical unloading. Cardiology 2002;97(4):203-9.

42. Malmqvist K, Wallen HN, Held C, Kahan T. Soluble cell adhesion molecules in hypertensive concentric left ventricular hypertrophy. J Hypertens 2002;20(8):1563-9.

43. Epshteyn V, Morrison K, Krishnaswamy P, et al. Utility of B-type natriuretic peptide (BNP) as a screen for left ventricular dysfunction in patients with diabetes. Diabetes Care 2003;26(7):2081-7.

44. Galindo-Fraga A, Arrieta O, Castillo-Martinez L, Narvaez R, Oseguera-Moguel J, Orea-Tejeda A. Elevation of plasmatic endothelin in patients with heart failure. Arch Med Res 2003;34(5):367-72.

45. Katz AM. The cardiomyopathy of overload: an unnatural growth response in the hypertrophied heart. Ann Intern Med 1994;121(5):363-71.

46. Hunter JJ, Chien KR. Signaling pathways for cardiac hypertrophy and failure. N Engl J Med 1999;341(17):1276-83.

47. Marks AR. A guide for the perplexed: towards an understanding of the molecular basis of heart failure. Circulation 2003;107(11):1456-9.

48. Bers DM. Calcium fluxes involved in control of cardiac myocyte contraction. Circ Res 2000;87(4):275-81.

49. Bers DM. Calcium and cardiac rhythms: physiological and pathophysiological. Circ Res 2002;90(1):14-7.

50. This work was supported by NIH grants to David Housman, Roger Hajjar, and Federica del Monte.

Appendix

Perl Algorithm 1:

What follows is an algorithm that we wrote using Perl language. The algorithm uses the 4237 array elements defined above as input to isolate SERCA2a target genes. It then clusters these genes into the 10 transcriptional profiles for SERCA2a targets described in the text (Figure 5).

```
# this program is analysisII, it extracts all the genes affected by SERCA
# command line: perl analysis2.txt input.txt >output.txt
# input.txt = dchip.txt
# $FV_F is a ratio where FV is the numerator and F the denominator


#enter here immediately below the >1 cutoff, ie 1.5
$hi=1.2;
$lo=1/$hi;
print "\ncutoff:\nHi=$hi\nLow=$lo\n\n";
print "This is the list of all the genes AFFECTED BY SERCA2a\n";

while (<>)
{
chomp;
if (/^((.*)\t(\d*.\d*)\t(\d*.\d*)\t(\d*.\d*)\t(\d*.\d*)\t(\d*.\d*)\t(\d*.\d*))$/)
        {

$FV_F=$7/$6;
$FS_FV=$8/$7;
$FS_F=$8/$6;
$F_NF=$6/$3;
$FS_F=$8/$6;
$FS_NF=$8/$3;
$FV_NF=$7/$3;

unless ((($FS_F > $lo) && ($FS_F < $hi)) || (($FS_FV > $lo) && ($FS_FV < $hi)))
{$SERCAaffected[$r]="$1"; $r=$r+1;}
        }
}

$number= @SERCAaffected;
print "number of genes affected by SERCA is = $number out of 4237 total\n";

print"\nPROBE SET  GENE ACCESSION  LOCUS LINKNF*    NFV    NFS*  F        FV*
        FS*    FV/F   FS/FV FS/F    F/NF   FV/NF FS/NF prioritycandidate gene probability
for SERCA effect\n\n";

foreach (@SERCAaffected)
{
chomp;
if (/^((.*)\t(\d*.\d*)\t(\d*.\d*)\t(\d*.\d*)\t(\d*.\d*)\t(\d*.\d*)\t(\d*.\d*))$/)
        {

$FV_F=$7/$6;
$FS_FV=$8/$7;
```

```
$FS_F=$8/$6;
$F_NF=$6/$3;
$FS_F=$8/$6;
$FS_NF=$8/$3;
$FV_NF=$7/$3;



if (($FV_F>$hi && $FS_FV>$hi && $FS_F>$hi) || ($FV_F<$lo && $FS_FV<$lo &&
$FS_F<$lo) || ($FV_F>$hi && $FS_FV<$lo && $FS_F<$lo) || ($FV_F<$lo && $FS_FV>$hi
&& $FS_F>$hi))
{$prob1 = 2; $prob2 = "high"; &analysisII;}


if (($FV_F>$hi && $FS_FV<$lo && $FS_F>$hi) || ($FV_F<$lo && $FS_FV>$hi &&
$FS_F<$lo))
{$prob1 = 3; $prob2 = "lower"; &analysisII;}


if (($FV_F>$lo && $FV_F<$hi && $FS_FV>$hi && $FS_F>$hi) || ($FV_F>$lo &&
$FV_F<$hi && $FS_FV<$lo && $FS_F<$lo))
{$prob1 = 1; $prob2 = "highest"; &analysisII;}
        }
}



# SUBROUTINE
sub analysisII
{
#set1, 40
if ($F_NF>$lo && $F_NF<$hi && $FS_F>$hi && $FS_NF>$hi)
{$set1[$n1]="$1        $FV_F $FS_FV        $FS_F  $F_NF $FV_NF        $FS_NF        $prob1
        $prob2"; $n1=$n1+1;}

#set2, 41=mir40
if ($F_NF>$lo && $F_NF<$hi && $FS_F<$lo && $FS_NF<$lo)
{$set2[$n2]="$1        $FV_F $FS_FV        $FS_F  $F_NF $FV_NF        $FS_NF        $prob1
        $prob2"; $n2=$n2+1;}

#set3, 46
if ($F_NF>$hi && $FS_F<$lo && $FS_NF>$hi)
{$set3[$n3]="$1        $FV_F $FS_FV        $FS_F  $F_NF $FV_NF        $FS_NF        $prob1
        $prob2"; $n3=$n3+1;}

#set4, mir46
```

```
if ($F_NF<$lo && $FS_F>$hi && $FS_NF<$lo)
{$set4[$n4]="$1	$FV_F $FS_FV	$FS_F $F_NF $FV_NF	$FS_NF	$prob1
	$prob2"; $n4=$n4+1;}

#set5, 42
if ($F_NF>$hi && $FS_F<$lo && $FS_NF>$lo && $FS_NF<$hi)
{$set5[$n5]="$1	$FV_F $FS_FV	$FS_F $F_NF $FV_NF	$FS_NF	$prob1
	$prob2"; $n5=$n5+1;}

#set6, 43
if ($F_NF<$lo && $FS_F>$hi && $FS_NF>$lo && $FS_NF<$hi)
{$set6[$n6]="$1	$FV_F $FS_FV	$FS_F $F_NF $FV_NF	$FS_NF	$prob1
	$prob2"; $n6=$n6+1;}

#set7, 47
if ($F_NF>$hi && $FS_F<$lo && $FS_NF<$lo)
{$set7[$n7]="$1	$FV_F $FS_FV	$FS_F $F_NF $FV_NF	$FS_NF	$prob1
	$prob2"; $n7=$n7+1;}

#set8, mir47
if ($F_NF<$lo && $FS_F>$hi && $FS_NF>$hi)
{$set8[$n8]="$1	$FV_F $FS_FV	$FS_F $F_NF $FV_NF	$FS_NF	$prob1
	$prob2"; $n8=$n8+1;}

#set9, 44
if ($F_NF>$hi && $FS_F>$hi && $FS_NF>$hi)
{$set9[$n9]="$1	$FV_F $FS_FV	$FS_F $F_NF $FV_NF	$FS_NF	$prob1
	$prob2"; $n9=$n9+1;}


#set10, 45=mir44
if ($F_NF<$lo && $FS_F<$lo && $FS_NF<$lo)
{$set10[$n10]="$1	$FV_F $FS_FV	$FS_F $F_NF $FV_NF	$FS_NF	$prob1
	$prob2"; $n10=$n10+1;}

#set11, 48
if ($F_NF>$lo && $F_NF<$hi && $FS_F>$hi && $FS_NF>$lo && $FS_NF<$hi)
{$set11[$n11]="$1	$FV_F $FS_FV	$FS_F $F_NF $FV_NF	$FS_NF	$prob1
	$prob2"; $n11=$n11+1;}

#set12, 49=mir48
if ($F_NF>$lo && $F_NF<$hi && $FS_F<$lo && $FS_NF>$lo && $FS_NF<$hi)
{$set12[$n12]="$1	$FV_F $FS_FV	$FS_F $F_NF $FV_NF	$FS_NF	$prob1
	$prob2"; $n12=$n12+1;}
}
```

```
#print set1
$num1=@set1;
print "\n\n\nset1 = $num1      profile = 40\n";
print "F UNCHANGED from NF, FS UPregulated from F\n\n";
foreach $set1 (@set1)
        {print "$set1\n"};

#print set2
$num2=@set2;
print "\n\n\nset2 = $num2      profile = 41 = mir40\n";
print "F UNCHANGED from NF, FS DOWNregulated from F\n\n";
foreach $set2 (@set2)
        {print "$set2\n"};

#print set3
$num3=@set3;
print "\n\n\nset3 = $num3      profile = 46\n";
print "F UPregulated from NF, FS<F but FS>NF\n\n";
foreach $set3 (@set3)
        {print "$set3\n"};

#print set4
$num4=@set4;
print "\n\n\nset4 = $num4      profile = mir46\n";
print "F DOWNregulated from NF, FS>F but FS<NF\n\n";
foreach $set4 (@set4)
        {print "$set4\n"};

#print set5
$num5=@set5;
print "\n\n\nset5 = $num5      profile = 42\n";
print "F UPregulated from NF, NORMALIZED by SERCA2a\n\n";
foreach $set5 (@set5)
        {print "$set5\n"};

#print set6
$num6=@set6;
print "\n\n\nset6 = $num6      profile = 43\n";
print "F DOWNregulated from NF, NORMALIZED by SERCA2a\n\n";
foreach $set6 (@set6)
        {print "$set6\n"};

#print set7
$num7=@set7;
```

```
print "\n\n\nset7 = $num7      profile = 47\n";
print "F UPregulated from NF, FS<F and FS<NF\n\n";
foreach $set7 (@set7)
        {print "$set7\n"};

#print set8
$num8=@set8;
print "\n\n\nset8 = $num8      profile = mir47\n";
print "F DOWNregulated from NF, FS>F and FS>NF\n\n";
foreach $set8 (@set8)
        {print "$set8\n"};

#print set9
$num9=@set9;
print "\n\n\nset9 = $num9      profile = 44\n";
print "F UPregulated from NF, FS UPregulated from F\n\n";
foreach $set9 (@set9)
        {print "$set9\n"};

#print set10
$num10=@set10;
print "\n\n\nset10 = $num10  profile = 45 = mir44\n";
print "F DOWNregulated from NF, FS DOWNregulated from F\n\n";
foreach $set10 (@set10)
        {print "$set10\n"};

#print set11
$num11=@set11;
print "\n\n\nset11 = $num11  profile = 48\n";
print "MARGINAL SERCA2a effect: FS UPregulated from F, F=NF\n\n";
foreach $set11 (@set11)
        {print "$set11\n"};

#print set12
$num12=@set12;
print "\n\n\nset12 = $num12  profile = 49 = mir48\n";
print "MARGINAL SERCA2a effect: FS DOWNregulated from F, F=NF\n\n";
foreach $set12 (@set12)
        {print "$set12\n"};
```

Perl Algorithm 2:

What follows is an algorithm that we wrote using Perl language. The algorithm uses the 4237 array elements defined above as input to isolate the genes that are natural adaptive responses to aortic banding needed for clinical non-failure. It then clusters these genes into the two transcriptional profiles described in the text (Figure 6).

```
# this program is analysisI, it extracts the genes not affected by SERCA
# nor the virus components of its vector
# command line: perl analysis1.txt input.txt >output.txt
# $FV_F is a ratio where FV is the numerator and F the denominator


#enter here immediately below the >1 cutoff, ie 1.5
$hi=1.2;
$lo=1/$hi;
print "\ncutoff:\nHi=$hi\nLow=$lo\n\n";

print "This is the list of all the genes NOT AFFECTED BY SERCA2a nor the virus components
of its vector\n";

while (<>)
{
chomp;
if (/^((.*)\t(\d*.\d*)\t(\d*.\d*)\t(\d*.\d*)\t(\d*.\d*)\t(\d*.\d*)\t(\d*.\d*))$/)
        {

$FV_F=$7/$6;
$FS_FV=$8/$7;
$FS_F=$8/$6;
$F_NF=$6/$3;
$FS_F=$8/$6;
$FS_NF=$8/$3;
$FV_NF=$7/$3;

if ($FS_F>$lo && $FS_F<$hi)
{$SERCAaffected[$r]="$1"; $r=$r+1;}
        }
}

$number= @SERCAaffected;
print "number of genes not affected by SERCA is = $number out of 4237 total\n";

print"\nPROBE SET  GENE ACCESSION  LOCUS LINKNF*    NFV    NFS*  F        FV*
        FS*     FV/F   FS/FV FS/F    F/NF   FV/NF FS/NF prioritycandidate gene probability
for natural beneficial effect\n\n";

foreach (@SERCAaffected)
{
chomp;
if (/^((.*)\t(\d*.\d*)\t(\d*.\d*)\t(\d*.\d*)\t(\d*.\d*)\t(\d*.\d*)\t(\d*.\d*))$/)
        {
```

```
$FV_F=$7/$6;
$FS_FV=$8/$7;
$FS_F=$8/$6;
$F_NF=$6/$3;
$FS_F=$8/$6;
$FS_NF=$8/$3;
$FV_NF=$7/$3;


# FS=F and FV=F and FS=FV
if (($FV_F>$lo && $FV_F<$hi) && ($FS_FV>$lo && $FS_FV<$hi))
{$prob1 = 1; $prob2 = "highest"; &analysisI;}

# (FS=F and FV=F and FS diff FV) or (FS=F and FS=FV and FV diff F)
if ((($FV_F>$lo && $FV_F<$hi) && ($FS_FV<$lo || $FS_FV>$hi)) || (($FV_F<$lo ||
$FV_F>$hi) && ($FS_FV>$lo && $FS_FV<$hi)))
{$prob1 = 2; $prob2 = "high"; &analysisI;}

# FS=F and (FV diff F) and (FS diff FV)
if ((($FV_F<$lo || $FV_F>$hi) && ($FS_FV<$lo || $FS_FV>$hi)))
{$prob1 = 3; $prob2 = "lower"; &analysisI;}
        }
}



# SUBROUTINE
sub analysisI
{
#set1, 61
if ($F_NF<$lo && $FS_F>$lo && $FS_F<$hi && $FS_NF<$lo)
{$set1[$n1]="$1        $FV_F $FS_FV        $FS_F  $F_NF $FV_NF        $FS_NF        $prob1
        $prob2"; $n1=$n1+1;}

#set2, 63=mir61
if ($F_NF>$hi && $FS_F>$lo && $FS_F<$hi && $FS_NF>$hi)
{$set2[$n2]="$1        $FV_F $FS_FV        $FS_F  $F_NF $FV_NF        $FS_NF        $prob1
        $prob2"; $n2=$n2+1;}

#set3, 62
if ($F_NF>$lo && $F_NF<$hi && $FS_F>$lo && $FS_F<$hi && $FS_NF>$lo &&
$FS_NF<$hi)
{$set3[$n3]="$1        $FV_F $FS_FV        $FS_F  $F_NF $FV_NF        $FS_NF        $prob1
        $prob2"; $n3=$n3+1;}

#set4, 64, 65=mir64, 66, 67=mir66
```

```
if (($F_NF>$hi && $FS_F>$lo && $FS_F<$hi && $FS_NF>$lo && $FS_NF<$hi) ||
($F_NF<$lo && $FS_F>$lo && $FS_F<$hi && $FS_NF>$lo && $FS_NF<$hi) || ($F_NF>$lo
&& $F_NF<$hi && $FS_F>$lo && $FS_F<$hi && $FS_NF>$hi) || ($F_NF>$lo &&
$F_NF<$hi && $FS_F>$lo && $FS_F<$hi && $FS_NF<$lo))
{$set4[$n4]="$1	$FV_F $FS_FV	$FS_F $F_NF $FV_NF	$FS_NF	$prob1
	$prob2"; $n4=$n4+1;}
}


#print set1
$num1=@set1;
print "\n\n\nset1 = $num1	profile = 61\n";
print "FS UNCHANGED from F, F DOWNregulated from NF\n\n";
foreach $set1 (@set1)
	{print "$set1\n"};

#print set2
$num2=@set2;
print "\n\n\nset2 = $num2	profile = 63 = mir61\n";
print "FS UNCHANGED from F, F UPregulated from NF\n\n";
foreach $set2 (@set2)
	{print "$set2\n"};

#print set3
$num3=@set3;
print "\n\n\nset3 = $num3	profile = 62\n";
print "F=NF and FS=F and FS=NF\n\n";
foreach $set3 (@set3)
	{print "$set3\n"};

#print set4
$num4=@set4;
print "\n\n\nset4 = $num4	profile = like 62 = 64, 65=mir64, 66, 67=mir66\n";
print "Like 62, ~(F=NF and FS=F and FS=NF)\n\n";
foreach $set4 (@set4)
	{print "$set4\n"};
```